Fakultät für Medizin

Analysis of different combinatory regimes on the antitumor efficacy of oncolytic YB-1 based virotherapy in glioblastoma

Maximilian Ehrenfeld

Vollständiger Abdruck der von der Fakultät für Medizin der Technischen Universität München zur Erlangung des akademischen Grades eines
Doktors der Naturwissenschaften (Dr. rer. nat.)
genehmigten Dissertation.

Vorsitz: Prof. Dr. Andreas Pichlmair

Prüfer*innen der Dissertation:
1: apl. Prof. Dr. Per Sonne Holm
2: Prof. Angelika Schnieke, Ph.D.

Die Dissertation wurde am 24.01.2022 bei der Technischen Universität München eingereicht und durch die Fakultät für Medizin am 07.06.2022 angenommen.

Abstract

The aim of this study was to enhance oncolytic virotherapy in glioblastoma by combining the oncolytic adenovirus XVir-N-31 with small molecule inhibitors. First, we established a reference point using the standard therapy consisting of chemotherapy and radiation to which we compared the new treatment regimes. Based on the findings a new viral construct was generated, to further increase our molecular understanding.

In the first step we investigated the effectiveness of XVir-N-31 treatment in combination with chemotherapy and radiation. As already published, we observed an increase in viral replication, particle formation and cell killing. When combining both treatment options together with the virus the benefit was only minor compared to the single treatments. These effects were expectable since this therapy approach leads to severe cellular stress, hindering the viral life cycle.

Therefore, the aim for the new treatment strategy lays in enhancing the viral life cycle using small molecule inhibitors.

It has been shown before that CDK4/6 inhibitors increase the viral replication, potency and particle formation of XVir-N-31 in bladder cancer. Therefore we combined XVir-N-31 with two CDK4/6 inhibitors that are able to penetrate the blood-brain barrier, namely Abemaciclib (LY-2835219) and Ribociclib (LEE011). Both CDK4/6 inhibitors lead to a cell cycle arrest in the G1 phase. While the effects on the viral parameters differed severely. Ribociclib enhanced the viral replication, particle formation and viral potency in concentration of only 100nM. It furthermore led to the downregulation of Rb and its dephosphorylation. Abemaciclib was also capable of reducing the cell viability, but the inhibitor interfered the viral life cycle and increased the other viral parameters not significantly. Ribociclib therefore was chosen as the inhibitor of choice for the treatment of glioblastoma in combination with XVir-N-31.

The second inhibitor class that we investigated were bromodomain inhibitors, namely JQ1. JQ1 inhibits the epigenetic reader protein Brd4, altering both cellular and viral parameters. The effects of JQ1 in the virotherapy context have already been published with mixed results, depending on the viral background. We were the first to validate the effectiveness using our XVir-N-31 construct. JQ1 was able to increase all viral parameters. The effects were highly significant and exceeded the benefits of the

CDk4/6 inhibitor therapy. Interestingly JQ1 could be also used in low concentrations of only 100nM, showing that this small molecule class is applicable *in vivo*.

To further improve our therapeutic approach we combined LEE011 and JQ1 in a triple therapy with XVir-N-31. This led to a further increase in cell killing, viral particle formation and replication. The triple therapeutic approach will now be further investigated *in vivo*, as well as in different other tumor entities.

Based on these results we constructed a new virus with deletions in the E2F binding sites, located in the E1 enhancer and E2 early promotor region. Here we found that the JQ1 treatment increases the viral replication independent of E2Fs.

We therefore conclude this translational thesis, with a new triple therapy approach as well as further insight in the mode of action of LEE011 and JQ1.

Zusammenfassung

Das Ziel dieser Arbeit war es die onkolytische Virotherapie in Glioblastoma, mittels der Kombination des onkolytisches Adenovirus XVir-N-31 und verschiedener Therapeutika, zu verbessern. Zu Beginn wurde als erstes die Kombination von XVir-N-31 mit der Standardtherapie, bestehend aus Bestrahlung und Chemotherapie, etabliert. Diese Ergebnisse wurden dann mit den neuen Therapieansätzen verglichen. Basierend auf den Resultaten wurde dann des Weiteren ein neues Virus kloniert, produziert und getestet, um weitere Einblicke in die molekularbiologischen Hintergründe zu gewinnen.

Bei der Kombination von XVir-N-31 mit Bestrahlung und Chemotherapie ergaben sich gesteigerte virale Parameter, wie Replikation, Partikelbildung und eine Erhöhung der Zelllyse. Wenn alle drei Therapien kombiniert wurden, war der Effekt geringer. Dies ist darauf zurückzuführen, dass die aggressive Kombination die Zellen zu sehr belastet, um einen funktionalen Lebenszyklus der Viren aufrecht zu erhalten.

Unser neuer Therapieansatz beruht darauf nicht nur die Zellen abzutöten, sondern gezielt den viralen Lebenszyklus positiv zu beeinflussen.

Es wurde bereits publiziert, dass CDk4/6 Inhibitoren die viralen Faktoren, wie Replikation und Partikelbildung von XVir-N-31 in Blasenkrebs erhöhen kann. Diesen Therapieansatz wollen wir nun auf das Glioblastom übertragen. Dazu wurden zwei verschiedene CDK4/6 Inhibitoren, die in der Lage sind, die Blut-Hirn-Schranke zu überwinden genutzt, namentlich Abemaciclib (LY2835219) und Ribociclib (LEE011). Beide Inhibitoren arretierten die Zellen in der G1 Zellzyklusphase. Jedoch waren die Effekte auf die viralen Parameter unterschiedlich. Während Ribociclib grundsätzlich positive Effekte auf die viralen Parameter aufweist, ergeben sich diese Steigerungen bei Abemaciclib nicht. Daher wurde für die weitere Therapie des Glioblastoms in Kombination mit XVir-N-31 eine Indikation mit Ribociclib empfohlen.

Bei dem zweiten Inhibitor, namens JQ1, handelt es sich um einen Wirkstoff aus der Klasse der Bromodomänen-Inhibitoren. Der Wirkstoff inhibiert epigenetische Aktivität von Brd4 und verändert damit sowohl zelluläre als auch virale Expressionen. JQ1 wurde bereits mit verschiedenen viralen Konstrukten kombiniert, die Ergebnisse waren aber von Virus zu Virus unterschiedlich. In dieser Arbeit untersuchen wir erstmalig die Effektivität von JQ1 mit XVir-N-31 in Glioblastoma. Hierbei zeigte sich eine massive

Erhöhung aller getesteten viralen Parameter, in einem so hohen Maße, dass die Wirkung von CDK4/6 Inhibitoren noch übertroffen wurde. Ein weiterer Vorteil der Therapie mit JQ1 ist die geringe Konzentration, von 100nM, bei der bereits das therapeutische Fenster erreicht ist. Dies spricht für eine Verwendung der Wirkstoffklasse *in vivo*.

Um die Therapie noch weiter zu verbessern, kombinierten wir im nächsten Schritt LEE011 und JQ1 in einer Dreifach-Therapie mit XVir-N-31. Hiermit konnten wir die virale Potenz, die Produktion infektiöser viraler Partikel und die virale Replikation noch weiter steigern. Dieser Ansatz wird jetzt sowohl *in vivo*, als auch in anderen Tumorentitäten getestet.

Basierend auf allen Ergebnissen konstruierten wir ein neues Adenovirus, mit deletierten E2F Bindestellen, lokalisiert im E1 Enhancer und dem E2 early Promotor. Dies ermöglichte uns zu zeigen, das JQ1 die virale Replikation unabhängig des E2F/Rb – Pathways erhöht.

In dieser translationalen Arbeit, konnten wir eine neue Therapieoption mit CDK4/6 Inhibitoren und Bromodomänen-Inhibitoren in Kombination mit dem onkolytischen Adenovirus XVir-N-31 für das Glioblastom etablieren und zu einem besseren molekularbiologischen Verständnis der zugrundeliegenden Wirkmechanismen gelangen.

Acknowledgement

First and foremost, I wish to thank Prof. Dr. Gschwend for giving me the opportunity to work in his urology department at the Klinikum rechts der Isar, MRI.

I would like to express my heartfelt and sincere gratitude to Prof. Dr. Per Sonne Holm, who gave me the opportunity to work on a highly interesting and urgent topic. He taught me many aspects of scientific methodology and the way to critically think through the experiments to fully harvest all information available. Furthermore, he taught me to plan and manage several simultaneous projects in the most effective way. His heartfelt joy and enthusiasm towards virotherapeutic research were highly contagious and motivational and I am very thankful about the time that we spent together in his lab, discussing, planning and coming up with new hypothesis and solutions.

Many thanks also to PD Dr. Roman Nawroth for his help and advice. His critical thinking always was helpful in discussions to ensure that all aspects are considered, when coming up with new ideas or trying to proof a hypothesis.

Furthermore, I would like to offer my greatest appreciation to Prof. Dr. Ulrike Naumann and Moritz Klawitter, our cooperation partners from the Hertie-Institute in Tübingen, for their contributions and excellent work.

My gratitude extends to all member of the urology research group, present and past. Research always thrived in active cooperation and a friendly working environment. Many thanks to Klaus, for his in-depth knowledge of cloning and adenovirus biology. Thank you Sruthi, Charlene, Judith, Lena, Yuling and Florian for your insights and encouragement.

I want to thank Prof. Dr. Klaus-Peter Janssen for his mentorship and guidance during my whole project.

Lastly, my deepest appreciation goes towards my wife Daniela, my family and all my friends. Thank you for your love, trust and patience. You always supported me along the way and encouraged me to purse this goal of mine.

Contents

List of Figures

List of Supplementary Figures

List of Tables

List of Symbols and Abbreviations

µl	microliter
ml	milliliter
nm	nanometer
µm	micrometer
cm	centimeter
ng	nanogram
µg	microgram
mg	milligram
nM	nanomolar
µM	micromolar
mM	millimolar
M	molar
V	Volt
°C	degree Celsius
min	minute
h	hour

5-ALA ..... *5-aminolevulinic acid*

AB ..... *antibody*
ADP ..... *adenovirus death protein*
AED ..... *anti-epileptic drug*
ATF ..... *activating transcription factor*

BBB ..... *blood-brain barrier*
bcl-2 ..... *B-cell lymphoma 2*
BRD4 ..... *bromodomain-containing protein 4*
BSA ..... *bovine serum albuminum*

CAR ..... *coxsackie adenovirus receptor*
CDK ..... *cyclin-dependent kinas*
CDK4 ..... *cyclin dependent kinase 4*
CDK4/6i ..... *CDK4/6 inhibitor*
CDKN2A/B ..... *cyclin-dependent kinase inhibitor 2A/B*
CDKN2B-AS1 ..... *CDKN2B antisense RNA 1 intronic convserved region*
CPE ..... *cytopathic effects*
CR ..... *conserved region*

CRAd ..... *conditionally replicative adenoviruses*

CTLA-4 ..... *cytotoxic T-lymphocyte-associated protein 4*

Ctrl ..... *control*

dpi ..... *days post infection*

EGFR ..... *epidermal growth factor*

GBM ..... *glioblastoma multiforme*

Gy ..... *gray*

HAdV ..... *human adenoviruses*

HSV-1 ..... *herpes simplex virus, type 1*

ICD ..... *immunogenic cell death*

IDH ..... *isocitrate dehydrogenase*

LEE ..... *ribociclib LEE011*

LY ..... *abemaciclib LY2935219*

mBC/ABC ..... *negative metastatic or advanced breast cancer*

MDR1 ..... *multidrug resistance gene 1*

MGMT ..... *O6-methylguanine–DNA methyltransferase*

MLP ..... *major late promotor*

MOI ..... *multiplicity of infection*

MRI ..... *magnetic resonance imaging*

MRP1 ..... *multidrug resistance associated protein 1*

NF1 ..... *neurofibromatosis type 1*

ns ..... *not significant*

OS ..... *overall survival*

OV ..... *oncolytic virus*

p ..... *probability*

p53 ..... *tumor protein p53*

PBMC ..... *peripheral blood mononuclear cell*

PBS ..... *phosphate-buffered saline*

PCR ..... *polymerase chain reaction*

PD-1 ..... *programmed cell death protein 1*

PDGFRα ..... *platelet derived growth factor alpha*

PD-L1 ..... *programmed cell death protein 1 ligand 1*

PP2A ..... *protein phosphatase 2a*

pRb ..... *phosphorylated retinoblastoma pocket protein*

qPCR ..... *quantitative PCR*

Rb ..... *retinoblastoma pocket protein*

RGD ..... *arginyl-glycyl-aspartic acid*

RT ..... *radiotherapy*

RTK ..... receptor tyrosine kinase

S.D. ..... *standand deviation*

TBP ..... *TATA-Box binding protein*

TERT ..... telomerase reverse transcriptase

TMZ ..... *temozolomide*

TNF-α ..... *tumour-necrosis factor alpha*

TP ..... *terminal protein*

TSP ..... *tumor-specific promotor*

T-VEC ..... *talimogene laherparepvec*

VEGF ..... *vascular endothelial growth factor*

VTE ..... *venous thromboembolism*

YB-1 ..... *Y-box binding protein 1*

1. Introduction

Glioblastoma is one of the worst diagnoses for a patient to receive, being extremely fast growing, highly aggressive, challenging to resect and highly resistant to both radiation and chemotherapy. Therefore, the overall survival of glioblastoma remains nearly unchanged over the past decades and the standard therapy still revolves around resection, followed by heavy use of chemotherapeutics and radiotherapy. These features as well as challenges make the development of new therapeutic approaches an urgent need.

One of these new approaches for the treatment of solid tumors is virotherapy, discovered already in the 1950s, but only in the early 21 century, when the molecular mechanisms were better understood, the first oncolytic viruses were developed.

Our research is based on adenoviruses, a group of double stranded DNA viruses, well known for their capabilities to replicate in tumor cells. There are three commonly known systems leading to tumor selectivity, besides the usage of tumor specific promotors. Either mutations in the E1A or in the E1B gene sequence.

Our system is based on the transactivation capabilities of viral E1A13S. By deletion of 10 base pairs, the E1A13S protein expression is lost, thereby the virus has to depend on E1A12S protein. The expression of E1A12S proteins only allows replication in cells in the presence of nuclear YB-1, restricting the viral lifecycle on tumor cells.

In this thesis we compare different treatment options, ranging from the classical therapy regime, with chemotherapy and radiation to specific small molecule inhibitors, including a CDK4/6 inhibitor and an BRD4 inhibitor.

1.1. Glioblastoma multiforme (GBM)

Glioblastoma multiforme (GBM) is a malignant primary tumor of the brain, accounting for the most deaths among patients suffering from brain tumors (Wen, Weller et al. 2020). With an age adjusted incidence of 3.22/100.000 person it is relatively rare, predominates in patients over 55 years and men are more affected than women with a ratio of 1.5:1 (Ohgaki and Kleihues 2013, Louis, Perry et al. 2016, Sung, Ferlay et al. 2021). The 5-year survival rate is very poor with less than 5% and did not improve over the last decades (Tamimi and Juweid 2017). Interestingly in England an increase in GBM incidence was observed over the past 20 years (Philips, Henshaw et al. 2018,

Philips, Henshaw et al. 2018). Ionizing radiation is considered a risk factor, but non-ionizing radiation originating from cell phones, while being heavily investigated did not support any association with an increase in GBM. Interestingly allergies, atopic diseases and early life exposure to infections are associated with a decreased risk of brain tumor development (asthma by 30%) (Ostrom, Adel Fahmideh et al. 2019). While there are genetic factors associated with GBM, only 5% of cases are familial (Ranger, Patel et al. 2014). There are 11 specific glioblastoma single nucleotide polymorphisms (SNPs) known, including alterations in *TERT* (5p15.33), *EGFR* (7p11.2) and *CDKN2B-AS1* (9p21.3) (Melin, Barnholtz-Sloan et al. 2017). Furthermore, several genes and pathways are associated with different genetic subtypes of glioblastoma that were developed over the past decade (Phillips, Kharbanda et al. 2006, Verhaak, Hoadley et al. 2010). The three main groups consist of the proneural group, with expression of receptor tyrosine kinase (*RTK*), amplifications of cyclin dependent kinase 4 (*CDK4*) and platelet derived growth factor alpha (*PDGFRα*) and association with younger adulthood. The second group, showing the „classic gene expression“ with *EGFR* amplifications, homozygous loss of *CDKN2A/B.* The last group the mesenchymal like subgroup bears enriched neurofibromatosis type 1 (*NF1*) loss and increased tumor infiltration with macrophages. Although these groups are considered the main types of GBM several other subgroups and mixed entities do exist. All groups are accompanied with *TERT* promotor mutations (Wen, Weller et al. 2020, Ostrom, Edelson et al. 2021).

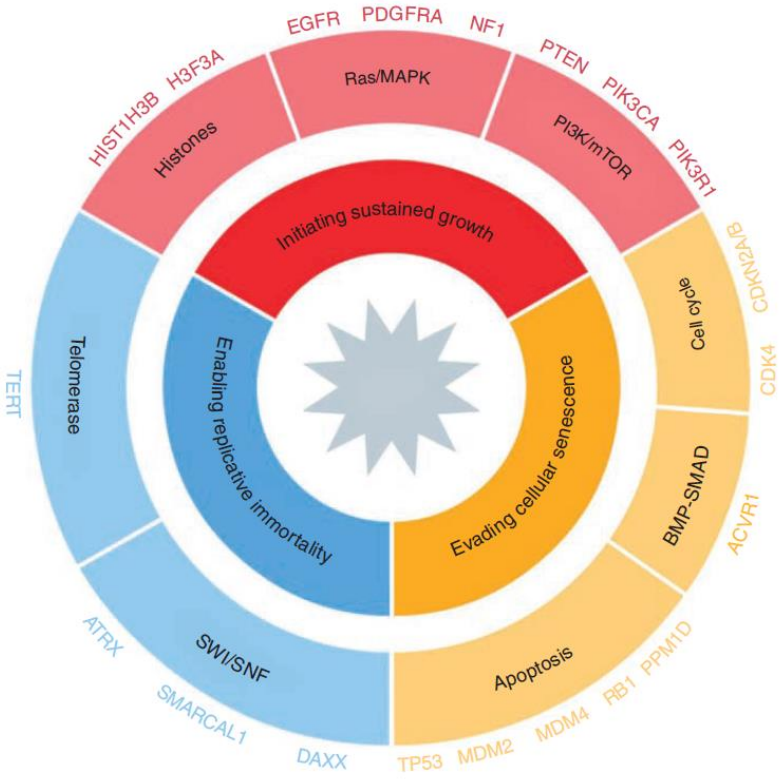

Figure 1: Somatic defects in three major processes characterise GBM. Initiating tumor growth, evading senescence and enabling replicative immortality are required for gliomagnesis, here shown with the most frequently altered genes and pathways. With permission from Neuro-Oncology 2021 (Wen, Weller et al. 2020).

1.1.1. Histopathology and predictive biomarkers

GBM is classified as a *de novo* grad IV tumor malignancy with astroglia appearance, microvascular proliferation and pseudopalisading necrosis. Besides the classical features, the absence of *IDH* mutations, and a combination of *TERT* promotor mutations, with loss of chromosome 7 and 10, or *EGFR* amplification is diagnosed as GBM, in the absence of histological features, based on similar patient survival and poor outcome. *IDH1/2* mutations allow by far the best prediction of patient survival. Originally discovered in 2008, and mostly occurring in low grade gliomas, *IDH1/2* mutations greatly benefit the patients prognosis and over 90% of mutations can be detected using a mutation specific immunohistochemistry screen against *IDH1-R132H* (Capper, Weißert et al. 2010, Cohen, Holmen et al. 2013). These mutations significantly increase the response to temozolomide, an alkylating agent, commonly used in GBM treatment (SongTao, Lei et al. 2012). In general, using next generation sequencing is common practise. Loss of *ATRX* is a second feature for

immunohistochemistry investigation commonly lost in tumor bearing *IDH1/2* mutations. In general, the terminology for *IHD1/2*-mutant glioblastoma was under discussion, based on the lower aggressiveness and better outcome of the patients and changed into IDH-mutant astrocytoma WHO grade IV (Brat, Aldape et al. 2020, Weller, van den Bent et al. 2021).

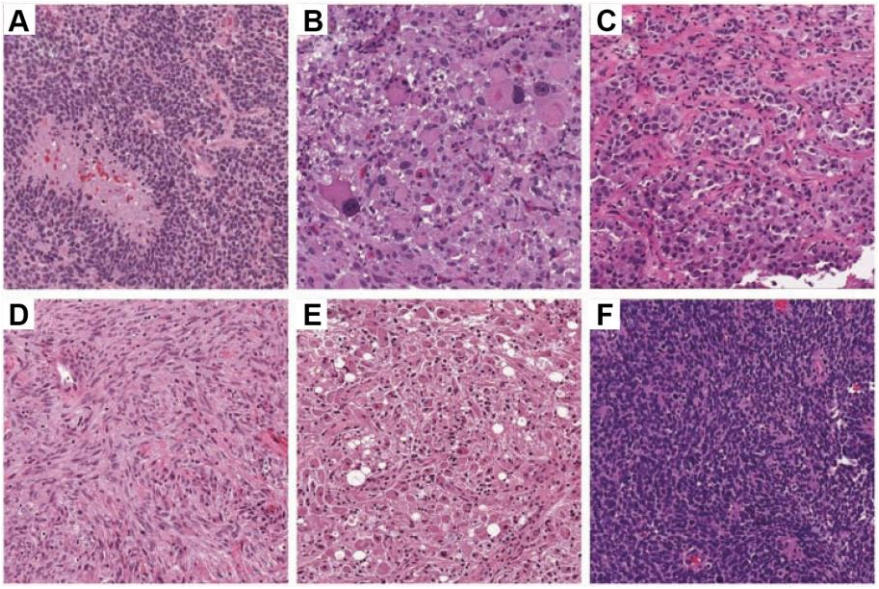

Figure 2: The many forms of GBM. (A) Classic GBM, with pseudopalisading necrosis and microvascular proliferation. (B) Giant cell GBM. (C) Epithelioid GBM with BRAF V600E. (D) Gliosarcoma. (E) Granular cell GBM. (F) Small cell GBM. All images are from the UPMC Neuropathology Virtual Slide Database, 200x magnification. With permission from Neuro-Oncology 2021 (Wen, Weller et al. 2020)

Genomic profiling of GBM has improved the understanding of the molecular mechanisms driving tumor progression, but so far, no direct genotype specific treatment could be found. The one predictive biomarker for GBM is the epigenetic silencing of the O^6-methylguanine–DNA methyltransferase (*MGMT*), leading to an improved outcome for the treatment with TMZ (Hegi, Diserens et al. 2005). There are several methods used to identify the methylation status of *MGMT*, most commonly used is a methylation specific-PCR, but pyrosequencing was shown to be more effective (Quillien, Lavenu et al. 2012). The usage of immunohistochemistry to investigate MGMT promotor methylation is unreliable and should therefore not be used (Wick, Weller et al. 2014).

1.1.2. Diagnosis and Imaging

Glioblastoma patients commonly present for the first time with neurological symptoms. New onset epilepsy, neurocognitive impairment and intercranial pressure are all known symptoms, based on the rapid tumor growth, infiltrating and displacing brain tissue (Weller, Van Den Bent et al. 2017). The gold standard for diagnosis is contrast-enhanced magnetic resonance imaging (MRI), typically showing a necrotic mass and in the surrounding a non-enhanced signal abnormality of edema and infiltrative tumor (Wen, Weller et al. 2020). Other common features include cystic changes and haemorrhage (Ly, Wen et al. 2020).

1.1.3. Treatment and Prognosis

The treatment of GBM has to be split up, into managing the symptoms and treating the underlying cause.

Treating symptoms is important not only for newly diagnosed patients, helping them battle the disease, but also as a supportive care for terminal ill patients. Dexamethasone is used to treat peritumoral vasogenic edemas, relieving neurologic deficits and intercranial pressure, but the usage of corticosteroids is currently debated, the side effects at high dosages and continued dosage duration could worsen the patients outcome (Cenciarini, Valentino et al. 2019). For patients showing seizures, before or during the disease course, anti-epileptic drugs (AEDs) are used, but there is no benefit for giving them prophylactically.

Venous thromboembolism (VTE) is a high risk in patients with GBM, making the use of anticoagulants important, even though the usage is not so well studied. But intertumoral hemorrhages occur regular following tumor resection, and are contraindications to anticoagulation agents (Yust-Katz, Mandel et al. 2015, Muster and Gary 2020). 91% of all patients show cognitive deficits, before treatment. Using acetylcholinesterase inhibitors or psychostimulants can improve the patients life quality, reducing fatigue, sleep disturbance as well as improving cognitive functions (Tucha, Smely et al. 2000).

Other important factors relevant for all cancer treatments are physical activities and a healthy diet. Giving the patient also the possibility to interact with his illness and a sense of self determination. The communication with the patients, informing them about the status of the illness, the progression, treatment options and as well

achievable goals in progression free survival and palliative care remain the most important topic (Fritz, Dirven et al. 2016). The patients should at all times be involved, giving them the chance to cope with all issues, concerning their life.

The standard therapy for newly diagnosed glioblastoma remains unchanged consisting of surgery, radiotherapy and temozolomide (TMZ) treatment (Wen, Weller et al. 2020). Not resulting in cure but increasing the overall survival (OS) significantly. The recurrence rate is over 90% with a median interval of 7 months and at this point the functional status of the patients is typically poor resulting in limited treatment options (Stupp 2005, Weller, Cloughesy et al. 2013). The tumor can again be resected and re-challenged with TMZ as well as radiation is possible, otherwise palliative best supportive care is applied. For all patients, with primary tumors or recurrent GBM, clinical trials are the treatment of choice, using different approaches, in the hope of benefiting both the patients and improving the treatment regime in general.

The steps of treatment have to be tailored for each individual patient's needs, based on risk factors, prognostic impact and patient status. The first step is a maximal safe gross total resection of the enhancing solid tumor mass (Ellingson, Abrey et al. 2018). To visualize the tumor 5-aminolevulinic acid (5-ALA) is used allowing the surgeon an improved resection and maximizing the extend of resection (Stummer, Novotny et al. 2000). But the risk of further permanent neurologic deficits remains high, therefore the prevention is more important than the removal of the complete tumor (Gulati, Jakola et al. 2011). Removed tumor mass is used for histological diagnosis and grading, as well as specific staining for *IDH1/2* mutations and analysis of the *MGMT* promotor methylation status (Eigenbrod, Trabold et al. 2014). Both resemble important factors for the following treatment. Resection alone never leads to a cure of GBM, and therefore is always accompanied by further treatment steps.

Following resection, the patient is treated with a combination of radiotherapy and concurrent TMZ treatment. The effect of TMZ treatment is predicted by the methylation status of the *MGMT* promotor. Only tumors with methylated MGMT promotor show strong response to TMZ, therefore TMZ treatment can be withheld for patients with MGMT unmethylated tumors. TMZ treatment (75mg/m^2/day x 6 weeks) is given with concurrent RT (60Gy, 30 x 2Gy fractions) and adjuvant TMZ treatment (150-200 mg/m^2/day x 5 days for six 28-day cycles) (Wen, Weller et al. 2020). In elderly patients (defined as over 65 years), hypo fractionated RT (40Gy in 15 fractions) is used to,

since these patients already show a worse prognosis and have a lower tolerance for toxicity (Roa, Brasher et al. 2004).

Given the horrible prognosis and fast progression, other therapy approaches are under heavy investigation. The usage of nitrosoureas (preferably lomustine), antibodies targeting the vascular endothelial growth factor (VEGF), has so far not shown significant benefits (Wick, Gorlia et al. 2017). Immunotherapy and molecular targeting are further treatment options, alone or in combination with stand of care treatment, but more research has to be conducted (Lim, Xia et al. 2018, Le Rhun, Preusser et al. 2019, Birzu, French et al. 2021). Our work focused on the usage of virotherapy and approach that is currently analysed, using different virus families and constructs (Stavrakaki, Dirven et al. 2021).

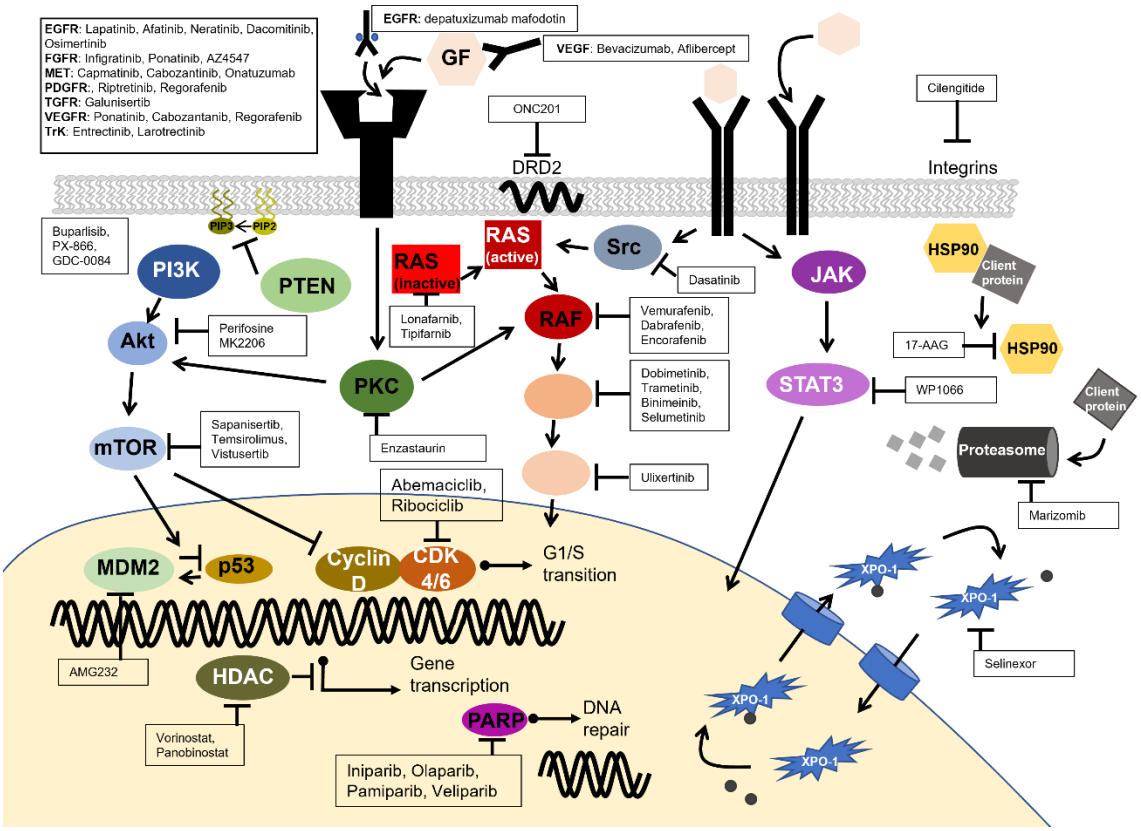

Figure 3: Selected recently completed or ongoing trials with targeted molecular therapies. CDK = cyclin-dependent kinase; EGF = epidermal growth factor; EGFR = epidermal growth factor receptor; FGFR = fibroblast growth factor receptor; GF = growth factor; HDAC = histone deacetylase; HSP = heat shock protein; MDM2 = murine double minute 2; mTOR = mammalian target of rapamycin; PARP = poly(ADP-ribose) polymerase; PDGFR = platelet derived growth factor receptor; PKC = protein kinase C; RTK = receptor tyrosine kinase; TGF-β = transforming growth factor beta; TGFβR = transforming growth factor beta receptor; TrK = tropomyosin receptor kinase; VEGF = vascular endothelial growth factor; VEGFR = vascular endothelial growth factor receptor; XPO1 = exportin 1. With permission from Neuro-Oncology 2021 (Wen, Weller et al. 2020)

1.2. Biology of adenovirus and oncolytic virotherapy

Adenoviruses are a group of linear double-stranded nonenveloped DNA viruses belonging to the family of adenoviridae and the genus mastadenovirus (Lynch III and Kajon 2016). The family of adenoviridae currently harbours besides mastadenovirus, 5 more genera and a total of 86 species. The genera mastadenovirus currently consists of 51 species, found in different mammals, ranging from bats, sheep and mice, apes as well as all human mastadenoviruses group A-G (HAdV-A through HAdV-G) (ICTV,

Virus Taxonomy, Adenoviridae, 2020). In general infections with an adenovirus leads to respiratory diseases, gastroenteritis or infections of the eye (adenoviral keratoconjunctivitis) (Russell 2009, Jhanji, Chan et al. 2015).

1.2.1. Human adenoviruses

Human adenoviruses (HAdV) were classified into seven species and historically defined as serotypes, based on their ability for agglutinate erythrocytes of humans, rats or monkeys and depending on serological cross-neutralisation (Hoeben and Uil 2013, Dhingra, Hage et al. 2019). Now genome sequencing, is the method of choice to define new adenovirus types. There are currently 104 HAdV genotypes known (hadvwg, 2021). Different species tropisms correlate with clinical properties, species B1, C and E cause respiratory disease, in contrast species B, D and E infect mainly the eye (Russell 2009). But infections of species F are responsible for gastrointestinal infections and species B2 leads to infections of the kidney and urinary tract (Russell 2009). For virotherapeutic approaches vectors are based on species C, type 2 and 5 (Braithwaite and Russell 2001).

1.2.2. Infection and replication

The first viral component to interact with the cell, during the infection is the fibre protein. Depending on the tropism, this can occur in the respiratory or gastrointestinal tract as well as in the oropharynx or conjunctiva. The major receptor for adenoviral infection is the coxsackie adenovirus receptor (CAR), belonging to the immunoglobulin superfamily, involved in the formation of tight junctions. Upon attachment of the Fibre protein to the cellular CAR receptor, the viral penton base protein located below the Fibre spikes, bind cellular αvβ3/αvβ5 integrins via their RGD motif. This leads to rapid viral internalization via clathrin-coated vesicles and endosomes (Russell 2009). The viral escape into the cytosol, using an acidic pH to disrupt the endosomes (Blumenthal, Seth et al. 1986). The particles are transported along microtubules to the nucleus using dynein/dynactin, where the virus docks via its hexon shell to a nuclear pore complex receptor CAN/Nup214 (Meier and Greber 2004, Cassany, Ragues et al. 2015). Now the viral core consisting of DNA and DNA associated proteins is released into the cellular nucleus and viral DNA gene expression and replication takes place (Russell 2009). The virus now alters its host to ensure perfect condition for viral gene expression and replication, via recruitment of cellular transcription factors, alteration of the cell

cycle status and epigenetic changes (Braithwaite and Russell 2001, Ben-Israel and Kleinberger 2002, Lynch, Gooding et al. 2019).

1.2.3. The viral genome organisation and viral proteins

Adenovirus particles are of icosahedral shape and have no envelope, they enclose a quasi-circular double stranded DNA genome with an approximate length of 26-45 kb. Each capsid consists of several minor proteins, VI, VIII, IX, IIIa, IVa2 and the three major capsid proteins hexon (II), penton base (III) and a knobbed fibre (IV) (Russell 2000). Each capsid hold 240 hexons grouped into four types, H1 to H4, based on their environment. The penton capsomere consists of penton base and a non-covalently bound fibre and is essential for the viral infection (Russell 2009). In the capsid core the dsDNA is covalently attached to the terminal protein (TP) at its 5´ termini as well as associated with the three core proteins V, VII, and Mu(µ) (Russell 2009).

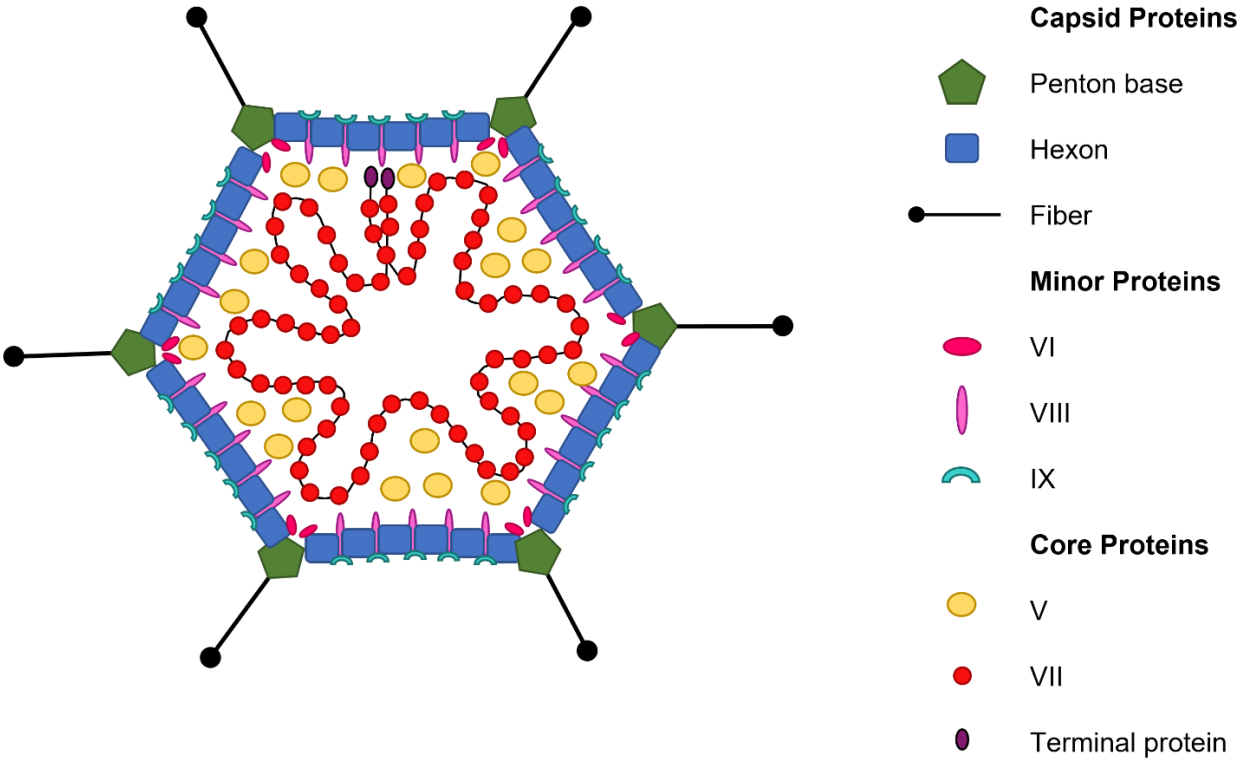

Figure 4: The adenovirus structure. A schematic overview of the icosahedral viral particle structure highlighting important structural proteins, like hexon, penton base and fibre, as well as the dsDNA stabilized by core proteins and the terminal protein. Figure adapted from (Russell 2009).

The linear dsDNA adenoviral genome is flanked by two inverted terminal repeats, these function as the origin of replication. The transcription follows a complex pattern with

eight transcription units from both strands, accompanied by two virus associated RNAs, respectively transcribed by RNA polymerase II and III. Due to alternative splicing and multiple polyadenylation sites, each transcription unit can act as a blueprint for several transcripts and therefore proteins (Braithwaite and Russell 2001).

Besides the complex transcription pattern the adenoviral transcriptions a highly organized temporal course, divided into three major groups (early, intermediate and late genes) (Braithwaite and Russell 2001). While the early genes E1A, E1B, E3, E4 and E2, transcribed from five different promotors are essential for the regulation of viral gene expression and DNA replication, the intermediate genes IX and IVa2 encode for minor components of the viral capsid, first expressed in lower levels at an early timepoint of infection, increasing over time. All five late genes L1-L5 are transcribed from the major late promotor (MLP) and encode for the viral capsid proteins (Braithwaite and Russell 2001).

E1A region

The E1A gene is the first transcribed gene located at the left side of the viral genome. If has a unique promotor structure, composed of the inverted terminal repeats and enhancer region as well as several binding sites for cellular transcription factors, e.g. E2F1 (Berk 1986).

The role of E1A protein in stimulating the transcription of other viral promotors makes it crucial for conductive viral gene expression during the early stages of replication (Braithwaite and Russell 2001). But the role of E1A is not limited to viral transactivation, but interactions with cellular promotors, in both activating and repressing manner lead to optimal conditions for viral replication. There are five different proteins encoded by the E1A gene (9S, 10S, 11S, 12S and 13S) produced by alternative splicing. The most important transcripts are E1A12S and E1A13S (Braithwaite and Russell 2001). There are four conserved regions (CR) located within the E1A transcript. E1A13S in the only splicing variant encoding all four conserved regions (CR1/2/3/4), E1A12S only shares three (CR1/2/4) (Avvakumov, Kajon et al. 2004, Akaike, Nakane et al. 2021). These conserved regions allow the interaction with other transcriptions factors. Interaction via the CR2 domain to the retinoblastoma pocket protein (Rb) leads to the release of E2Fs, thereby promoting cell cycle progression and S-phase induction (Nakajima, Masuda-Murata et al. 1987, Ben-Israel and Kleinberger 2002). Besides the cellular S-phase

induction targeting the Rb/E2F1 complex followed by release of E2F1, enables the binding of E2F1 at the E2-early promotor, increasing viral protein expression (Kovesdi, Reichel et al. 1986, Zajchowski, Boeuf et al. 1987, Bandara and La Thangue 1991). Furthermore E1A can directly interact with E2F1 via DP-1 binding (Pelka, Miller et al. 2011). But several publications also show the stabilization of the Rb/E2F complex via E1A, supposedly to decrease the cellular apoptotic response to the viral infection (Nemajerova, Talos et al. 2008, Seifried, Talluri et al. 2008). The CR3 domain of E1A13S play a crucial role in the transactivation of cellular and viral promotors like the E2 early promotor, already in the early stages of viral infection ensuring viral gene expression and replication (Ablack, Pelka et al. 2010). The CR3 region of the E1A protein recruits p300 to the E4 promotor (Pelka, Ablack et al. 2009).

All these factors resulted in the development of different E1A mutated viral constructs for cancer therapy. CR2 deletion constructs like delta24 and dl-922-947, which cannot bind to the Rb protein, thereby being unable to induce S-phase entry and are only able to replicate in cells with mutated Rb (Fueyo, Gomez-Manzano et al. 2000, Heise, Hermiston et al. 2000). Deleting the CR3 region leads to a viral construct depending on the much weaker transcriptional activity of E1A12S (Rognoni, Widmaier et al. 2009).

E1B region

The E1B gene is located on the left side of the viral genome near E1A. Its promotor possesses several binding sites for transcription factors, within close proximity allowing interaction with one another (Berk 1986). But the promotor does not contain any E2F binding sites (Kovesdi, Reichel et al. 1987).

Two proteins are encoded by E1B and produced via alternative splicing, namely E1B19k and E1B55k. E1B19k, expressed strongly at late times during infection, belongs to the B-cell lymphoma 2 (bcl-2) family inhibits apoptosis via p53 and other cell death proteins (Braithwaite and Russell 2001). E1B55k on the other hand, forms a complex with the viral E4orf6 proteins and is serving several purposes. It is important for the transportation of late viral mRNAs to the ribosomes as wells as binding p53, thereby leading to p53 degradation (Braithwaite and Russell 2001). Furthermore E1B55k-E4orf6 allows the translocation of Y-box binding protein 1 (YB-1) from the cytosol into the nucleus, which acts as a transcription factor for the E2-late promotor, bearing three YB-1 binding sites (Holm, Bergmann et al. 2002, Holm, Lage et al. 2004).

The complex of E1B55k and E4orf6 act as a stabilizer for E1A, amplifying the activation of E2F1, increasing DNA replication and gene expression (Dallaire, Schreiner et al. 2015).

E2 region

The E2 region is one of two early genes transcribed on the opposite, lower DNA strand leftwards. It possesses two promotors, E2-early and E2-late, that show as their name implies activity at different timepoint during infection. The E2-early promotor is active during early transcription, as well as at later timepoint, but its activity is overshadowed by the E2-late promotor in later stages of viral infection. The E2-early promotor contains two E2F1 binding sites, like the E1A promotor, the binding of a transcription complex consisting of E2F1, TATA-Box binding protein (TBP) and activating transcription factor (ATF) activates the promotor (Seifried, Talluri et al. 2008). Both E4orf6/7 and E1A boost the activity of the E2-early promotor, 5 to 21-fold respectively (Swaminathan and Thimmapaya 1996). The E2-late promotor bears three YB-1 promotor binding sites using cellular YB-1 for its activation (Holm, Bergmann et al. 2002).

The products of the E2-gene are of utmost importance for viral DNA synthesis, like DNA polymerase, primase or the DNA binding protein (DBP.E2A). The E2A protein binds single stranded DNA, active during viral replication. E2B protein serves as DNA polymerase as well as the primer for the initiation of DNA synthesis (Braithwaite and Russell 2001).

E3 region

The E3 region is located between the late protein regions L4 and L5 on the upper stand of the adenoviral genome. Its promotor region overlaps with the E2-early promotor located on the lower DNA strand continuing upstream. While not containing any E2F binding sites, this close proximity to the E2-early promotor elements and transcription factors could affect the E3 transcription (Berk 1986, Kovesdi, Reichel et al. 1987).

E3 proteins modulate the anti-viral immune response of the host, making it an attractive genome area for virotherapy, since deletion of this region leads to an increased inflammatory response (Braithwaite and Russell 2001, Rognoni, Widmaier et al. 2009). There are seven proteins encoded by the E3 region (Lichtenstein, Toth et al. 2004). For example the 14.7 protein prevents tumour-necrosis factor alpha (TNF-α) induced

apoptosis and the T-cell induced apoptosis by downregulation of immunodominant antigens (Braithwaite and Russell 2001). The E3gp19k protein sequestrates MHC class I molecules inside the endoplasmic reticulum (ER) by binding of MHC class I molecules and formation of a complex, disallowing the presentation of antigen-peptides on the cell surface, leading to a reduction of cell killing via cytotoxic T cells specific for adenovirus (Lichtenstein, Toth et al. 2004). In the end of the viral replication cycle host cell lysis is necessary to allow the release of the virions, this step is induced by another E3 protein, namely the adenovirus death protein (ADP) (Lichtenstein, Toth et al. 2004).

E4 region

Besides E2 of all early genes only E4 is transcribed on the lower DNA strand, located on the far-right side. Like E3 the promotor region of E4 does not contain E2F binding sites, but is activated by E1A induced transcription factors p50E4F and ATF (Täuber and Dobner 2001). The activity of the promotor is negatively regulated by E2A and a feedback loop of the E4orf4 protein phosphatase 2a (PP2A) complex, leading to the dephosphorylation of transcription factors like E1A (Täuber and Dobner 2001).

The E4 proteins, produced by alternative splicing are regulators of viral DNA synthesis, mRNA shuttling, cellular protein synthesis and cell death (Braithwaite and Russell 2001). Many functions have already been described above. E4orf4 leads in a complex with PP2A to the dephosphorylation of E1A, thereby reducing E1A regulated gene expression (Täuber and Dobner 2001), but is as well responsible for the induction of p53 or viral protein independent cell death (Braithwaite and Russell 2001). The E4orf6-E1B55K complex play an important role in the regulation of viral gene expression, viral DNA replication and cell death (Braithwaite and Russell 2001). E2 gene expression is enhanced by the formation of different complexes with E4orf6/7, stabilizing E2F1 (Braithwaite and Russell 2001).

Table 1: Summary of important early viral proteins and their function on viral and cellular level.

Protein	Function
E1A	Transactivation of viral gene promotors
E1B19k	Inhibition of Bcl-2 mediated cell death
E1B55k/E4orf6	Inhibition of p53 mediated cell cycle arrest, contribution to viral replication
E1B55k/E5orf6/7	Stabilization of E2F1 for E2 gene expression
E2A, E2B	Replication machinery for viral DNA
E3 ADP	Initiation of cell lysis for virion release
E3gp19k	Complexing of MHC I class molecules to inhibit antigen presentation
E4orf4	Induction of p53 independent apoptosis

Intermediate genes

The two promotors IX and IVa2 located on the upper and lower DNA strand respectively, regulate the transcription of the intermediate genes. They become active when the viral DNA replication has started (Berk 1986). The IX protein has both structural and transcriptional roles, it is incorporated into the viral capsid, but acts as an transcription factor for the MLP (Lutz, Rosa-Calatrava et al. 1997). The IV2a protein acts as well as a transcription factor for the MLP as well as interacting with the L1 52/55k protein, resulting in viral DNA packaging (Tribouley, Lutz et al. 1994, Zhang and Imperiale 2003).

Late genes

All late proteins are controlled by the MLP, which does not possess any E2F1 binding sites. It is located on the upper DNA strand and the transcripts include all 5 major late proteins L1 to L5, encoding for viral capsid proteins like Hexon (L3) or Fibre (L5) (Braithwaite and Russell 2001, Young 2003).

1.3. Oncolytic virotherapy

The usage of viruses as potential therapeutics has increased over the last decades, with deeper understanding of viral biology. There are two strategies for viral therapeutics, either the usage as vectors for gene therapy or as oncolytic viruses. For gene therapy non replicating viruses are used, acting as shuttles, whereas for oncolytic virotherapy, either wild-type or genetically engineered viruses, targeting tumor cells while leaving healthy cells unharmed, are the system of choice (Chaurasiya, Fong et al. 2021).While the idea of using viruses to actively destroy tumor cells already dates back into the 1950s (Moore 1952), to this date there is only one FDA approved oncolytic virus, Talimogene laherparepvec (T-VEC). T-VEC is an attenuated herpes simplex virus, type 1 (HSV-1), adapted for both selective tumor cell replication and the induction of host immunity (Rehman, Silk et al. 2016). Oncolytic virotherapy is tested with a huge variety of different viral families, both DNA and RNA viruses, including adenoviridae, poxviridae, herpesviridae, rhabdoviridae, reoviridae, paramyxoviridae, parvoviridae and picornaviridae (Vähä-Koskela, Heikkilä et al. 2007, Chaurasiya, Fong et al. 2021).

1.3.1. History and Concept

Viruses have been used as therapeutic agents, like vaccines, already centuries ago (Pasteur 1885), and stating in the early 1900s several cases of cancer remission in context of viral infection were observed (Choi, O'Leary et al. 2016). After the observation of this effect, the first clinical trials followed, using different viruses for the treatment of cancer. But even though brief remission was observed in some patients the side effects were severe, leading to the patient's death by viral causes, via hepatitis or neuro-encephalitis, or anamnestic response of the immune system, allowing cancer progression (Choi, O'Leary et al. 2016).

While these results showed the potential of oncolytic virotherapy, the side effects made improvements of both cancer cell selectivity and efficacy necessary. In the 1950s the development of cell culture techniques and animal models, increased virus research and deepened the molecular understanding, further clinical trials followed, ending unsatisfactory. This led to a halt in research until in the 1990s the development of tools to manipulate the viral genome, allowed improvements for selectivity and decreased toxicity (Choi, O'Leary et al. 2016). This led to the development of new viral constructs

with ONYX-015, being the first adenoviral construct in a phase I clinical trial, and H101 becoming the first OV approved for cancer treatment (Choi, O'Leary et al. 2016).

While the concept to aim viruses against cancer cells, leading to cancer cell lysis, holds true to this point. Recent developments shifted the focus to the immune system of the patient. Harnessing the immunogenicity of viral constructs, like adenoviruses, release of tumor antigens via cell lysis, induces local inflammation and thereby an antitumor immune response (Sato-Dahlman, Roach et al. 2020). This "priming", with increased infiltration of immune cells, alters the tumor microenvironment, from "cold" to "hot" (LaRocca and Warner 2018).

Using viruses like adenovirus, activates the immune system even prior to infection, both toll like receptors or the complement system, directly react upon binding of virions and lead to the release of proinflammatory cytokines (Supplementary Figure 1). When cells are infected more cellular anti-viral response pathways are tiggered. When tumor cells are lysed to release freshly generated virions, the anti-viral response leads to more immune cell infiltration of the tumor altering the tumor microenvironment (Farrera-Sal, Moya-Borrego et al. 2021).

To improve the immunity against tumor antigens several methods can be used. Fractionated dosing allows a broader intra tumoral tissue distribution of the agent, thereby increasing the area of tumor lysis and microenvironmental change. Another idea is applying repeated cycles of the viral agent to increase the systemic response triggered by viral infection (Supplementary Figure 2). One issue here is the production of anti-viral antibodies, hindering the effectiveness of the viral construct. Therefore viral constructs are mostly applied in a combinational therapy, using chemotherapeutics, small molecule inhibitors or anti-immune-checkpoint antibodies (Thangamathesvaran, Shah et al. 2018, Farrera-Sal, Moya-Borrego et al. 2021).

1.3.2. Overview about current clinical trials

There are currently over 110 studies using oncolytic virus therapy for cancer therapy (clinicaltrials.gov, 2021), with over 40 active trials. Studies include both the usage of oncolytic viruses in a mono therapeutic approach, as well as combining OV with different therapeutic agents (for review (Chaurasiya, Fong et al. 2021)). Here standard chemotherapeutic drugs are used as well as targeted therapy approaches. Current studies focus on herpes simplex virus-1 (HSV-1), like T-VEC; vaccinia virus (VACV)

constructs like Pexa-Vec and adenovirus constructs (further broken down in the next chapter).

1.4. Oncolytic adenoviruses

One major class of viruses used for virotherapy are adenoviruses. They have a large packing capacity, well known infection route, can infect both dividing and non-dividing cells and do not integrate into the host genome. These factors together with only mild symptoms make them a valuable tool for both gene therapy and virotherapy (Gonzalez-Pastor, Goedegebuure et al. 2021). The most commonly used adenovirus serotypes are 2 and 5, well characterised and used for the generation of conditionally replicative adenoviruses (CRAd). There are two strategies used to achieve tumor selectivity. Either the usage of cancer- or tumor-specific promotors (TSP) or deletion if E1A or E1B genes preventing replication in healthy cells, depending on alterations in tumor cells (Gonzalez-Pastor, Goedegebuure et al. 2021). TSPs are used for both gene delivery as well as oncolytic virotherapy, inserting cancer or tumor-specific promotors before the E1A gene, couples the expression of E1A, fundamental for the initiation of AdV replication, to the expression of a selected tumor protein. As an example Telomelysin (OBP-401) needs the expression of human telomerase reverse transcriptase (hTERT) for effective replication (Montaño-Samaniego, Bravo-Estupiñan et al. 2020). This tumor specificity comes with the disadvantage, that while some proteins are highly overexpressed in certain tumors, others tumors lack these proteins, making the vector useless in other entities. The deletion of E1A or E1B parts, depends on the malfunction of the cellular machinery. Deletion of 24 bp in the CR2 region of E1A (dl922-947 or delta24) hinders the ability of E1A to bind the Rb protein, leading to a virus dependency of mutated Rb (Whyte, Ruley et al. 1988). This leads to the viral incapability to release E1A in normal cells, resulting in no viral replication. Only in cells with deregulated or mutated pRB, E2F promotes the viral transcription (Fueyo, Gomez-Manzano et al. 2000). Deletion of the E1B-55k gene (Onyx-015) hinders the inactivation o p53, thereby allowing replication only in cells with mutated p53 status (Gonzalez-Pastor, Goedegebuure et al. 2021). However, this concept has been questioned by several research groups, since the tumor selectivity seems to be limited (Harada and Berk 1999, O'Shea, Johnson et al. 2004).

XVir-N-31

We developed an adenoviral construct bearing several deletion sites as well as one addition, making XVir-N-31 cancer cell specific, more inflammatory and increasing its general infectivity. XVir-N-31 was first described in 2011 by (Holzmüller, Mantwill et al. 2011). By deletion of 10bp in the CR3 domain in the E1A gene, no E1A13S can be formed. Since E1A13S is the main transactivator of viral gene expression via the E2-early promotor, the virus depends on the E2-late promotor. The E2-late promotor bears three YB-1 binding sites. YB-1 is relocated from the cytoplasm to the nucleus upon adenoviral infection by the E1B55k/E4orf6 complex. By deleting E1A13S, the transactivation on E1B55k and E4orf6 is greatly reduced. Consequently, cytoplasmic YB-1 is not shuttled into the nucleus, leading to the dependency of nuclear YB-1 for effective viral replication (Holm, Bergmann et al. 2002, Holm, Lage et al. 2004). Additionally, in XVir-N-31 the E1B19k gene is deleted to allow cellular apoptosis. In the E3 region of XVir-N-31 2681 bp were deleted, increasing the host´s inflammatory response as well as allowing the construction of further viruses with additional transgene expression like an anti-PD-L1 antibody (Lichtenegger, Koll et al. 2019). Besides deletions, one addition was given to XVir-N-31, encoding the integrin-binding arginyl-glycyl-aspartic acid (RGD) motif in its Fibre knob, enhancing cell tropism independent of CAR expression (Holzmüller, Mantwill et al. 2011).

1.5. Enhancing oncolytic virotherapy

While oncolytic virotherapy approaches show promising results preclinically, in vivo efficacy remains low. Improving the virotherapy therefore remains an urgent need. As described above the usage of transgene expression in the context of viral vectors is one option. In adenoviruses the E1 and E3 region are used, for cytotoxic, anti-angiogenic or immunostimulatory protein expression (Chaurasiya, Chen et al. 2018, Chaurasiya, Fong et al. 2021). Increasing the viral uptake by improved tropism via e.g., RGD expression on the Fibre knob (XVir-N-31), is another opportunity. All these options are based on alterations within the virus, but the next chapter will highlight the combination of oncolytic virotherapy with clinical anti-tumor agents, including radiation, chemotherapy, immunotherapy, or small molecule inhibitors.

1.5.1. Enhancing viral therapy with standard chemotherapeutic agents and radiation

Chemotherapy and radiation are both fundamentally used methods for the treatment of cancers (Bieler, Mantwill et al. 2008, Harrington, Freeman et al. 2019, Sato-Dahlman, Roach et al. 2020). Chemotherapeutics include mitotic inhibitors, antibiotics, platine salts, alkylating agents and antimetabolites. Crosslinking cellular DNA, leads to cell cycle arrest and apoptosis in cells, but this effect is not linked to tumor cells, as normal cells are similarly affected, leading to severe side effects (Bressy and Benihoud 2014). Interestingly it was already shown that the combination of oncolytic virotherapy with chemotherapeutics could lead to an increase in viral replication and tumor cell death. Even though the molecular basis of these effects were not well investigated or understood (Bressy and Benihoud 2014).

Our group has already shown the influence of chemotherapeutics and radiation on the viral replication and production of adenoviruses and the effects on tumor cell survival. In 2006 we published data investigating the effects of two chemotherapeutic agents, irinotecan and trichostatin A on virotherapy (Bieler, Mantwill et al. 2006). The topoisomerase I inhibitor irinotecan leads to DNA breaks, this leads to the translocation of YB-1 into the nucleus as well as the activation of the Akt pathway, again activating YB-1 further increasing the nuclear YB-1 fraction. This accumulated nuclear YB-1 can bind at viral E2 late promotor promoting viral replication. Trichostan A, as a histone deacetylase inhibitor, increased the toxicity of irinotecan. As a triple therapy this approach of stronger replication and cell lysis was observed.

Interestingly YB-1 plays an important role in the chemoresistance of cancer cells. So do ATP-binding cassette transporters, like multidrug resistance gene 1 (MDR1) and multidrug resistance associated protein 1 (MRP1) correlate not only with chemotherapy resistance but are also activated by YB-1 (Mantwill, Köhler-Vargas et al. 2006). Facilitating the use of nuclear YB-1 at the E2 late promotor hinders its ability to activate both MDR1 and MRP1 genes, resulting in a downregulation of MDR1 and MRP1. This results in a resensibilisation of the tumor cells to chemotherapeutic agents, improving their effectiveness as well as synergistically improving viral replication and cell killing (Rognoni, Widmaier et al. 2009).

Besides chemotherapy the effects of radiation on viral cell killing have been investigated in our lab. Radiotherapy is capable of increasing the amount of nuclear

YB-1, again leading to enhanced viral replication and higher viral yield, both *in vitro* and *in vivo* (Bieler, Mantwill et al. 2008).

Interestingly besides cell lysis, we could as well observe an anti-angiogenesis effect of our viral constructs, compared to using wildtype adenovirus typ 5 (Holzmüller, Mantwill et al. 2011). The infection with XVir-N-31 resulted shows in contrast to ADWT also an increase in immunogenic cell death, releasing damage-associated molecular patterns (DAMPs) like high mobility group protein 1 (HMGB1) as well as exosomal 70 kilodalton heat shock proteins (Hsp70) (Lichtenegger, Koll et al. 2019).

1.5.2. Targeted therapies and immunotherapy

While chemotherapeutics and radiation affect the cells in a general manner, activating several pathways at once, targeted therapies try to inhibit specific highly activated pathways in tumor cells (Bressy and Benihoud 2014). Early examples of targeted therapies involve the usage of mammalian target of rapamycin (mTOR) inhibitors like RAD011 or histone deacetylases like Valporic acid or Trichostatin A. While the effect on viral replication was not always observed or even tested, significantly reduced tumor growth was observed, compared to the single treatments.

The usage of monoclonal antibodies directed against epithelial growth factor receptor (EGFR), cetuximab or anti -vascular endothelial growth factor (VEGF) antibody bevacizumab not always resulted in effects when analysing the combination *in vitro*. Nonetheless promising outcomes were observed *in vivo* (Bressy and Benihoud 2014).

Recent studies focused on the usage of immune checkpoint inhibitors (ICI) in combination with viral therapies. In general, three major inhibitor classes are in use namely cytotoxic T-lymphocyte-associated protein 4 (CTLA-4), programmed cell death protein 1 (PD-1) and programmed cell death protein 1 ligand 1 (PD-L1) inhibitors (Thangamathesvaran, Shah et al. 2018, Farrera-Sal, Moya-Borrego et al. 2021).

CTLA-4, acts as a down regulator of the immune response and is located on T cells. Upon binding to the B7 receptor on antigen presenting cells (APC) a tyrosine kinase signal cascade is triggered resulting in lower T cell response to stimulatory signals (Thangamathesvaran, Shah et al. 2018). This interaction as well hinders the binding of B7 to CD28 and loosening the interaction of the T cell with the APCs. Inhibiting CTLA-4 via antibodies like ipilimumab, increases T cell proliferation, T cell survival and the production of cytokines (Thangamathesvaran, Shah et al. 2018). The PD-1 receptor

as well with two ligands of the B7 family, namely PD-L1 and PD-L2. Binding leads to the inhibition of T cell proliferation as well as downregulated inflammatory marker expression. Both PD-1 and its ligands are prominent targets for ICD, to alter the tumor microenvironment benefiting tumor suppression (Thangamathesvaran, Shah et al. 2018).

1.6. Usage of oncolytic virotherapy in glioblastoma

As described previously, glioblastoma is a devastating disease with very limited treatment options and overall poor prognosis. As described above tumor heterogeneity is a common feature of glioblastoma, with alterations in both oncogenes (EGFR, PDGF) or tumor suppressor genes (RB1, TP53) and even inter tumoral heterogeneity (Stavrakaki, Dirven et al. 2021). Allowing the tumor to adapt to environmental changes, like targeted therapy. The high recurrence rate after initial response, is marked with further alterations, leading to drug resistance, while further infiltration of the surrounding tissue makes total tumor resection impossible (Stavrakaki, Dirven et al. 2021). Although numerous therapeutic approaches were tested in glioblastoma, so far clinical trial often led to unsatisfactory endpoints (Stavrakaki, Dirven et al. 2021). Over 10 different virus families are used for virotherapy in various cancer types (Harrington, Freeman et al. 2019) as well as over 6 in GBM, including DNA and RNA OVs, like Herpesvirus, Adenovirus or Reovirus (Stavrakaki, Dirven et al. 2021).

There are several oncolytic adenovirus constructs in clinical trial for the treatment of glioblastoma, both as a monotherapy or in combination with other drugs. Both replication defective and replication-competent viruses are being tested (Chiocca, Nassiri et al. 2019).

For gene delivery replication defective adenoviral vectors were used to deliver the herpes simplex virus type 1 thymidine kinase (HSV1-*tk*), *p53* or *IFN-β*. The thymidine kinase expressed by the viral vector can phosphorylate nucleoside analogues, like valacyclovir (VCV), which is used by the cancer cells to repair, radiation caused, DNA stand breaks, resulting in DNA replication arrest and immunogenic cell death (Chiocca, Nassiri et al. 2019). The idea is to retarget the tumor for the immune system, by the induction of local inflammation and immune cell invasion. A subset of patients showed a durable response even with recurrent GBM with 15% of patients reaching the 3 year mark (Chiocca, Nassiri et al. 2019).

The usage of replication competent adenoviral vectors is based on targeting pathways, that are frequently altered in tumors, using mutations in the Rb pathway, defects of p53/p14ARF or the dependency on nuclear YB-1. The first replication competent adenoviral vector used in clinical trial phase I for glioblastoma was dl1520 (ONYX-015), bearing a 827bp deletion in the E1B region. This results in the incapability of ONYX-015 to degrade *p53* via E1B55k. In normal cells the accumulation of *p53* leads to aberrant viral replication, while in tumor cells with defective *p53*, viral replication is not disturbed (Ries and Korn 2002). In the viral E1A gene a deletion of only 24bp, results in viral constructs, depending on a dysfunctional Rb pathway, altered in over 80% of GBM tumors (Stavrakaki, Dirven et al. 2021). As described above our group focused on the dependency of nuclear YB-1, a factor found in the nucleus of drug resistant cancer cells (Holm, Bergmann et al. 2002, Holm, Lage et al. 2004).

Table 2: Used virus families for oncolytic virotherapy in glioblastoma. Figure adapted from (Stavrakaki, Dirven et al. 2021).

Family	Genome	OV Examples	Genetic Engineering	Entry Receptor	Tumor specificity
Herpes virus	dsDNA	G207	ICP34.5 and ICP6-deleted mutant oHSV	HVEM, 3-O-sulfated heparin sulfate and nectin-2	Defects in the p16/Rb, PKR or interferon pathways
		G47Δ	ICP34.5, ICP6 and α47-deleted mutant oHSV	HVEM, 3-O-sulfated heparin sulfate and nectin-2	Defects in the p16/Rb, PKR or interferon pathways
		rQnestin-HSV-1	ICP34.5-deleted mutant oHSV, in which 134.5 gene was reinserted under control of nestin promoter	HVEM, 3-O-sulfated heparin sulfate and nectin-2	Expression of nestin
Adenovirus	dsDNA	Onyx-015	E1B-55k and E3B - deleted mutant group C adenovirus	CAR	Defects in p53 pathway, defects in cell cycle, late viral RNA export

		Delta24-RGD	24-base pair deletion in the E1A gene and insertion of an RGD sequence in the viral knob	CAR, αβv3 and αβv5 integrins	Defects in Rb pathway
Paramyxoviridae	(-) ssRNA	MV-CEA	Edmonston (MV-Edm) vaccine strain with insertion of the human carcinoembryonic antigen gene	CD46, nectin-4, SLAM	Overexpression of CD46, defects in the interferon pathway
		NDV	Natural tropism	Sialic acids	Defects in the interferon pathway
Reovirus	dsRNA	R124	Natural tropism	JAM-A, Nogo Receptor NgR1	Defects in the Ras signaling pathway
Picornaviridae	(+) ssRNA	PVSRIPO	Poliovirus type 1 (Sabin) vaccine with replacement of the internal ribosomal entry site (IRES) with the human rhinovirus type 2 IRES	CD155	Overexpression of CD155
Parvovirus H1	ssDNA	Parvovirus H-1PV	Natural tropism	Sialic acids	Defects in interferon pathway, defects in cell proliferation pathways

1.7. Cell cycle

The cell cycle is tightly regulated network, using different transcription factors, pocket proteins, cyclins, cyclin-dependent kinases (CDKs) and regulators. Each step is highly controlled and organized in a timely manner, with consecutive expression of different CDKs and cyclins, depending on the cell cycle phase (Pan, Sathe et al. 2017).

There are four distinct cell cycle phases, gap 1 (G1/G0), synthesis (S), gap 2 (G2) and mitosis (M) (Finn, Aleshin et al. 2016). Mitotic stimuli result in the production of cyclin D1 in G0/G1 phase cells. Next, cyclin D1 activates CDK4 and CDK6 leading to a complex formation. The now active CDK4/6-cyclin D1 complex phosphorylates several pocket proteins including Rb, p107 and p130, resulting in their inactivation. While hypophosphorylated Rb binds transcription factors of the E2F family, the

hyperphosphorylated Rb dissociates of the complex, releasing E2F. These E2Fs act as transcription factors for proteins involved in the trans transition, like cyclin A, cyclin E and dihydrofolate reductase (DHFR) (Blake and Azizkhan 1989, Mudryj, Devoto et al. 1991, Ohtani, Degregori et al. 1995). The interaction of cyclin A and cyclin E with CDK2, leads to further phosphorylation of Rb and other cell cycle mediators, inducing a positive feedback loop, allowing the cell to pass the restriction point and pass on to the S phase. From there cyclin A and cyclin B activate CDK1 continuing the cell cycle and progression of mitosis (Matthews, Bertoli et al. 2021).

Two families regulate the CDKs and cyclins during the cell cycle. The INK4 family proteins p15, p16, p18 and p19 inhibit CDK4/6 by reduction of their binding to cyclin D1 or interference at their catalytic domain (Finn, Aleshin et al. 2016). The second group of cyclin kinase inhibitors is the CIP/KIP protein family, including p21, p27 and p57 involved in both activating and repressing fashion on the cell cycle machinery (Finn, Aleshin et al. 2016).

Accumulated p53, results in higher transcription of p21 and CDK2 inhibition, arresting the cells in the G1 phase (Fischer, Prodeus et al. 2016). Interestingly p21 expression increases viral replication (Flak, Connell et al. 2010).

As described above the adenovirus requires S-phase induction, for optimal replication (Nakajima, Masuda-Murata et al. 1987, Ben-Israel and Kleinberger 2002). Using the E1A protein, adenoviruses interfere in the Rb/E2F pathway, leading to the release of E2Fs, promoting S-phase induction (Nakajima, Masuda-Murata et al. 1987). While at the same time using the E1B55k protein degrading p53 to prevent G1 cell cycle arrest and apoptosis (Braithwaite and Russell 2001).

In tumor cells the cell cycle is highly deregulated, allowing the cells to proliferate. Mutations in the Rb pathway are very common (Pelka, Miller et al. 2011). Therefore, targeting the cell cycle progression with small molecules was an appealing strategy.

Targeting the CDK4/6 axis prevents the phosphorylation of Rb, thereby preventing E2F release and cell cycle progression. The first generation of CDK4/6 inhibitors including flavopiridol, R-Roscovitine and UCN-01 had a broad spectrum of targets, targeting also other CDKs, Akt, Chk1 or protein kinase. This pan-CDK inhibition led to severe side effects and toxicities in clinical studies, while the efficacy was limited (O'leary, Finn et al. 2016) .

The next generation of ATP-competitive CDK4/6 inhibitors were much more specific. This leads oder led to an improved efficacy as well as less toxicity (Wu, Zhang et al. 2020). Ribociclib (LEE011, Novatis), Abemaciclib (LY2835219, Eli Lilly) and Palbociclib (PD-0332991, Pfizer) are FDA and EMA approved for the treatment of hormone receptor (HR) positive, human epithelial growth factor two (HER2) negative metastatic or advanced breast cancer (mBC/ABC) and are under evaluation in other tumor entities, including leukaemia, breast cancer, melanoma, glioma, pancreatic cancer, hepatocellular carcinoma, lung adenocarcinoma, sarcoma, ovarian cancer, renal cancer, prostate cancer and muscle invasive bladder cancer (Pan, Sathe et al. 2017). As a monotherapeutic approach CDK4/6 inhibitors have proven to be ineffective, therefore several different combinations are under clinical trial, involving chemotherapeutics as well as further selective targeting therapies (e.g. PI3K inhibitors, MTOR inhibitors etc.) (Knudsen and Witkiewicz 2017). Further combinatory approaches use the PD-L1 checkpoint inhibitors to both activate effector T-cells and inflammation, while downregulating the tumor cell proliferation (Schaer, Beckmann et al. 2018).

For glioblastoma treatment the blood-brain barrier (BBB) plays an important role for the permeability of the drug (Li, Jiang et al. 2021). All three CDK4/6 inhibitors are able to cross the BBB, but with different affinities. The two inhibitors Abemaciclib and Ribociclib have better brain penetrating capabilities, compared to Palbociclib (Li, Jiang et al. 2021).

Successful implementation of virotherapy in combination with CDK4/6 inhibitors have already been conducted in our group focusing on bladder and head and neck cancer. It is well established that the E1A protein is capable of overwriting the cell cycle arrests induced by CDK4/6 inhibitors and pushes cells into the S phase (Nakajima, Masuda-Murata et al. 1987). Interestingly the highest production of viral particles can be achieved if cells were infected in the G1 phase (Goodrum and Ornelles 1997).

1.8. Epigenetic alterations using Bromodomain Inhibitors

Brd4 is a member of the bromodomain and extraterminal (BET) protein family, playing a fundamental role in the organization of super-enhancers promoting the expression of oncogenes (Donati, Lorenzini et al. 2018). In 2010 P. Filippakopoulos, in the lab of J. Bradner, discovered a new selective BET inhibitor, called JQ1 (Filippakopoulos, Qi et al. 2010).

JQ1 is a small molecule, capable to penetrate the cell membrane and binds competitively to the acetyl-lysine recognition motif of BRD4. Targeting this protein, allowed for the first time the downregulation of c-Myc, one of the most common altered gene in cancers (Delmore, Issa et al. 2011). JQ1 interferes with c-Myc on two levels, by interfering with the transcription of the MYC gene as well as abrogating recruitment of enhancer complexes (Qi 2014). Interestingly besides c-Myc, JQ1 inhibition of BRD4 leads to the downregulation of further genes. Sun et al. reported that CDK4/6 was as well downregulated upon treatment with JQ1 in mantle cell lymphoma (MCL) cells and lead to a G1 phase arrest (Sun, Shah et al. 2015). The G1 arrest has already been observed with other BET inhibitors (Pastori, Daniel et al. 2014), but JQ1 leads to dephosphorylation of the RB protein (Zhu, Enomoto et al. 2017) as well as direct downregulation of further important cell cycle regulators like CDK4 and CDK6 (Sun, Shah et al. 2015). This downregulation is accompanied by an increase in HEXIM1 as well as boosting the transcription of HI-Virus proteins (Bartholomeeusen, Xiang et al. 2012). The interaction of BRD4 with the HIV TAT protein results in lower HIV-1 replication, using JQ1 latent HIV-1 infections could be reactivated and therefore targeted (Zhu, Gaiha et al. 2012). The influence of JQ1 on the BRD4 protein leads to the allocation of a complex consisting of CDK9 and RNA polymerase II (RNAP II) to viral promotors thereby increasing HSV replication (Ren, Zhang et al. 2016). Interestingly for the Eppstein Bar virus (EBV) the treatment of cells with JQ1 inhibits the production of the long EBV message, via viral C promotor (Cp) driven EBV transcription and thereby preventing their expression. Here JQ1 plays a role as an anti-EBV agent (Palermo, Webb et al. 2011). In human papillomavirus infections the BRD4 protein acts as an activator in early viral infections, with Bromodomain inhibitors like JQ1, reducing immediate early viral gene expression. But HPV can also accidently integrate into the host genome. Therefore, it is suggested that BRD4 inhibitors like JQ1 could be used in HPV associated cancers to prevent the expression of viral E6 and E7 oncogenes, leading to carcinogenesis (McBride, Warburton et al. 2021).

In the context of acetylated histones, bound by BET bromodomain inhibitors a prominent factor is the acetyltransferase p300. This protein plays a further important role in the acetylation of the viral genome and is regulated by the viral E1A region via both the CR1 and CR3 domain (Pelka, Ablack et al. 2009). Interestingly the complex is needed for the acetylation at all major early promotors in the viral genome, E2-early, E3 and E4 (Hsu, Pennella et al. 2018). The interaction of p300 and the viral E1A gene

modulates cellular protein expression, and is even considered to reduce the tumorgenicity (Miura, Cook et al. 2007). P300 role in the cell cycle progression can not be excluded here, leading to acetylation of phosphorylated Rb as well as being capable of binding to CDK4/6 (Nguyen, Baglia et al. 2004, Jin, Valanejad et al. 2016). JQ1 has a relatively short half-life and high toxicity resulting in low efficacy in vivo applications, therefore further inhibitors for BRD4 are in development (Li, MacKenzie et al. 2020). These include degraders of BRD4 like dBET6 or ARV-825 (Xu, Chen et al. 2018, Lu, Ding et al. 2019).

Interestingly JQ1 is capable to cross the blood brain barrier (Matzuk, McKeown et al. 2012) and, tested also in different combinatory approaches for glioma, both *in vitro* and *in vivo* (Lam, Morton et al. 2018, Xu, Chen et al. 2018, Chen, Zhang et al. 2020).

The effects on histone acetylation and epigenetic alterations induced by JQ1 treatment, are not limited to cellular factors. JQ1 also improves the effectiveness of adenoviral infection, replication as well as adenoviral gene delivery (Lv, Li et al. 2018, Qiao, Chen et al. 2020).

After presenting both the advantages and weaknesses of both CDK4/6 and bromodomain inhibitors, the combination of both is a valid treatment strategy. Interestingly the usage of CDK4/6 inhibitors can prevent JQ1 resistance via DUB3 phosphorylation (Jin, Yan et al. 2018). As shown in Figure 5, either treatment approach using the oncolytic adenovirus XVir-N-31, uses a specific target, further boosting viral replication. While the viral construct is limited to replication in cancer cells (Fig. 5 A/B), the usage of CDK/6 inhibitors results in G1 arrested cells, thereby weakening the antiviral response via the Rb/E2F complex (Fig. 5 C). If a bromodomain inhibitor like JQ1 is applied simultaneously to the viral infection, the viral gene expression gets severely increased (Fig. 5 D). In a combinatory approach, both individual drug effects are combined, resulting in the highest reduction of tumor cells, while allowing lower individual concentrations of the inhibitors used (Fig. 5 E).

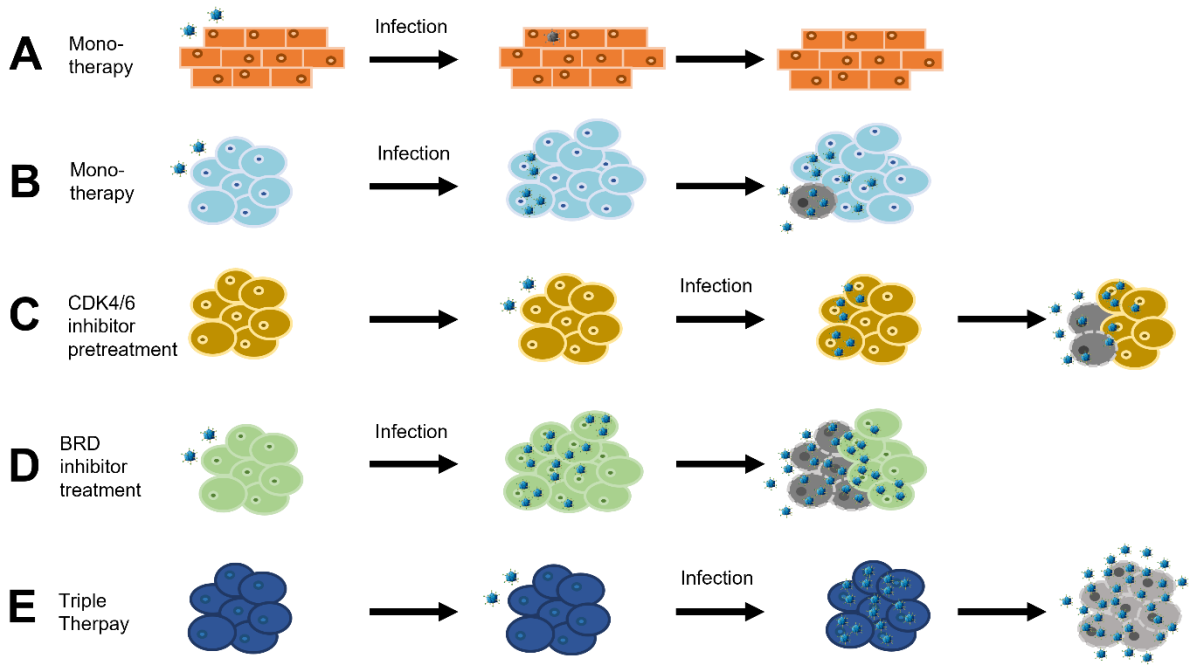

Figure 5: Proposed model of the combination therapy with XVir-N-31. A, in healthy cells XVir-N-31 can infect the cells but fails to successfully replicate. This leads to no further viral spread. B, In cancer cells after viral infection, viral replication occurs, thereby killing tumor cells, reactivating the immune system and spreading to further cells via the production and release of viral particles C, The pre-treatment with CDK4/6 inhibitors, like LEE011, leads to a growth arrest in cancer cells (in the G1 phase), this benefits the ability of the virus to overcome the initial replication burden, resulting in higher replication and particle formation. D, The usage of bromodomain inhibitors, e.g. JQ1, results in a strong increase in adenoviral gene expression and replication. Amplifying the viral life cycle. E, The combination of both CDK4/6 inhibitors and bromodomain inhibitors, work synergistically, removing the burden in initial viral gene expression as well as boosting further one all viral parameters, resulting in the most beneficial therapeutic approach.

1.9. Aim and objectives

Successful therapy against glioma require a combinatorial treatment strategy (Weller, van den Bent et al. 2021). Thus, the aim of this study was to validate the effectiveness of YB-1 based adenoviral oncolytic virotherapy in glioblastoma cell lines in combinations with classical treatment options as well as new targeted therapy approaches.

1. Radiation and alkylating agents (TMZ) are the fundaments in clinical treatment of glioblastoma multiforme, both *de novo* and recurrent (Wen, Weller et al. 2020). Its is well established that radiation and TMZ increase YB1 and by that viral replication (Bieler, Mantwill et al. 2008, Holzmüller, Mantwill et al. 2011, Bressy and Benihoud 2014). In order to deepen or knowledge, these two approaches were included into the combinatory approaches.

2. The usage of CDK4/6 inhibitors as monotherapeutic agents proof to be difficult, resulting short growth arrest followed by a relative fast resistance and further cancer cell proliferation (Portman, Alexandrou et al. 2019). The combination of CDK4/6 inhibitors with oncolytic adenoviral constructs has proven beneficial for viral replication, cell lysis and viral particle production in bladder cancer (manuscript under revision). We analysed the role of Rb downregulation in the context of glioblastoma in combination with viral infection. AG Holm was recently able to show that CDK4/6 synergises with XVir-N-31 in bladder and head and neck cancer, therefore we want to confirm these results in glioblastoma.

3. Bromodomain inhibitors like JQ1, are a relatively new approach for cancer treatment, focussing on the epigenetically alterations induced by BRD4 inhibition. Initial results have shown beneficial results of Adv replication (PSH personal information) therefore we wanted to analyse this in the context of glioblastoma. As well as establish a translational therapy approach using both CDK4/6 inhibitors as well as JQ1 in low concentrations, thereby avoiding adverse effects in patients.

The overall goal of this work was to identify and characterise a treatment which support adenoviral oncolysis.

2. Materials and Methods

2.1. Materials

2.1.1. Adenoviral constructs

Several Adenoviral constructs were used and constructed during the thesis.

Table 3: Adenoviral constructs

Name	Producer
AdWt 2xE2Fm	Klaus Mantwill and Maximilian Ehrenfeld, Klinikum rechts der Isar der TUM, Germany
AdWT 2xE2Fm mutated	Klaus Mantwill and Maximilian Ehrenfeld, Klinikum rechts der Isar der TUM, Germany
AdWt Trap	Klaus Mantwill, Klinikum rechts der Isar der TUM, Germany
XVir-N-31	Klaus Mantwill, Klinikum rechts der Isar der TUM, Germany

2.1.2. Antibodies

All antibodies were used for western blots, except for the anti-hexon antibody (used for hexon titer test) and its respective secondary antibody (HRP conjugated rabbit-anti-goat) and YB-1 plus goat anti-rabbit Alexa 488, which were used for immunofluorescence.

Table 4: Antibodies

Name	Cat. no.	Dilution	Producer
E1A	Sc-25	1:100	Santa cruz
E2A		1:100	Kindly provided by M. Dobbelstein, Göttingen University, Germany
E2F1	3742	1:1000	Cell Signaling Technology
GAPDH (14C10)	2118	1:1000	Cell Signaling Technology
Goat anti-rabbit Alexa 488	A32731	1:500	Thermo Fisher Scientific
HRP conjugated rabbit-anti-goat	P0449	1:1000	Dako
Peroxidase-conjugated anti-mouse IgG	715-036-150	1:10.000	Dianova

Peroxidase-conjugated anti-rabbit IgG	711-036-152	1:10.000	Dianova
Rb (D20)	9313	1:1000	Cell Signaling Technology
Phosphor Rb (Ser 780) (D59B7)	8182	1:1000	Cell Signaling Technology
YB-1 (EP2708Y)	ab76149	1:500	abcam

2.1.3. Bacteria

The bacteria were amplified and made chemically competent in the laboratory.

Table 5: Bacteria

Name	Cat. no	Producer
DH5α	EC0112	Invitrogen
Top10	C404003	Invitrogen

2.1.4. Buffers and solutions

Table 6: Buffers and solutions

Buffer	Composition
Blocking solution	1% BSA (w/v) in PBS
DNA Lysis buffer	10mM Tris-HCl (pH 8) 100mM NaCl 25mM EDTA (pH 8) 0.5% SDS
Enzymatic tissue dissociation solution	50% of a 0.05% Trypsin/EDTA solution 25% Collagenase IV (2000U/ml) 25% HBSS calcium and magnesium free
Immunoblotting antibody dilution buffer	5% BSA in TBS-T 0.02% Sodium azide
Immunoblotting blocking solution	5% non-fat milk powder in TBST
LB agar	LB medium 1.5% Select agar 0.1% Antibiotic
LB medium	0.01% Tryptone 0.005% Yeast extract 0.01% NaCl

Protein loading buffer (4x)	0.25M Tris-HCl (pH 6.8) 8% SDS 0.04% Bromophenol blue 40% Glycerin 100µl 1M DTT to 500µl prior to use
SDS page running buffer (10x)	25nM Tris 192mM Glycine 0.1% SDS (w/v)
SDS protein lysis buffer (1%)	10mM Tris-HCl (pH 7.2) 1% SDS 1mM Na-orthovanadate one Mini-Protease Inhibitor tablet 10µl/ml phosphatase inhibitor prior to use
Separating gel buffer	1.5M Tris/HCl pH 8.8
SRB staining solution (0.5%)	0.5% SRB (w/v) in 1% acetic acid
Stacking gel buffer	0.5M Tris/HCl pH 6.8
TBE (10x)	1M Tris 1M Boric acid 0.02M EDTA
TBS (10x)	0.5M Tris pH 7.6
TBS-T	0.1% Tween-20 in TBS (1x)
TCA (100%)	0.3M TCA in 22.7ml dH_2O
TE (0.1x)	0.1% TE (100x, pH 8)
Transfer buffer (10x)	25nM Tris 192mM Glycine
Transfer buffer (1x)	10% Transfer buffer (10x) 20% Methanol
Tris base (10mM)	1% Tris Base (1M)
Trypsin stop solution	50 % trypsin inhibitor 50% DMEM/F12 0.02% DNase I
Virus lysis buffer	20mM Tris 25mM NaCl
Virus storage buffer	20 mM NaCl 25 mM Tris 2.5 % Glycerol

2.1.5. Cell culture

Cell lines

Table 7: Cell lines

Cell lines	Source
HEK293	American type culture collection, Manassas, VA, USA
LN229	A kind gift of Prof. Naumann, Hertie-Institute, Tübingen
T98G	A kind gift of Prof. Naumann, Hertie-Institute, Tübingen
U373	A kind gift of Prof. Naumann, Hertie-Institute, Tübingen
U87	A kind gift of Prof. Naumann, Hertie-Institute, Tübingen

Cell culture medium

Table 8: Cell culture media

Medium	Composition
Culture Medium for cells cultured at 10% CO_2	DMEM 5% FBS 1% P/S
Freezing Medium	50% DMEM 40% FBS 10% DMSO
Infection medium for cells cultured at 10% CO_2	DMEM 1% P/S

2.1.6. Chemicals, enzymes and reagents

Table 9: Chemicals, enzymes and reagents

Material	Source
2-Mecaptoethanol	Sigma-Aldrich Chemie GmbH
100% Ethanol	Sigma-Aldrich Chemie GmbH
Agarose Ultrapure	Thermo Scientific
Acetic Acid	Sigma-Aldrich Chemie GmbH
Ammonium persulfate (APS)	Sigma-Aldrich Chemie GmbH
Ampicillin	Sigma-Aldrich Chemie GmbH
Boric acid	Sigma-Aldrich Chemie GmbH
Bovine serum albumin (BSA)	Sigma-Aldrich Chemie GmbH

Bromophenol blue	Serva
Calcium chloride ($CaCl_2$)	Merck Chemicals GmbH
Chloroform	Sigma-Aldrich Chemie GmbH
Color Prestained Protein Standard, Board Range	New England Biolabs
Complete mini protease inhibitor	Roche
Dimethyl sulfoxide (DMSO)	Sigma-Aldrich Chemie GmbH
Dithiothreitol (DTT)	Cell Signaling
DNA loading buffer (6x)	Thermo Scientific
Dulbecco´s Modified Eagle´s Medium (DMEM)	Biochrom
Ethidiumbromide (10mg/ml)	Sigma-Aldrich Chemie GmbH
Ethylenediaminetetraacetic acid (EDTA, 0.5M)	AppliChem
Fetal bovine serum (FBS)	Biochrom
Fluoroshield with DAPI	Sigma-Aldrich Chemie GmbH
FuGENE HD Transfection Reagent	Promega Cooperation
GeneRuler 100bp Plus DNA ladder	New England Biolabs GmbH
GeneRuler 1kb DNA ladder	New England Biolabs GmbH
Glucose	Sigma-Aldrich Chemie GmbH
Glycine	Sigma-Aldrich Chemie GmbH
GoTaq qPCR master mix	Promega Cooperation
GoTaq Green PCR master mix	Promega Cooperation
Hydrogen chloride (HCl)	Merck Chemicals GmbH
Isopropanol	Sigma-Aldrich Chemie GmbH
Lipofectamine RNAimax	Invitrogen
Magnesium chloride (MgCl)	Sigma-Aldrich Chemie GmbH
Methanol	Sigma-Aldrich Chemie GmbH
Opti-MEM	Invitrogen
Penicillin Streptomycin (P/S; 100x)	Sigma-Aldrich Chemie GmbH
Phenol Chloroform Isoamyl Alcohol (PCI)	Sigma-Aldrich Chemie GmbH
Phospahte buffered saline (PBS, 1x, 10x, 20x)	Biochrom
Phosphatese inhibitor Mix II	Serva Electrophoresis GmbH
Phusion High-Fidelity PCR Master Mix	Thermo Scientific
Precision plus protein standard	BioRad

Proteinase K	Qiagen
Restriction enzymes and buffers	New England Biolabs GmbH
Potassium chloride (KCl)	Merck Chemicals GmbH
Select agar	Sigma-Aldrich Chemie GmbH
Skimmed milk powder	Sigma-Aldrich Chemie GmbH
Sodium acetate	Merck Chemicals GmbH
Sodium azide	Sigma-Aldrich Chemie GmbH
Sodium chloride (NaCl)	Merck Chemicals GmbH
Sodium dodecyl sulfate (SDS)	Sigma-Aldrich Chemie GmbH
Sodium orthovanadate	Sigma-Aldrich Chemie GmbH
Sodium phosphate dibasic	Merck Chemicals GmbH
Sulforhodamine B (SRB)	Sigma-Aldrich Chemie GmbH
T4 DNA Ligase	Thermo Scientific
Taq DNA polymerase	Thermo Scientific
Tetramethylethylenediamine (TEMED)	Carl Roth
Trichloroacetic acid (TCA)	Sigma-Aldrich Chemie GmbH
Tris(hydroxymethyl)-aminomethane	Merck Chemicals GmbH
Triton X-100	Sigma-Aldrich Chemie GmbH
Trypan blue (0.5%)	Biochrom
Trypsin/EDTA	Biochrom
Tween-20	Serva Electrophoresis GmbH
Yeast extract	Sigma-Aldrich Chemie GmbH

2.1.7. Equipment disposable

Table 10: Equipment disposable

Equipment	Source
Amersham hybond-P PVDF-Membrane	GE Healthcare
Cell culture plates (96-well, 24-well, 12-well, 6-well, 10cm, 15cm)	Corning Incorporated
Cell culture plates (24-well)	Techno Plastic Products AG
Cell lifter	Sigma-Aldrich Chemie GmbH
Chromatography paper Watman	GE-Healthcare
Conical tubes Falcon (15ml, 50ml)	Greiner GmbH
Cryogenic vials Nunc (1.8ml)	Thermo Scientific
Gel Saver II – Tips 1-200µl	Kisker Biotech GmbH
Glass coverslips	Corning Incorporated

Hard-shell PCR plates (96-well)	BioRad
Lens cleaning paper	The Tiffen company
Needles (27 Gauge)	BD Biosciences
PCR reaction tubes (0.5ml)	Biozym Scientific
PCR sealers microseal ´B´ film	BioRad
Pipette tips with/without filter	Sarstedt
Reaction tubes (0.5ml, 1.5ml, 2ml)	Sarstedt
Serological pipettes (5ml, 10ml, 25ml)	Greiner Bio-One International AG
Slides, microscope	Merck Chemicals GmbH
Sterile filter Nalgene (0.25µm, 0.4µm)	B. Braun Melsungen AG
Syringes	B. Braun Melsungen AG
White polystyrene plates (96-well)	Corning Incorporated

2.1.8. Equipment multiple use

Table 11: Equipment multiple use

Equipment	**Source**
Analytic balance AT250	Mettler Toledo
Autoclave Sytec DX-65	Systec GmbH
Avanti JXN-30	Beckman Coulter
Biological safety cabinet Herasafe KS12	Thermo Scientific
BVC professional laboratory fluid aspirator	Vacuubrand GmbH
Centrifuge 5430R	Eppendorf GmbH
Centrifuge 5810R	Eppendorf GmbH
Centrifuge ROTINA 35R	Hettich
ChemiDoc XRS Imaging System	BioRad
ChemiDoc MP Imaging System	BioRad
CO_2 incubator HERA Cell240	Thermo Scientific
CO_2 incubator HERA Cell240i	Thermo Scientific
Cold light source Leica L2	Leica Microsystems GmbH
Cryogenic freezing container, 1 Deg C	Nalgene
Electrophoresis power supply EPS 601	Amersham Pharmacia Biotech
Glassware	Schott AG
Heating and drying oven Heraeus FunctionLine B6	Thermo Scientific
Heating and drying oven Heraeus FunctionLine UT20	Thermo Scientific

Heating block thermostat BT100	Kleinfeld Labortechnik
Ice machine Manitowoc	Manitowoc Ice
Intellimixer RM-2L	Elmi Ltd. Laboratory Equipment
Magnetic Stirrer	Heidolph Instruments GmbH
Microcentrifuge 5430R	Eppendorf GmbH
Microcentrifuge QikSpin QS7000 personal	Edwards Instrument Co.
Micropipettes Pipetman	Gilson Inc.
Microplate reader Vmax Kinetic	Molecular Devices
Microscope AxioVert 135	Carl Zeiss
Microscope AxioVert A1	Carl Zeiss
Microscope camera AxioCam ERc 5s	Carl Zeiss
Microscope EVOS M5000	Invitrogen
Mini protean system	BioRad
Mini trans-blot cell transfer system	BioRad
Mini-protean tetra cell gel system	BioRad
Minishaker IKA MS2	IKA Works Inc.
Multilabel plate reader Victor X3	Perkin Elmer
Neubauer chamber	LO Laboroptik
Orbital shaker K15	Edmund Buehler GmbH
Perfect blue gelsystem Mini M	PEQLAB Biotechnologie GmbH
pH Meter 691	Metrohm
Power supply PowerPac HC	BioRad
Pressure cooker	Fissler & Fissler
Spectrophotometer Nanodrop 2000c	Thermo Scientific
Stereo microscope Stemi DV4	Carl Zeiss
Thermal cycler C1000 CFX96	BioRad
Thermal cycler iCycler iQ Real-time PCR detection system	BioRad
Thermal cycler MJ Research PTC-200	BioRad
Trans-Blot Turbo Transfer System	BioRad
Vortex-Genie 2	Scientific Industries
Water bath W350	Memmert
Water purification system, Purelab	ELGA Lab water

2.1.9. Kits

Table 12: Kits

Kit	Cat. No	Source
CellTiter-blue Cell Viability Assay	G8080	Promega
High-Capacity cDNA Reverse Transcription Kit	4368813	Thermo Scientific
Liquid DAB + Substrate Chromogen System	K3468	Dako
mirVANA miRNA Isolation Kit	AM1560	Thermo Scientific
Monarch Gel Extraction Kit	T1020S/L	New England Biolabs
HiSpeed Plasmid Midi Kit	12643	Qiagen
Pierce BCA Protein assay	23225	Thermo Scientific

2.1.10. Plasmids

Table 13: Plasmids

Plasmid	Source
pShuttle AdEasy wtE1	Klaus Mantwill
pAdEasy AdWtE1-E2-earlyMutDeltaE3 RGD	Klaus Mantwill
pAd5wt E1A/E2-mutE2F RGD	Maximilian Ehrenfeld and Klaus Mantwill

2.1.11. Primers

Table 14: Primers

Name	Company	Forward primer	Reverse Primer
β-actin	Eurofins	TAAGTAGGTGCA CAGTAGGTCTGA	AAAGTGCAAAGAA CACGGCTAAG
E2F1	Life Technologies	ACGCTATGAGAC CTCACTGAA	TCCTGGGTCAA CCCCTCAAG
Fiber	Eurofins	AAGCTAGCCCTGC AAACATCA	CCCAAGCTACCAG TGGCAGTA
GAPDH	Eurofins	TGGCATGGACTGT GGTCATGAG	ACTGGCGTCTTCA CCACCATGG

2.1.12. Programs and software

Table 15: programs and software

Program	Website
Adobe Illustrator	https://www.adobe.com/de/products/illustrator.html
Adobe Photoshop	https://www.adobe.com/de/products/photoshop.html

GraphPad Prism 5	https://www.graphpad.com/scientific-software/prism/
Microsoft Office	https://www.microsoft.com/de-de/microsoft-365
Serial Cloner	https://serial-cloner.de.softonic.com/
Snap gene	https://www.snapgene.com/
Zen Lite 2012	https://www.zeiss.com/microscopy/int/products/microscope-software/zen-lite.html

2.1.13. siRNAs

Table 16: siRNAs

Name	Sequence	Company
siCtrl #1022076	no human sequence similarity	Qiagen
siCtrl pool	no human sequence similarity	SiTOOLs Biotech
siRb #1	AAGGTTCAACTACGCGTGTAA	Qiagen
siRB #2	CAGGAGTGCACGGATAGCAAA	Qiagen
siRb pool	30 preselected siRNAs	siTOOLs Biotech

2.1.14. Small molecule inhibitors

Table 17: Small molecule inhibitors

Name	Target	Stock conc.	Dissolvent	Company
LEE011 (Ribociclib)	CDK4/6	10mM	DMSO	Selleck Chemicals
LY2935219 (Abemaciclib)	CDK4/6	10mM	DMSO	Selleck Chemicals
Temozolomide	Alkylating agent	10mM	DMSO	Sigma Aldrich Chemie GmbH
JQ1	BET4	1mM	DMSO	Selleck Chemicals

2.2. Methods

2.2.1. Cell Culture

All four human glioblastoma cell lines were cultured in DMEM high glucose medium at 37°C with 10% CO_2 in sterile 10cm plates, if greater quantities of cells were needed for experiments sterile 15cm plates were used. The cells were always kept in sub-confluency, checked daily, and split when they reached 70-80% confluency. At this point the medium was aspirated and the cells were washed once with PBS, to remove residual FCS, interfering with the following trypsinization step. Two millilitres of trypsin were used for a 10cm plate and depending on the cell line incubated until the cells detached from the plate. To stop the digestion, fresh medium was added to the plates and the solution, containing the cells, transferred into a 15ml Falcon tube. The cells were then pelleted at 300rcf, for 3 minutes and after removal of the supernatant, resuspended in fresh medium. If the cells were only passaged, a fraction was seeded on fresh 10cm plates for cultivation. Cells were passaged only for up to 30 times, before being replaced with a lower passage number, to avoid any culturing artifacts.

Otherwise 20µl of the cell solution was mixed with 20µl of Trypan blue (1:1) and 10µl were pipetted on a Neubauer counting chamber. The concentration of cells per millilitre was calculated as follows:

$$\textit{Number of cells/ml} = \textit{Average of cells/quadrant} * 2 * 10^4$$

With the now known concentration of cells, dilutions could be done, depending on the experimental setup. For 10cm plates 0.5-1x10^6 cells/plate, 6 well plates 1-2x10^5 cells/well, 12 wells 1-2x10^4 cells/well, 96 well plate 5x10^3 cells/well were seeded, respectively.

2.2.2. Cryoconservation of cell lines

To cryoconserve the used cell lines, the cells were prepared as described above. After counting the cells, the cells were again centrifuged and diluted in freezing medium at a concentration of 1-2x10^6 cells/ml. Each cryotube was filled with 1ml of the solution and directly transferred into a freezing container. The container was put at -80°C soon after to avoid cytotoxicity due to the 10% DMSO in the freezing medium. After 1-2 days the tubes were transferred into the liquid nitrogen tank, were they were stored until further use.

For cell thawing the cells were taken out of the liquid nitrogen tank, fast thawed in a 37°C water bath, and directly diluted with fresh medium. After a centrifugation step (300rcf, 5 minutes) the cells were resuspended in fresh medium and cultured on 10cm plates.

2.2.3. Small molecule inhibitor treatment

All inhibitors were diluted in DMSO (Table 17) at a concentration on 10mM. These stocks were used for the preparation of working solutions, in medium, for direct use. To avoid any DMSO artefacts, no final concentration over 1% DMSO was used.

2.2.4. Cell viability assay

To investigate the cell viability under different small molecule inhibitors, the CellTiter-Blue assay and a Sulforhodamine B (SRB) assay were used. 500 cells/well were seeded in 96 well plates, each inhibitor concentration as triplets. At the next day the cells were treated with increasing concentrations of the inhibitors and after 72h, the cell viability was measured. For the CellTiter-Blue assay, the reagent was added to each well and the absorbance measured over a time span of 6 hours once per hour using a multilabel plate reader at 590nm. For the SRB assay the medium was aspirated, the cells fixed using 10% TCA, and stained using a 0.5% SRB solution. Excess SRB was washed out using 1% acetic acid. The bound SRB was solved in 100µl of 10mM Tris base and measured using a multiplate reader at 560nm.

2.2.5. Potency assay and combination treatment

The viral cell killing capabilities were tested alone and in combination with small molecule inhibitors, alkylating agents and radiation. All experiments were conducted in 12 well plates, with 1-2x10^5 c/well respectively. The day after seeding, the cells were treated with temozolomide or CDK4/6 inhibitors or underwent radiation. If no pre-treatment was required, the cells were directly infected the day after seeding. Otherwise one day after the treatment the cells were infected with increasing amount of virus (multiplicity of infection, MOI). For infection, the medium was aspirated and 250µl medium without FCS containing the virus was added in triplicates. The MOIs were calculated using the following formula:

$$virus\ stock/well = \frac{MOI * amount\ of\ cells/well}{virus\ concentration\ [\frac{pfu}{\mu l}]}$$

As an example if there were $2x10^5$ cells in one well and to be infected with 100 MOI and the virus has a concentration of $2x10^6$ pfu/µl, the calculation goes as follows:

$$\frac{100 * 2x10^5 c/well}{2x10^6 pfu/\mu l} = 10\mu l/well$$

The infection medium was kept for 1 hour on the cells in the incubator and to ensure even distribution the plates are carefully rotated ever 15 minutes. One hour post infection (hpi) fresh medium, with FCS, was added to the plates with our without the inhibitors. The Bet4 inhibitor JQ1 is an exception here, being only added after the infection and not before. Four or five days post infection (dpi) the medium was aspirated, the plates washed once with PBS and fixed using 10% Trichloracetic acid (TCA). The plates were transferred for 1 hours to a 4° fridge, before being stained using SRB for 20-30 minutes at room temperature (RT). The plates were then washed three times with 1% acetic acid, to remove any not bound SRB and air dried overnight (ON). The SRB was solved in 10mM tris base and the solution was photometrically measured and quantified using a multilabel plate reader at 560nm. Each mean with the corresponding standard deviation (SD) was calculated in GraphPad Prism and the values normalized to their respective control.

2.2.6. Hexon titertest

To measure the infectious viral particle production in glioblastoma cells Hexon-titertests were conducted. The first part of the assay was done in 6 well plates. For this $1x10^5$ cells were seeded and pre-treated with CDK4/6 inhibitors or temozolomide 24 hours before infection. Cells were infected with different MOIs depending on the cell line (U87, U373 and LN229: 20 MOI; T98G: 50MOI) in 400µl infection medium. At 1hpi 2ml fresh medium, containing the used inhibitors were added. For JQ1 the treatment again only starts after the infection. After 3 days the cells and the supernatant are transferred into falcon tubes. The cells are harvested using cell scrapers. To release viral particles inside intact cells, three freeze-taw cycles are used. Afterwards the detritus was pelleted using 1000rcf for 10 minutes at RT. The supernatant was transferred into new tubes and each sample was tested for its infectiveness and infectious particles, using HEK293 cells. HEK293 cells were seeded at a concentration of $4x10^5$ c/ml in 24 well plates using 0.5ml per well. Directly after seeding, the prepared cell supernatants were serial diluted in 1:10 steps in medium and of each dilution, either 50µl or 10µl were added to the HEK293 cells. At 2dpi, the plates were analysed for

cytopathic effects (CPE) and starting at the wells where no clear cell lysis could be observed fixed and stained for the viral Hexon protein. After aspirating the medium, the plates were air dried for 10min, before adding 0.5ml 100% ice cold methanol. The plates were incubated for 10 minutes at -20°C, then the methanol was aspirated and the plates washed twice with a 1% BSA-PBS solution. The primary antibody (AB) goat-anti-hexon was diluted 1:500 in the 1% BSA-PBS solution and 250µl was added to each well. After 1 hour at 37°C, the plates were again washed twice with 1% BSA-PBS and 250µl of the secondary rabbit-anti-goat-HRP AB, diluted 1:1000, was added to each well and incubated again for 1h at 37°C. The plates were then washed twice with 1% BSA-PBS and 250µl DAB staining solution was added to each well. The HRP converts the DAB solution and leaves a dark-brown staining in virus infected cells. These dark stained cells can be counted under a microscope at a 20x magnification and 10 field of site are counted per sample. Using the following formular the viral titer (infectious units or particle forming units per ml, PFU/ml) can be calculated:

$$Titer\ [pfu/ml] = \frac{average\ number\ of\ positve\ cells/fields * fields/well}{volume\ of\ diluted\ virus\ used\ per\ well\ (ml) * dilution\ factor}$$

2.2.7. Viral replication

To investigate the viral replication alone or in combination with different treatment options quantitative PCR (qPCR) for viral Fibre DNA copies per cell (normalised to Actin) were conducted. Using the ΔΔCT method (chapter 2.1.8) the replication was analysed in comparison to the respective viral entry levels (4hpi value)

Seeding, pre-treatment and infection of cells

Glioblastoma cells were seeded in 6 wells with a concentration of $1x10^5$ c/well and treated according to the treatment strategy. At the next day, the cells were infected with different MOIs according to the respective cells (Table 7). After 1hpi, medium was added with or without the inhibitors. After 4 h.p.i., 1 d.pi. and 2 d.p.i the DNA was extracted, by first aspirating the medium. Afterwards the wells were washed with PBS once and the cells were lysed using 200µl of DNA lysisbuffer. To ensure complete DNA extraction the cells were scraped of the well and transferred into fresh tubes. To each tube 3µl Proteinase K was added and the samples were incubated at 56°C between 1 hour and ON.

DNA Isolation

To isolate the DNA the phenol chloroform extraction method (PCI) was used. First 200µl of phenol chloroform isoamyl alcohol was added to each tube and mixed thoroughly via vortexing. Then the tube were incubated on ice for 5 minutes before being centrifuged at 16500rcf, 4°C for 3 minutes. The upper phase was transferred in fresh tubes and mixed with 200µl of chloroform, again vortexed, incubated on ice and centrifuged, removing residual phenol in the sample. Again the upper phase was transferred in new tubes and mixed 800µl of EtOH and 50µl of a 3M Na-acetat solution. To enhance the DNA precipitation one drop of glycogen was added. The tubes were inverted, not vortexed and centrifuged for 30 minutes at 4°C. Next the supernatant was discarded and the DNA pellets were washed with a 70% EtOH solution and centrifuged for 10 minutes at RT. The EtOH was removed and the pellets are dried until they are colourless, before being resuspended in 50-100µl 0.1xTE buffer. To ensure complete DNA dissolving the samples are incubated at 40°C in the thermomixer. The DNA concentrations and purity were quantified in a Nano drop and diluted to a concentration of 10ng/µl in H_2O for qPCR analysis.

2.2.8. qPCR

To analyse the viral replication or (expression) of viral genes, qPCRs were performed using either DNA samples of cDNA.

qPCRs were done in 96 well plates using master mixes, prepared after following recipes (Table 18). Briefly, 10µl of master mix were mixed with 5µl of sample (10ng/µl), sealed and after a brief centrifugation step, analysed via a Real-Time PCR detection system (Figure 6). Each sample and condition were done in triplicates. The relative quantification was based on the ΔΔCT method together with the calculation of error bars:

$$\Delta CT = CT\ (gene\ of\ interest) - CT\ (house\ keeping\ gene)$$

$$\Delta\Delta CT = \Delta CT\ (treated\ sample) - \Delta CT\ (control\ sample)$$

$$relative\ normalsied\ gene\ expression = 2^{-(\Delta\Delta CT)}$$

$$SD\ \Delta CT = SD\ \Delta\Delta CT = \sqrt{CQ\ SD\ (gene\ of\ interest)^2 \quad + CQ\ SD\ (house\ keeping\ gene)^2}$$

$$SD\ UP = \Delta\Delta CT - 2^{-(\Delta\Delta CT - SD\ \Delta\Delta CT)};\ SD\ DOWN = \Delta\Delta CT - 2^{-(\Delta\Delta CT + SD\ \Delta\Delta CT)}$$

As the housekeeping gene Actin was used and the samples were normalised to their 4hpi values.

Table 18: Dilution schematic for fibre and actin master mixes.

	Fibre master mix	**Actin master mix**
GoTaq qPCR Master Mix	7.5	7.5
Forward primer (1:10)	0.75	0.75
Reverse primer (1:10)	0.75	0.75
Ultra pure H_2O (DNase/RNase free)	1	1
Total [µl]	**10**	**10**

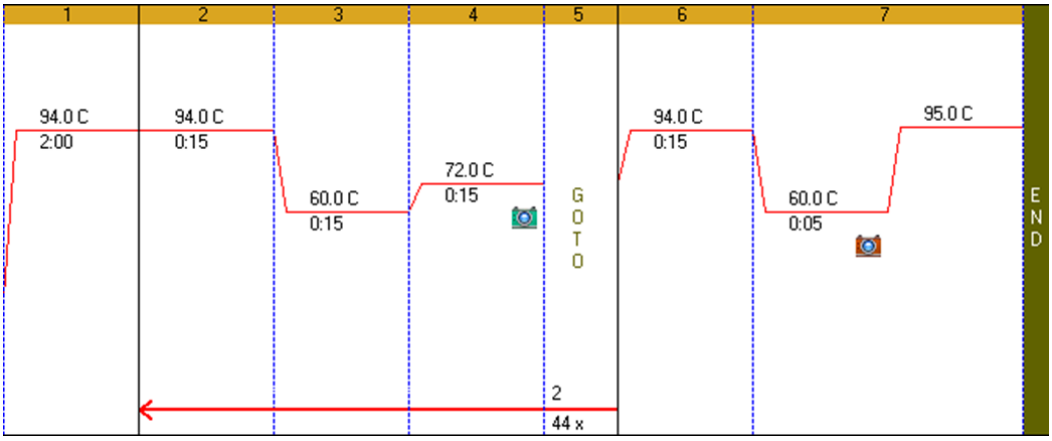

Figure 6: qPCR temperature profile used for the qPCRs.

2.2.9. Immunoblotting

To investigate alterations in cellular and viral proteins upon inhibitor treatment or radiation, immunoblots were performed. Protein lysates were, separated by size via gel electrophoresis, transblotted on membranes and the alterations in protein levels and phosphorylation checked with specific antibodies. Using HRP-tagged secondary antibodies and ECL reagents, the changes could be visualized and measured using a ChemoDoc MP Imaging System.

Seeding, pre-treatment and infection of cells

All experiments were performed in 10cm plates to ensure enough material, $1x10^6$ cells were seeded per plate. The next day the cells were treated with the inhibitors and lysates were performed 24 or 48 hours later. If the expression of viral proteins was investigated, one day after the treatment with inhibitors, the plates were infected. To ensure good infectivity, the medium was aspirated and virus dilutions in 2ml infection medium, without FCS, were added to the plates. After one hour in the incubator,

carefully swirling the plates every 15 minutes, fresh medium with the corresponding inhibitors were added. Again, 24hpi and 48hpi protein lysates were made.

Preparation of protein Lysates

After indicated time points protein lysates were made, by first putting the plates on ice. Then the medium was aspirated, and the plates carefully washed three time with ice cold PBS, before adding 300-400µl 1% SDS protein lysis buffer (containing both phosphatase and protease inhibitors), depending on the cell density. The SDS lysis buffer, also opens the nuclei, releasing the DNA. This DNA interferes with the gel separation, due to its high viscosity, therefore the DNA was broken down using a syringe and a 27-gauge needle to apply sheer forces. The detritus of the cells was removed via a centrifugation step at 30.000rcf for 30 minutes at 10°C. Afterwards the supernatant was transferred into fresh tubes and the protein concentration measured using the BCA Assay. The samples were stored at -80°C.

BCA Assay

To quantify the protein concentrations in each sample a BCA assay was performed, according to the manual in a 96 well plate. The samples were compared to a BSA standard and measured in duplicates. Each well contained 112.5µl of the BCA solution (ratio Part A to Part B 1:50) and 12.5µl either BSA standard or sample. The plate was incubated for 30 minutes at 37°C. Depending on the concentration of proteins the colour of the solution changed to a deep purple. The absorbance was measured at 562nm in a multiplate reader and compared to the BSA standard curve to calculate the protein concentration. Each set of samples was adjusted on the same protein concentration, by dilution in 1% SDS protein lysis buffer. For the gel electrophoresis each sample consists of 30µl sample and 10µl of 4x loading buffer, containing DTT (ration 6:1), denaturating the proteins, for size dependent separation. To ensure complete denaturation, the samples were boiled for 5 minutes at 100°C prior to performing the gel electrophoresis.

SDS Gel Electrophoresis

For separation of the proteins by size 10% polyacrylamide separating gels were cast. The separation gel was cast inside gel casting chambers and to exclude oxygen from interfering with the polymerisation covered with isopropanol. After the gel was fully set, the isopropanol was removed, and remaining rest were washed out with H_2O. The

stacking gel was poured over the separation gel and the combs were inserted. The complete cast gels were transferred into a gel electrophoresis chamber and the protein samples were loaded, as a standard 10µl of Precision plus protein standard was added to each first pocket of the gels. The electrophoresis followed in 1x SDS page running buffer, first at 90V until the samples reached the separating gel and upon entering changed to 150V.

Table 19: Recipes for the separation and stacking gel

	Separation gel (10%)	**Stacking gel**
ddH_2O	1.5ml	1.4ml
30% Acrylamide	3.3ml	0.5ml
Separation buffer (pH 8.8)	5ml	-
Stacking buffer (pH 6.8)	-	2ml
10% APS	100µl	40µl
TEMED	10µl	4µl
Total [ml]	**10ml**	**4ml**

Protein Transfer and Blocking

A wet tank transblotting system was used to transfer the proteins off the polyacrylamide gel onto PVDF membranes. The PVDF membranes were activated in methanol, blotting paper and sponges were prepared in 1x blotting buffer. To separate the stacking gel from the separation gel, first one glass plate was removed and then, using a paper towel, the stacking gel could be discarded. The separation gel containing the loaded protein samples was washed in 1x blotting buffer. Now the sandwich blots were assembled, between one sponge, one blotting paper on each side, the gel and the membrane were stacked. To ensure the complete transfer of the proteins, any air between the membrane and the gel should be avoided. The protein transfer was carried out at 100V for 2h. Afterwards, the membrane was removed and placed in a falcon tube containing 5% milk powder in PBS-T and rotated for 1h at room temperature, thereby blocking any nonspecific antibody binding sites.

Immunodetection

Each primary antibody used was diluted according to Table 4. After blocking the membranes, they were washed with PBS-T three times and incubated with the primary

antibody, either ON at 4°C or for 1h at RT. Again, three washing steps with PBS-T followed, then 5ml of secondary antibody solution was added to each falcon tube and incubated for 30min–1h at RT. A last washing step with PBS-T followed before adding ECL solution to the membranes and placing them into the BioRAD Developing system, were the chemiluminescent signals were detected. The membranes were afterwards washed again and reused with new primary and secondary antibodies. If not longer required, the membranes were frozen away at -20°C.

2.2.10. siRNA Transfection

All siRNA transfections were performed following the Lipofectamine RNAiMAX Reagent Protocol (Protocol Pub. No. MAN0007825 Rev.1.0; life technologies). In 6 well plates $1.25x10^5$ cells were seeded and on the next day transfected with either control siRNA or two different siRNAs against Rb. For every well 9µl of the Lipofectamine RNAiMAX Reagent was diluted in 150µl Opti-MEM and in a second tube 3µl of a 10µM siRNA solution was as well diluted in 150µl Opti-MEM. The siRNA solution was added into the Lipofectamine solution and after a vortexing step incubated for 5 minutes. Then of the 300µl total volume 250µl was added to the well. At the next day the plates were infected as described before and samples were taken 4hpi, 24hpi and 48hpi. To analyse the effectivity of the siRNAs protein samples were collected 24 and 48 hours after the transfection. To ensure a higher protein concentration for each sample, the lysates were a collection of two, equal treated wells.

2.2.11. Immunofluorescence

Viral infection leads to the accumulation of YB-1 in the nucleus (Holm, Bergmann et al. 2002), to investigate this effect under different therapy approaches, immunofluorescence staining against YB-1 were conducted. Glioblastoma cells were seeded with a concentration of $2.5x10^4$ c/well on glass coverslips, precoated with a 0.1% gelatine/PBS solution, in 24 well plates. On the next day, the cells were treated with inhibitors. After overnight incubation, the cells were either directly infected or underwent radiotherapy, 6 hours before infection. The cells were infected in 150µl infection medium, without FCS and 1hpi fresh medium containing the respective inhibitors was added. After 24 hours the plates were fixed by first aspirating the medium and one washing step with PBS. As a fixative solution a 1:1 Methanol-Acetone solution was used. The plates were incubated for 1 hour at -20°C, then the fixative was removed and the plates were blocked using a 3% BSA/PBS solution for 1 hour at room

temperature to saturate any unspecific epitope bindings. The primary anti-YB-1 antibody (EP2708Y) was diluted 1:1000 in the blocking solution and the plates were incubated for 1 hour at room temperature. Afterwards the antibody solution was aspirated and the plates washed three times with 3% BSA/PBS. The secondary antibody tagged with an Alexxa488-fluorophore, again diluted 1:500 in 3% BSA/PBS was applied to each well and the plates incubated for 1 hour at RT, in the dark. After three more washing steps the coverslips were removed from the wells and using ProLong mounting medium (containing DAPI for nuclear staining) put on glass slides. The mounting medium dried overnight and the edges of the cover slips were sealed using nail polish. Pictures were taken using the Evos M5000 microscope and analysed using the ZEN 2012 (Zeiss) program.

2.2.12. Establishing primary glioblastoma cell lines from patient material and isolating PBMCs of patient blood

Of eight patients at the neurosurgery department at the Klinikum rechts der Isar (MRI, Munich) tumor material and 150ml blood was collected. The surgical specimen were dissected and converted into primary cell cultures. The blood was processed to isolate the peripheral blood mononuclear cells (PBMCs).

Establishing primary glioblastoma cell lines

The isolation of single cells from glioblastoma specimen was based on the protocol of (Hasselbach, Irtenkauf et al. 2014).

The tumor specimen were collected in 15ml falcon tubes filled with 4°C cold isotonic saline solution and transported into the laboratory for further dissection on petri dishes. Using scalpels and tweezers necrotic tissue was removed and the sample placed on a fresh petri dish already containing PBS. Here the tissue was minced with two scalpels before transferring it into a 50ml tube. To further disassemble the tumor the solution was pipetted several times. The sample was centrifuged at 500rcf for 5 minutes and the pipetting was repeated up to 100 times. Following another centrifugation step, the already dissected sample was enzymatically minced using 4ml enzymatic tissue dissociation solution per gram tumor specimen (5ml 0.05% Trypsin/EDTA solution, 2.5 ml Collagenase IV (2000U/ml), 2.5ml HBSS calcium and magnesium free) for 30 minutes at 37°C. The enzymatic digestion was stopped with twice the volume of stop solution (5ml trypsin inhibitor, 5ml DMEM/F12, 2µl DNase I). To separate the cells from

undigested debris, the sample was filtered through a 40µm cell strainer and pelleted down at 800rcf for 5 minutes. The supernatant was aspirated, and the sample resuspended in DMEM/F12 medium This step was repeated two more times, before seeding the cells in low concentration in DMEM/F12 growth medium, containing growth factors (LIF, FGF and EGF) and B27 supplement. The samples were grown without serum in suspension conditions to induce spheroid formation. The medium was changed weekly, by transferring the cells into 15ml falcon tubes, sedimenting by gravity, removing half the volume and addition of fresh growth medium.

Isolation of PBMCs from whole patient blood

Of each patient 150ml whole blood was collected and mixed with twice the amount of 2mM EDTA/PBS. In 50ml tubes 15ml bicoll solution was prepared and carefully 30ml of the whole blood/PBS solution was layered on top. The falcon tubes were centrifuged at 1200rcf for 30 minutes without brakes. The white layer containing the leukocytes of two tubes were combined in one 50ml falcon tube and diluted up to 50ml in PBS. The tubes were centrifuged again for 10 minutes at 900rcf. The supernatant was aspirated. To remove all red blood cells the cells were incubated in 2ml ACK buffer solution for 10 minutes and again diluted in PBS. Of the solution 10µl was collected mixed with 10µl Trypan blue and counted using a Neubauer counting camber. After another centrifugation step the cells were resuspended at a concentration of $5x10^7$ cells/ml in freezing medium (RPMI, 10%FCS, P/S) containing 10% DMSO. The PBMC samples were put in a freezing container at -80°C and after one day transferred into the liquid nitrogen tank.

2.2.13. Standard T-Test and ANOVA

Graphs were plotted in GraphPad Prism 5 as their mean and corresponding standard deviation (S.D.). For statistical analysis 2-tailed Students t-tests or 2 way ANOVA were conducted. A p-value of ≤ 0.05 was considered as statistically significant.

2.2.14. Production of chemical competent *E. coli* bacteria

First one colony of Top10 or DH5α grown on an LB plate was inoculated in 2ml LB liquid medium and shaken overnight at 37°C. A 0.1M $CaCl_2$ and 0.1M $CaCl_2$ containing 15% Glycerol were prepared and kept in the fridge at 4°C until use. In 100ml LB medium 1ml overnight culture was diluted and shaken vigorously until a OD_{600} of 0.25-0.3 was measurable. The culture was put on ice for 15 minutes. The solution was

centrifuged at 3.300rcf for 10 minutes at 4°C. The supernatant was discarded, and the cell pellet was resuspended in 30ml 0.1M $CaCl_2$ solution. The cells were incubated on ice for 30 minutes, before another centrifugation step followed. The supernatant was removed, and the pellet resuspended in 6ml $CaCl_2$ containing 15% glycerol. The solution was pipetted as 50µl aliquots in 1.5ml tubes and stored at -80°C until further use.

2.2.15. Virus generation

The generation and production of WT 2xE2Fm and XVir-N-31 2xE2Fm was based on previous viral constructs generated in the lab and done with the help of Klaus Mantwill.

Plasmid restriction and ligation

Using the program serial cloner, restriction sites in the plasmids were identified and cut using the corresponding restriction enzymes and buffers. The restrictions were performed ON and for backbone restrictions an alkaline phosphatase was used to leading to a dephosphorylation of the restriction sites, disallowing self-ligation of the backbone in the ligation step.

For the ligation, both insert, and backbone were first purified following the phenol chloroform extraction method and the DNA concentration measured using a Nanodrop. Then both fragments were ligates using a T4 DNA ligase and its corresponding buffer overnight. The samples were again purified before being used to transform competent *E. coli* bacteria.

E. coli transformation and colony screen

The production of plasmids was done in Top10 or DH5α *E. coli* strains. Therefore 10µl of purified ligation preparation was mixed with 50µl bacteria solution and put on ice for 10 minutes. To allow penetration of the bacterial membrane a heat shock of 46°C was applied for 10 seconds, the tubes were afterwards directly transferred to ice and incubated again for 10 minutes. The bacteria was multiplied by adding 300µl of LB medium and shaking rigorously for 1 hour at 37°C. The bacteria solution was plated on LB Agar plates containing the corresponding selection antibiotic expressed on the plasmid backbone over night until colonies grow.

Colony PCR was performed to preselect clones containing the correct insert. A PCR master mix was prepared containing the GoTaq master mix, the forward and reverse

primers. Of the master mix 24µl were put into 100µl PCR tubes and in each tube a colony picked dipped into the master mix solution and then put in 700µl LB Medium (+antibiotic) in 2ml tubes and incubated at 37°C, rigorously shaken. The PCR was conducted, and the products analysed on a 1% agarose gel (containing EtBr). The length of the product was compared to a DNA ladder and the estimated product length, calculated with serial cloner.

Plasmid production and purification

The colonies grown on LB agar plates were transferred into 2ml tubes containing 700µl LB medium (+antibiotic). If more plasmid should be produced the colonies were put in 15ml tubes containing 5ml of LB medium (+antibiotic). The bacteria were then grown while shaking at 37°C, until cloudiness was observed. Now the solution was split, 700µl were used for the glycerol stocks (10% glycerol) the rest was centrifuged down for 10 minutes at 3000rcf. The supernatant was removed and the pellet purified either using the monarch kit (NEB Biolabs) or Quiagen Midi or Maxi Kit.

The pellets were resuspended in 200µl of P1, then 200µl of P2 was added and the tube shaken. After addition of 200µl P3 (+ one drop chloroform) the tubes were centrifuged for 10 minutes at 15.000rcf. Then the supernatant was loaded on pre equilibrated (with QBT) columns, washed twice with QC buffer and eluted in QF buffer. The concentration of the plasmids were measured using the Nanodrop.

Sequencing and restriction analysis

To ensure correct insertion and orientation in the plasmids they were analysed using both restriction analysis and for the final construct also by sequencing. As described above restriction enzymes were used to check the correct length of both inserts and the complete plasmids. If the correct band were achieved for the final constructs the mutated inserts were sequenced to ensure no mutations occurred during the construction and production of the plasmids.

2.2.16. Virus production

Both new constructs, like WT or XVir-N-31 2xE2Fm and already established constructs like XVir-N-31 were produced on regular bases in the laboratory.

Transfection of linearized viral plasmids

HEK293 cells were transfected with linearized viral plasmids. First $5x10^4$ HEK293 cells were seeded in 12 well plates. After 24 hours these cells were transfected following the FuGene protocol.

Generation of crude virus stocks (G1 and G2 stock)

A successful transfection leads to cytopathic effects (CPE) after 7 to 14 days. Both the cells and the supernatant were harvested, to open the cell membrane without harming the infectivity of the viral particles three freeze thaw cycles were performed. The detritus was removed by centrifuging the samples at 600rfc for 5 minutes. The infectious particles remain in the supernatant, which were transferred into fresh 1.5ml tubes. Then the aliquot was split, one half was used to infect a 15cm plate containing HEK293 cells at a confluency of 50%, the other half was mixed with glycerol and stored as G1 stock at -80°C. When CPE could be observed in the 15cm plate, cells and supernatant were collected, underwent three freeze and thaw cycles, and a centrifugation step at 600rcf for 5 minutes. The supernatant was mixed with glycerol and stored in aliquots as -80°C as the G2 stock.

Virus production

To produce virus, freshly thawed HEK293 cells were used. HEK293 cells were seeded in 20 15cm plates and at a confluency of 80% infected with 20 MOI of the G2 stock. For each plate the G2 stock was diluted in 4ml infection medium. First the growth medium on each plate was aspirated and the cells carefully layered with 4ml of infection medium containing the G2 stock. The plates were incubated for 1h at 37°C and carefully swivelled every 15 minutes. After 1 hour 10ml of growth medium was added to each plate. Two days after infection, at the first sign of CPE the medium and cells were collected carefully, not destroying the cells and centrifuged at 1000rcf for 10 minutes. The supernatant was discarded and the pellet was resuspended in 8ml lysis buffer. Three freeze thaw cycles followed to release the viral particles and the solution was either stored at -80°C until caesium chloride purification of directly processed.

Virus purification

To purify the virus, first a centrifugation step at 3000rcf for 15 minutes was used, separating virus from cellular debris. The supernatant was withdrawn into a fresh tube and incubated with 12.5U/ml Benzonase and 1mM $MgCl_2$ for two hours at room temperature. Benzonase digests any free DNA in the solution, thereby destroying the cellular DNA. To isolate pure virus concentrate a caesium chloride density gradient purification was used. In ultracentrifuge tubes two caesium chloride solutions were pipetted on another. First 17ml of a 1.33g/ml was pipetted and carefully layered with 9ml of a 1.45g/ml caesium chloride solution. On top of the two caesium chloride parts, the virus solution was added, and the tubes centrifuged using a Avanti JXN-30 ultracentrifuge at 53.000rcf for 3 hours at 10°C. A clear white band containing the virus forms in the ultracentrifuge tube and was removed using a syringe. To further increase the purity of the virus solution, a second caesium chloride density gradient ultracentrifugation step followed, again at 53.000rcf for 18hours. The final product was obtained, using a syringe, and desalted, using PD-10 desalting columns. The freshly produced virus was obtained in virus storage buffers, aliquoted and stored at -80°C.

3. Results

3.1. Virotherapy

To analyse the potential of the oncolytic Adenovirus XVir-N-31 on glioblastoma multiforme (GBM) cell lines potency assays were performed. Three different glioblastoma cell lines were infected with increasing MOIs of XVir-N-31 and the cell viability was analysed 5 days post infection (d.p.i.). U87 cells shows good infectivity with XVir-N-31 and already a strong decrease in cell viability after infection with 10 multiplicity of infections (MOI). In LN229 the viability does not follow a direct decrease in viability, instead at low MOIs the relative absorption is increased compared to the control. For T98G the results resembled the decrease of cell viability in U87 cells, but only at higher MOIs. All cell lines were effected of XVir-N-31 at levels under 100 MOI.

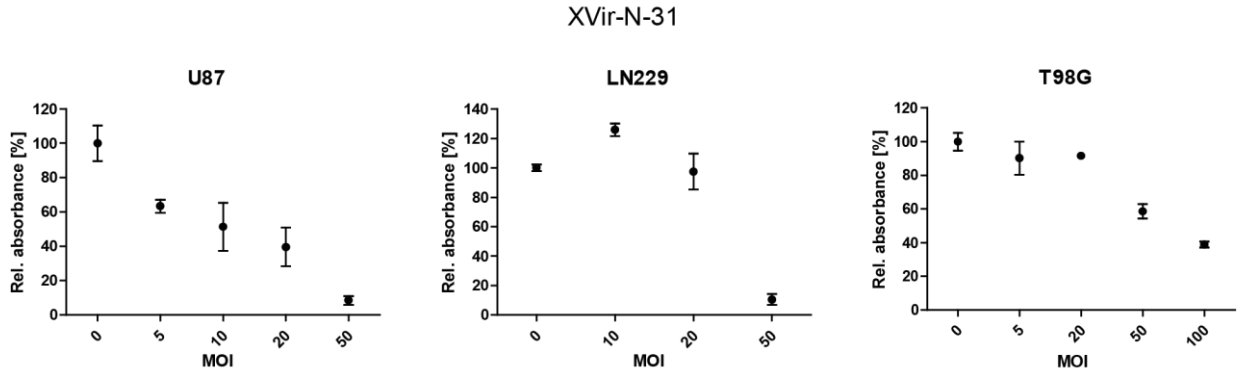

Figure 7: **Effectivity of oncolytic virotherapy in glioblastoma multiforme cell lines.** GBM cancer cell lines were infected with different MOIs of XVir-N-31 and analysed 5 days post infection. Error bars S.D.

3.2. Radiation and Chemotherapy in combination with virotherapy

The classical treatment regime for glioblastoma multiforme involves resection followed by radiation and chemotherapy. To assess the effects of radiation and chemotherapy in a combinatory approach with oncolytic adenovirus treatment, we investigated combinations and analysed different viral parameters.

3.2.1. Radiation

The combination of radiation with oncolytic virotherapy was shown in Bieler et al. 2008 (Bieler, Mantwill et al. 2008). Therefore, we wanted to investigate the effectivity, using our oncolytic adenovirus XVir-N-31 in three different GBM cell lines.

The effects of radiation on the cell cycle

Virus effectivity is influenced by the cell cycle state present at the time of infection. First, we wanted to analyse the effect of radiation on the cell cycle. U87 cells showed no clear increase in any cell cycle phase. In LN229 an increase in the portion of G1 cells could be observed, the increase disappeared after 48 hours. For T98G cells the increase in G1 cells at 24 hours post radiation was small and again gone at the 48 hour mark.

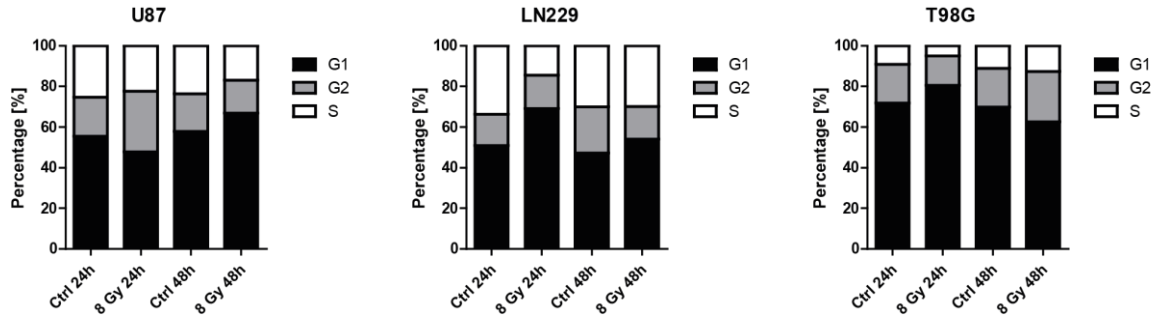

Figure 8: **Effects of radiation on the cell cycle**. GBM cell lines were radiated with 8 Gy and after 24 and 48 hours the cell cycle was analysed using FACS. Cell cycle phases are shown relative to the number of counted cells in all three phases.

Viral potency of XVir-N-31 can be increased in combination with radiation

Using radiation, which leads to an increase in YB-1 in the nucleus, the potency-effects of XVir-N-31 were analysed in three different cell lines. Radiation alone influenced all three cell lines. The strongest effect was observed in U87 cells. While in U87 and T98G the virus alone was able to decrease cell viability, XVir-N-31 showed little effect on LN229 cells. In the combinational approach only in U87 cells the cell viability decreased further. In LN229 and T98G a combination of radiation and virus, did not successfully improve the cell killing.

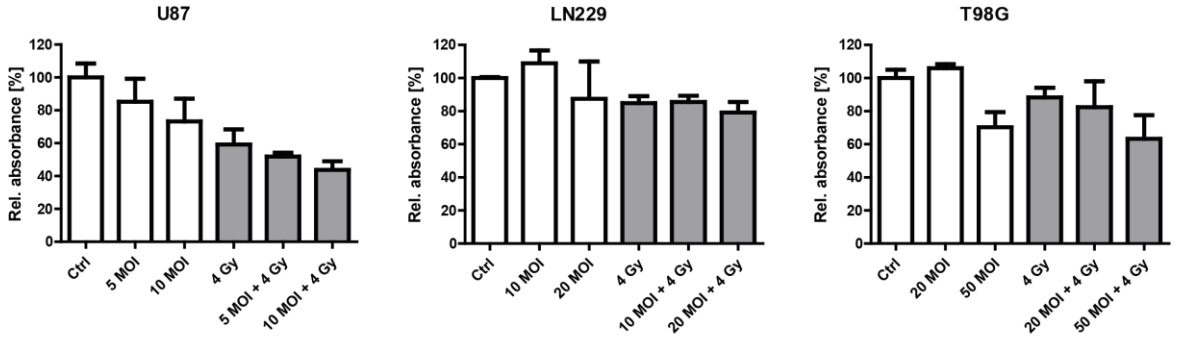

Figure 9: **Viral potency only increases in one cell line in combination with radiotherapy.** In three cell lines the effect on cell killing of radiation in combination with XVir-N-31 treatment was observed. Cells were treated with 4Gy radiation and 6 hours later infected with XVir-N-31. After 4d.p.i. the cells were fixed and stained. Error bars S.D.

Viral replication was increased when cells underwent radiation therapy

A second aspect of viral effectiveness is its ability to replicate. To analyse if the effects of on cell viability are accompanied by enhanced viral replication, all three glioblastoma cell lines were first radiated with 6 Gy, according to our previous publication (Bieler, Mantwill et al. 2008) and then infected with XVir-N-31.

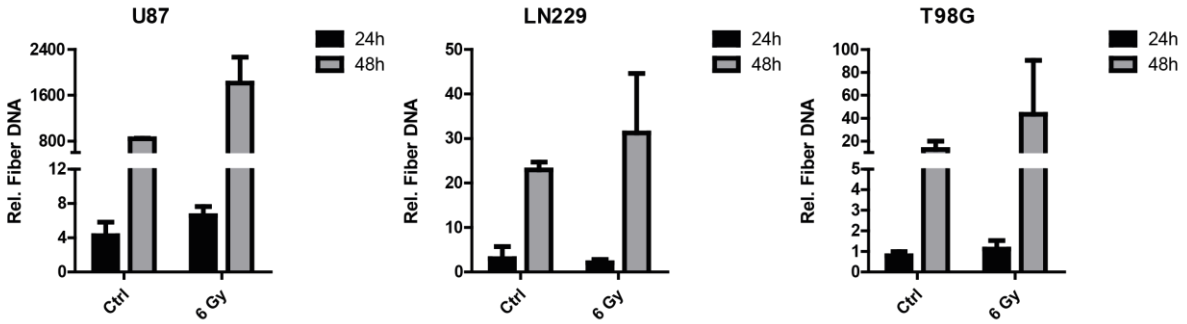

Figure 10: **Radiotherapy increases viral replication with U87 cells.** Cells were radiated with 6 Gy and 6h later infected with XVir-N-31 (U87, LN229: 20 MOI; T98G: 50 MOI). Viral replication was analysed at indicated timepoints. Error bars S.D.

In both LN229 and T98G there was no significant difference between the control group and the samples, which were radiated, at 24h and 48h timepoints, but there is a trend observable. In U87 cells the replication was doubled compared to the control group at 24h and tripled at 48h.

3.2.2. Chemotherapy

Besides resection and radiation there is a third treatment option. The used chemotherapeutic for GBM is Temozolomide (TMZ), a blood brain barrier penetrable agent. GBM becomes quickly resistant against TMZ in vivo and Glioblastoma cell lines are as well highly resistant against TMZ, making it inadequate for single use. Here we try to combine TMZ again with virotherapy to overcome the tumor resistance. LN229 is classified as TMZ sensitive, whereas both U87 and T98G are classified as TMZ resistant (Gaspar, Marshall et al. 2010, Taspinar, Ilgaz et al. 2013).

Temozolomide does not change the cell cycle status of glioblastoma cell lines

First we wanted to examine the capability of TMZ to push the three GBM cell lines into an G1 arrest, within the first 24 hours. This was done to analyse the cell cycle state at the timepoint of infection, which was 24 hours post treatment.

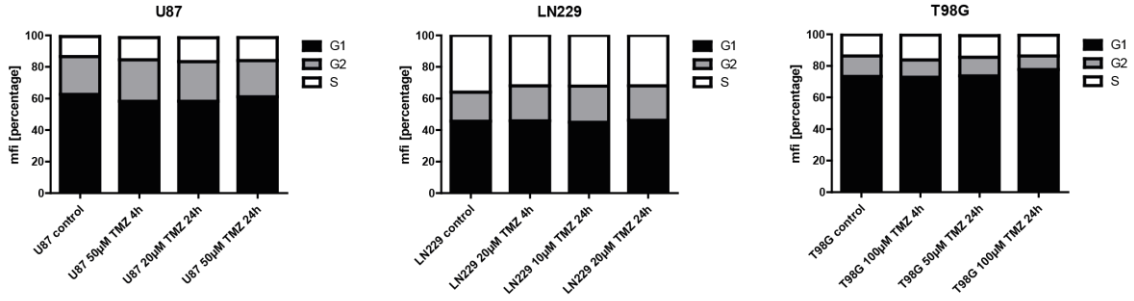

Figure 11: **TMZ does not alter the cell cycle state of all three GBM cell lines tested.** Cells were treated with two different concentrations of TMZ each. For the higher concentration, the first sample was assessed at 4 hours post treatment. Following the samples after 24 hours, the timepoint of an infection.

All three cell lines showed no alteration of the cell cycle at any timepoint and with any concentration of TMZ used. This indicates that TMZ has no direct influence on the cell cycle status within the first 24 hours post treatment. Therefore, no G1 arrest contributes to the induction of viral cell death or replication.

Expression of cell cycle proteins are not altered by TMZ

To validate the results of the cell cycle status, western blots were performed in two GBM cell lines. Here we checked the expression of cell cycle related proteins.

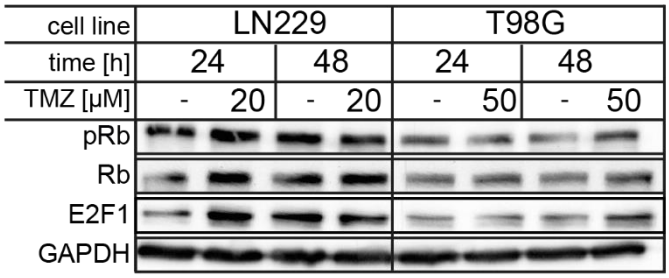

Figure 12: **Treatment with TMZ does not alter cell cycle related proteins in two GBM cell lines.** Cells were treated with TMZ and samples were taken after 24h and 48h. GAPDH acts as a housekeeping control.

In both LN229 and T98G for Rb, pRb and E2F1 there were no alterations in the expression of protein levels, both at 24h and 48h after treatment. This confirmed the results of the FACS analysis.

Combination of TMZ and virotherapy leads to increased potency in two cell lines

Next we investigated the effects of TMZ on cell viability in combination with XVir-N-31. We therefore treated cells with indicated amounts of TMZ and infected them with different MOIs, based on MOIs described above.

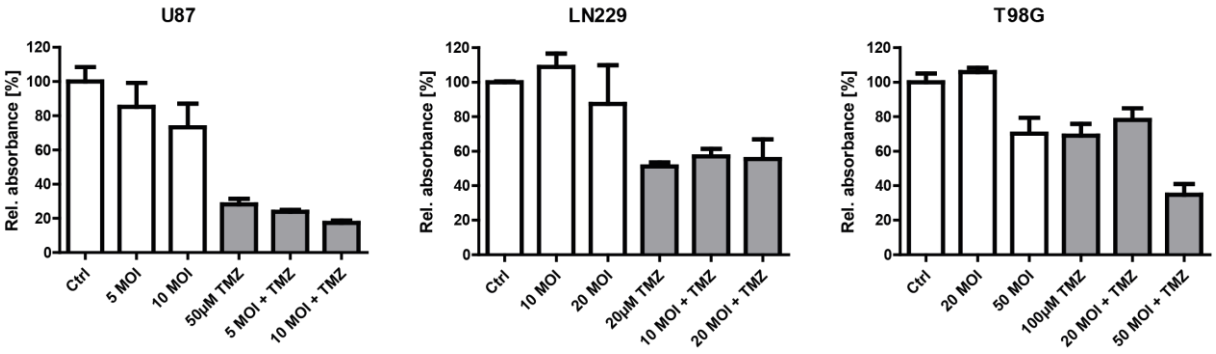

Figure 13: **The viral potency is increased in combination with TMZ in two of three GBM cell lines.**

The effect of TMZ alone varied in all three cell lines. In U87 cells 50µM TMZ was potent, leading to a strong decrease in cell viability. This effect could be increased only by a

small portion in combination with virus but led to an 80% decrease in cell viability with TMZ and 10 MOI. In LN229 low MOIs between 10 and 20, did not alter the cell viability. The TMZ treatment halved the cell viability, but there was no increase when applied in combination with virus. Here higher MOIs could lead to a stronger decrease in cell viability. In T98G cells 100µM TMZ only decreased the cell viability by 30%, this was an equal strong effect as if a monotherapy with XVir-N-31 at 50 MOI was applied. The combination of both 100µM TMZ and 50 MOI of XVir-N-31 did improve the therapeutic effect and decreased cell viability to 40%.

Increase in viral replication can be observed in two GBM cell lines in a combination treatment of TMZ and XVir-N-31

Following the viral potency results we sought to investigate the effects of TMZ treatment on viral replication of XVir-N-31.

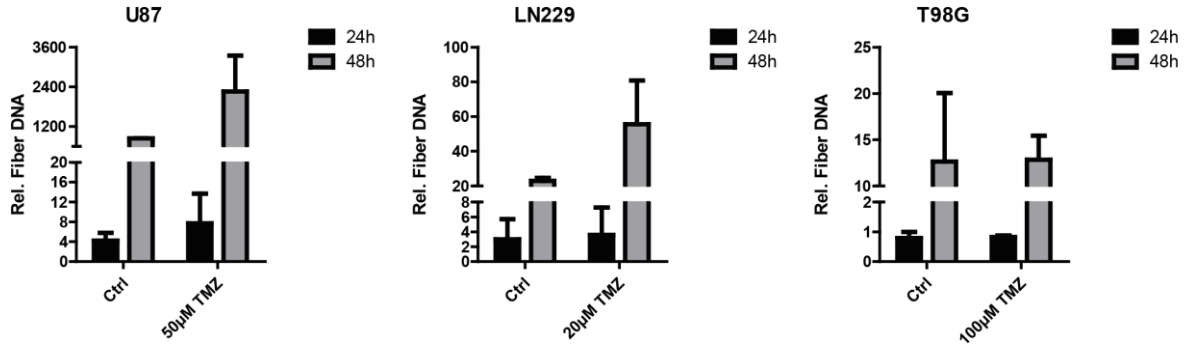

Figure 14: **Viral replication is increased upon TMZ treatment in two of three GBM cell lines.** Cells were pre-treated with TMZ and 24 hours later infected. All values are relative to their 4 hour control. Error bars S.D.

In U87 the viral replication was tripled compared to the control at the 48 hour mark. The same was observed in LN229 cells. Interestingly these results were not observed in the viral potency assays of LN229. This could be, because LN229 can survive long even when heavily infected and tend to bloat before apoptosis, misleading in potency assays. In T98G the viral replication was not increased in comparison to the control, at both 24h and 48h. This showed that higher viral potency could also be achieved even when the viral replication is not increased.

Viral particle formation is increased in all three cell lines in a combinatory approach of TMZ and virotherapy

Viral particle formation is a key component in virotherapy, allowing not only the reinfection of previously non infected cells, but in vivo also strongly boosting the immune system, thereby retargeting it to the previously “cold” tumor. We therefore analysed the production of infectious particles in the three GBM cell lines.

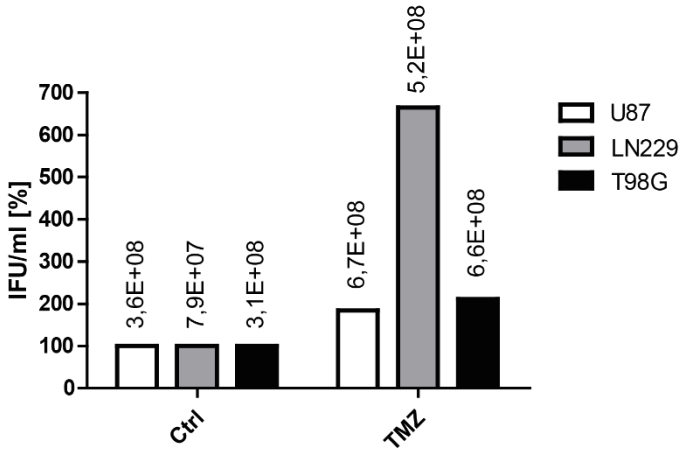

Figure 15: **Infectious viral particle formation was increased in all cell lines in a combinatory approach of TMZ and XVir-N-31.** Cells were pretreated with TMZ (U87: 50µM, LN229: 20µM, T98G: 100µM) and 24 hours later infected with XVir-N-31. After 72 hours the cells were scraped of the plate and underwent three freeze thaw cycles. The supernatant was used to reinfect HEK293 cells and after 40 hours the plates were stained, and the infected cells were counted. All values are relative to their control group. Values on top of the bars are IFU/ml

The production of viral particles is doubled in U87 and T98G. In LN229 interestingly the control value of infectious particles was three times lower compared to U87 and T98G, but upon TMZ treatment the particle formation is increased six fold and the total value of particles produced per ml was close to both other cell lines.

3.2.3. Combination both radiation and chemotherapy with oncolytic virotherapy

In the classical treatment regime for glioblastoma multiforme resection is followed by radiotherapy and chemotherapy. Having already checked both monotherapies in combination with oncolytic virotherapy. Here we investigated whether combing the classical therapy approach with virotherapy could lead to a better outcome, based on viral parameters, like viral potency and replication.

First we analysed the viral potency of a triple therapy with Radiation, TMZ and XVir-N-31.

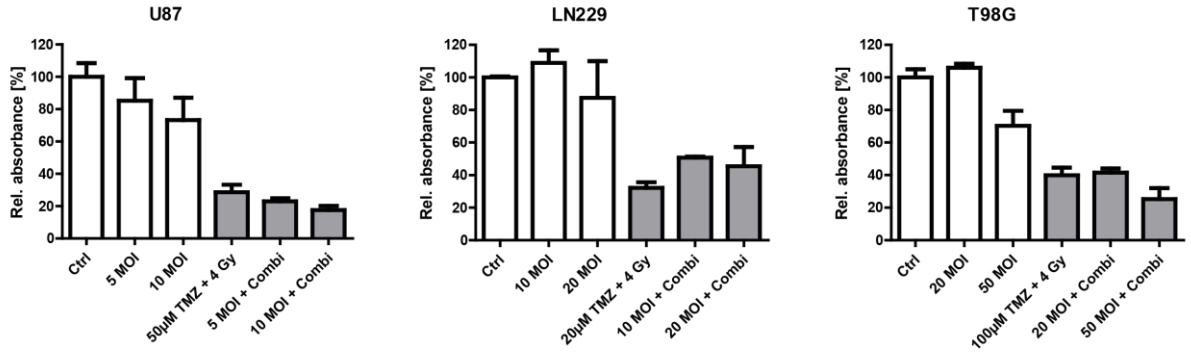

Figure 16: **Viral potency of XVir-N-31 in combination with radiation and chemotherapy.** Cells were pretreated with TMZ, on the next day radiated and 6 hours later infected. Error bars S.D.

The combination of TMZ and Radiation led to strong effects on the cell viability in all cell lines. Interestingly as observed before both U87 and T98G had increased cytotoxicity in a combinational approach with virotherapy. In LN229 the cell viability was not decreased. In comparison to either double therapy (Radiation + XVir-N-31 or TMZ + XVir-N-31), the effects were stronger compared to radiation and viral therapy. Compared to the TMZ treatment regime no strong increase was observable.

Next, we analysed the effects of the double therapy on the viral replication in the three GBM cell lines.

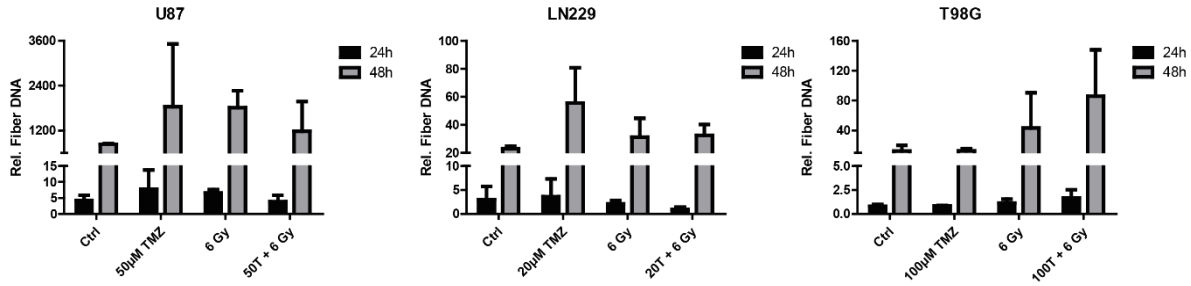

Figure 17: **Analysis of viral replication in triple therapy, compared to the monotherapies.** The cells were treated with TMZ, on the next day radiated and 6 hours later infected with XVir-N-31 (U87, LN229: 20 MOI; T98G: 50 MOI). Error bars S.D.

In U87 and LN229 cells the combinational therapy did not lead to an increase in viral replication compared to the TMZ treatment. Compared to the control group in all three

cell lines the combinational approach displayed higher values. Interestingly only in T98G cells the virus benefited in its ability to replicate. This could be based on the differences of the cell lines and the severe adverse effects of the combination of radiation and chemotherapeutic. T98G cells displayed the highest resistance against both radiation and chemotherapeutics, which also allowed the highest increase in potency and replication of XVir-N-31.

The combination of oncolytic virotherapy with radiation and chemotherapeutics showed good results, but the improvements were not highly significant. A new therapeutical approach was needed to further improve the virotherapy. Our recent findings described in Koch et al., 2021 opened a new therapeutic approach, for the treatment of bladder cancer in combination of CDK4/6 inhibitors and oncolytic adenovirus constructs.

3.3. CDK4/6 Inhibitors: In combination with virotherapy

There are several specific CDK4/6 inhibitors available, namely Palbociclib (PD-0332991), Abemaciclib (LY2835219) and Ribociclib (LEE011). All three are blood brain barrier penetrable (Miller, Traphagen et al. 2019)), as well as already used in clinical trials (Wu, Zhang et al. 2020). In this project we worked with two different CDK4/6 inhibitors, namely Abemaciclib and Ribociclib.

3.3.1. Abemaciclib

Abemaciclib was the first CDK4/6 inhibitor used in this project. First, we investigated the IC_{50} values in three different glioblastoma cell lines. Then we analysed its capability for G1 Arrest and further investigated its capability to enhance viral potency, replication, and infectious particle formation.

Analysing the IC_{50} values of Abemaciclib in three glioblastoma cell lines

CDK4/6 inhibitors led to cell growth arrest and therefore decreased absorption, in comparison to the control group.

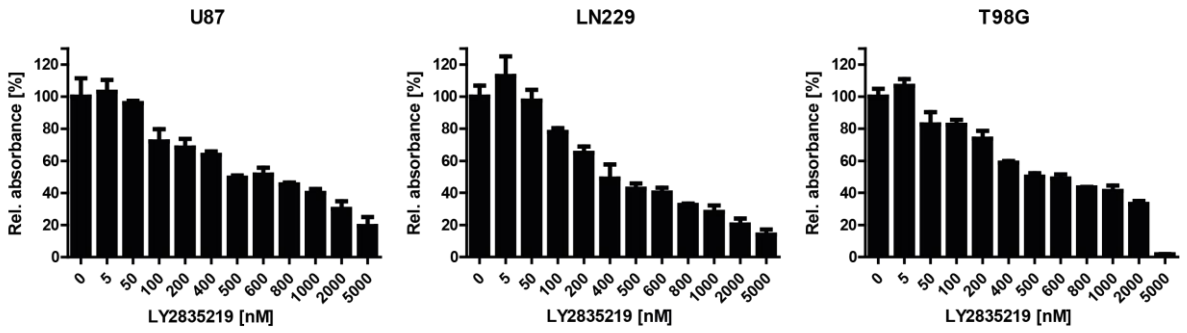

Figure 18: **Analysing the IC_{50} values of LY2835219 in three different glioblastoma cell lines.** Cells were seeded in 96 well plates, after one day treated with LY2835219 and incubated for four days, before fixation with 10% TCA and staining with SRB. The absorption was measured using a plate reader. Error bars S.D.

Only in higher concentrations cytotoxicity was observed. The effects of Abemaciclib on all three cell lines was comparable with IC_{50} values of 500nM LY. In U87 and LN229 the highest concentration of 5µM LY led to a decrease of cell viability by 80%. In T98G a concentration of 5µM proved to decrease the cell viability nearly 100%. For further combinatory experiments 100nM LY as the IC_{80} value and 1µM LY, showing a strong effect, were chosen.

Abemaciclib leads to a G1 Arrest in two glioblastoma cell lines

Following the monotherapy of Abemaciclib on cell viability, we analysed the functional effects of the CDk4/6 inhibitor on the cell cycle status of glioblastoma cell lines.

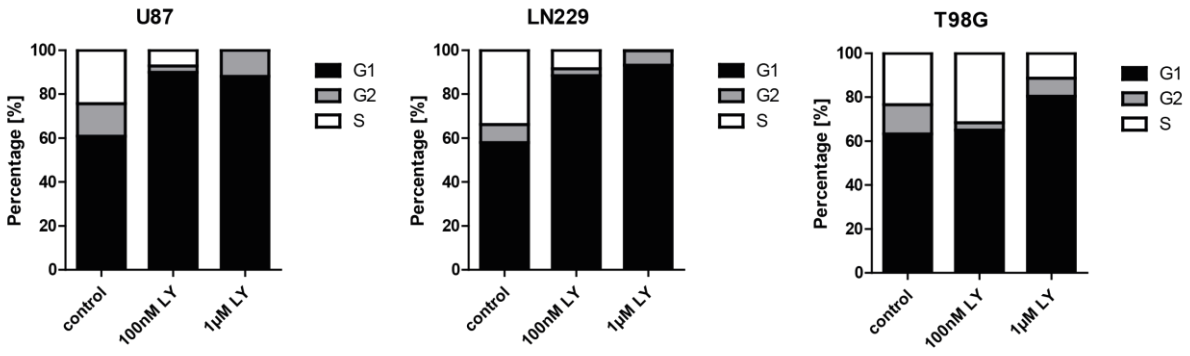

Figure 19: **CDK4/6 inhibitor LY2835219 led to G1 arrest in two GBM cell lines.** Cells were treated with LY2835219 and 24 hours later fixed, stained with PI and analysed for their cell cycle status.

CDK4/6 inhibitor Abemaciclib led to a G1 Arrest in U87 and LN229 cells, at concentrations of 100nM and 1µM. In T98G cells no clear G1 Arrest could be observed with 100nM and 1µM LY, but there was an increase in the G1 phase of 20% compared to the control and 100nM LY samples.

The CDK4/6 Inhibitor Abemaciclib increases the viral potency of XVir-N-31

After confirming the effects on the cell cycle in two cell lines, we focused on the improvement of oncolytic virotherapy in combination with Abemaciclib. First we investigated the viral potency and its effectiveness to reduce cell viability after pretreating cell with 100nM and 1µM LY2835219.

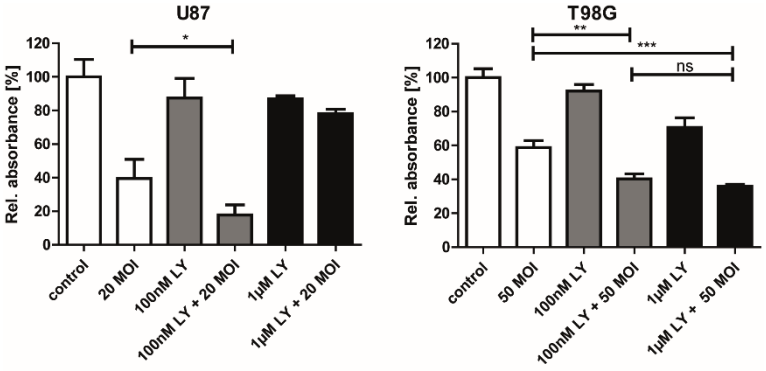

Figure 20: **Reduced cell viability in a combinatory approach of Abemaciclib with the oncolytic adenovirus XVir-N-31.** Cells were pretreated with Abemaciclib and infected with indicated MOIs, 24 hours later. The plated were fixated 4d.p.i. Error bars S.D., statistic analysis is done via students t-tests (ns>0.05; * p≤0.05; ** p≤0.01; *** p≤0.001)

XVir-N-31 as a monotherapy proved ineffective, therefore we analysed the combinatory effects of Abemaciclib with virotherapy. In U87 cells, CDK4/6 treatment with both 100nM and 1µM of Abemaciclib did not show effects as strong as observed in the IC_{50} experiments, 1µM LY did not lead to a decrease of cell viability by over 50%. In combination with virus 100nM LY decreased the cell viability up to 80%, significantly higher than 20 MOI alone. The higher concentration of 1µM LY diminished the combinatory effects of CDK4/6 inhibitor and virotherapy. In T98G no G1 arrest was observed but highly significant benefit on cell killing in combination with LY was observed at both 100nM and 1µM Abemaciclib.

High concentrations of Abemaciclib diminish effective viral replication and particle formation

Based on these results, we investigated the effects of higher concentrations of Abemaciclib on viral replication in both cell lines that reacted to a combinatory approach of CDk4/6 inhibitor and virotherapy.

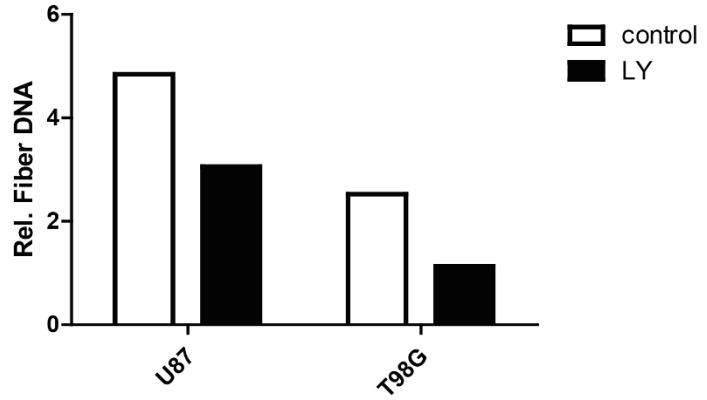

Figure 21: **Using 1µM of LY at 24 hours diminished effective viral replication.** Cells were pretreated with 1µM of LY and infected at the next day. At 4h and 24h samples were taken and the viral replication analysed.

Interestingly in both cell lines U87, showing no beneficial effect of a combinatory treatment of Abemaciclib and XVir-N-31 in decreasing the cell viability and T98G where a benefit could be observed, no improved viral replication was shown. Higher concentrations of LY interfered with the viral replication, this could also decrease viral particle formation.

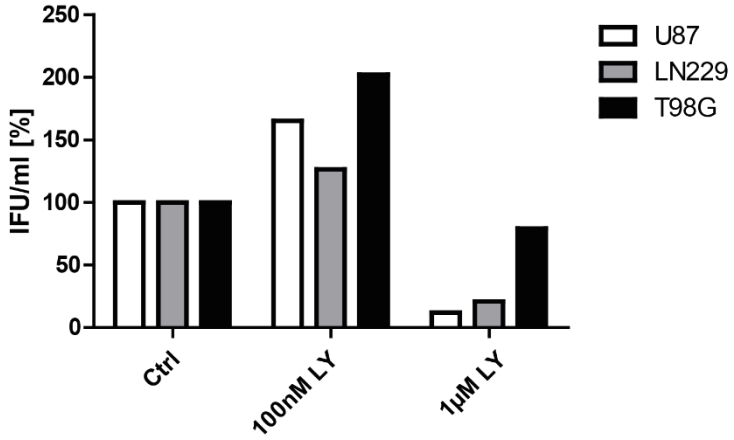

Figure 22: **Particle formation of XVir-N-31 is increased at low concentrations of Abemaciclib, but 1µM LY diminished the particle formation in all tested cell lines.** Cells were treated with Abemaciclib and infected at the next day (U87, LN229: 20 MOI; T98G: 50 MOI), three day later samples were collected and tested using HEK293 cells, infected with the supernatant.

The results observed in both viral potency assays and replication could be confirmed, when analysing the infectious particle formation of XVir-N-31 in all three cell lines. The

lower concentration of LY led to small increases in all three cell lines, that did not exceed 2-fold. For the higher concentration 1µM, the viral particle formation was impaired in all cell lines. U87 cells showed the strongest negative impact, with a decrease over 85%, compared to the control.

Based on these results the decision was made to investigate the second CDK4/6 inhibitor Ribociclib, which is a more specific CDK4/6 inhibitor, with less side effects. (Quelle)

3.3.2. Ribociclib

Following the analysis of Abemaciclib, we investigated the inhibitory effect of Ribociclib on cell viability, cell cycle arrest and expression of cell cycle relevant proteins. Next, we examined the therapeutic potential in combination with oncolytic virotherapy.

Ribociclib effectively decreases cell growth and leads to a G1 arrest

The effects on cell growth were analysed for all three cell lines with increasing concentrations of Ribocilib.

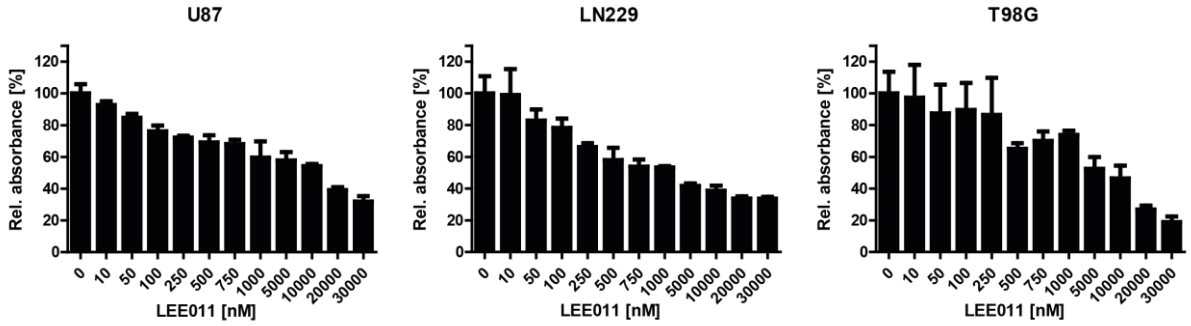

Figure 23: **The CDK4/6 Inhibitor LEE011 decreased cell viability in all three cell GBM cell lines.** Cells were seeded in 96 well plates, after one day treated with LY2835219 and incubated for four days, before fixation with 10% TCA and staining with SRB. The absorption was measured using a plate reader. Error bars S.D.

Increasing concentrations of Ribociclib led to a decline in cell division and resulted in lower absorption, compared to the control in all cell lines. The highest concentration of 30µM LEE011 did not diminish complete cell viability. U87 and LN229 reached a plateau at 40% cell viability. In T98G the highest concentration led to an 80% decline compared to the controls. These values were significantly higher compared to the results achieved with Abemaciclib.

Next, the capability of Ribociclib to arrest dividing cells in the G1 phase was assessed.

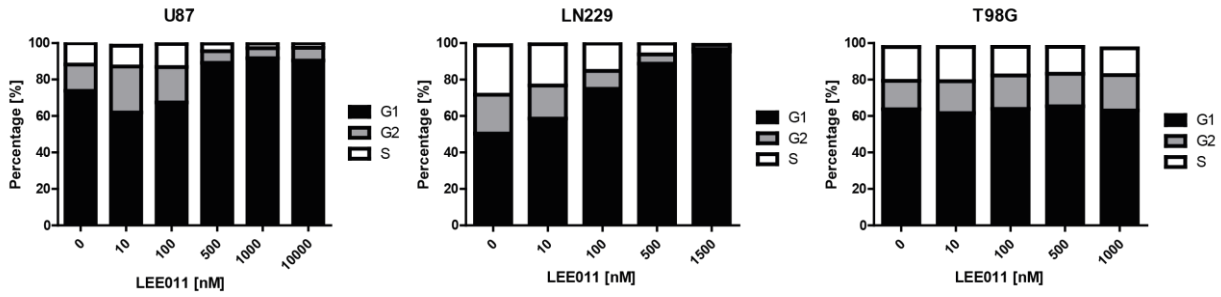

Figure 24: **Ribociclib led to a G1 arrest in two GBM cell lines.** Similar to the CDK4/6 Inhibitor Abemaciclib. Cells were treated with LEE011 and 24 hours later fixed, stained with PI and analysed for their cell cycle status.

With 500nM Ribociclib a clear G1 arrest was achieved in both U87 and LN229 cells. Like the results with Abemaciclib, a G1 arrest was not accomplished in T98G cells, even at concentrations of 10µM (data not shown)

Ribociclib is capable of decreasing the expression of cell cycle protein expression

In the next step, the biochemical effects of Ribociclib on the expression of cell cycle proteins were investigated. Three different GBM cell lines were therefore treated with two different concentrations of Ribociclib, and the expression of cell cycle proteins was examined after 24 hours, resembling the timepoint of infection.

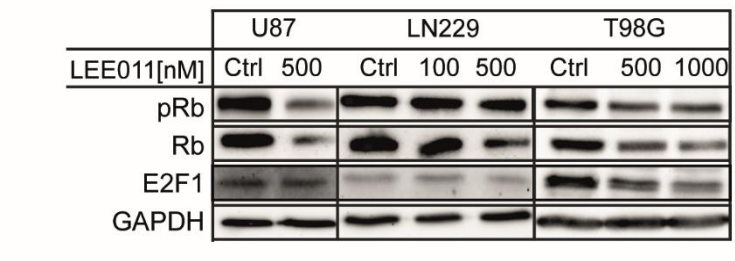

Figure 25: **Ribociclib effected the expression of cell cycle proteins.** Cell were treated with different concentrations of LEE011, and the expression of cell cycle proteins was analysed after 24 hours.

In all three cell lines a small decrease of Rb protein was observed. In U87 cells this was accompanied with a lower phosphorylation status of Rb protein. The E2F1 protein shoed no decrease in all cell lines. In both cell lines that show a G1 arrest upon Ribociclib treatment a light downregulation of Rb could be observed, as well as a

decrease in phosphorylated Rb. In T98G cells, not G1 arrest upon LEE011 treatment, only a small decrease in protein expression could be observed.

Ribociclib increased the oncolytic capabilities of XVir-N-31

Following the positive monotherapeutic results of Ribociclib, we assessed the effects of Ribociclib on viral potency, replication and infectious particle formations. Cell were treated with different concentrations of LEE011 and infected with XVir-N-31.

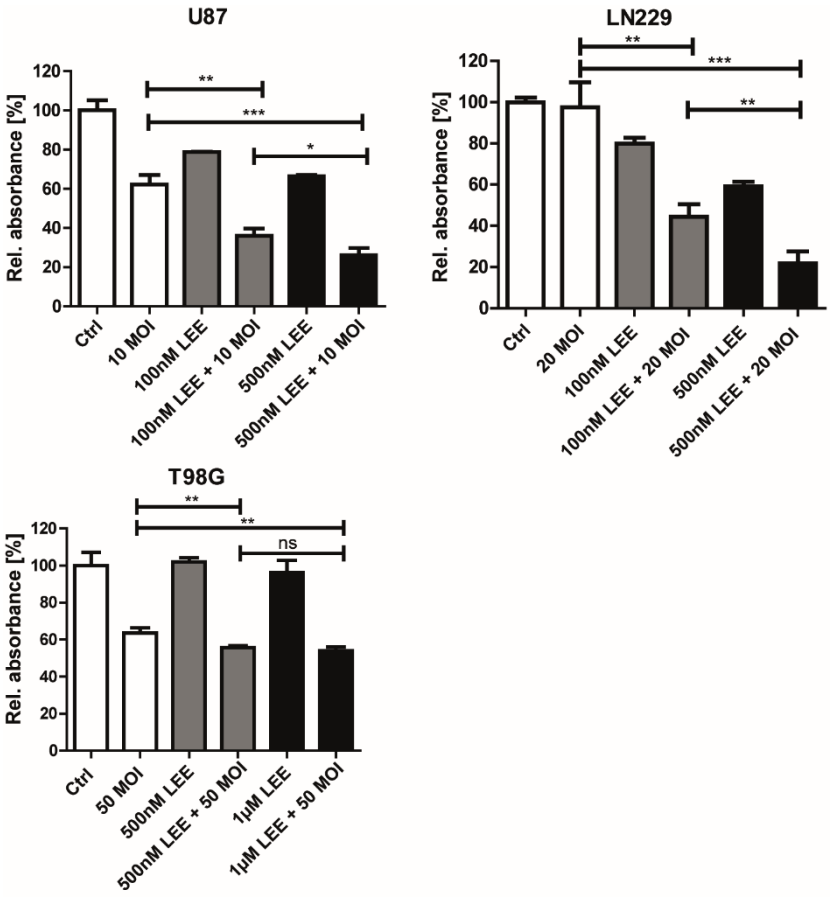

Figure 26: **Increased viral potency in combination of XVir-N-31 and Ribociclib.** Cells were pretreated with Ribociclib at indicated concentrations and infected with different MOIs, 24 hours later. The plated were fixated 4d.p.i. Error bars S.D, statistic analysis is done via students t-tests (ns>0.05; * p≤0.05; ** p≤0.01; *** p≤0.001)

The combinatory treatment with Ribociclib and XVir-N-31 decreased cell viability in U87 cells. The decrease was stronger at higher concentrations, but already 100nM LEE led to a pronounced decrease of cell viability in combination with 5 and 10 MOI. In LN229, 50 MOI was capable of decreasing the cell viability as a monotherapy, whereas 20 MOI, did not. In the combination with Ribociclib, already at 100nM, cell viability was halved. This could be further improved with higher concentrations up to

20% cell viability at 20 MOI with 1mM LEE011. T98G cells were not effectively G1 arrested with Ribociclib, here we could show that the viral potency could as well not be significantly increased. Based on these results we examined the effects on viral replication of XVir-N-31, in the combinational therapy with Ribociclib.

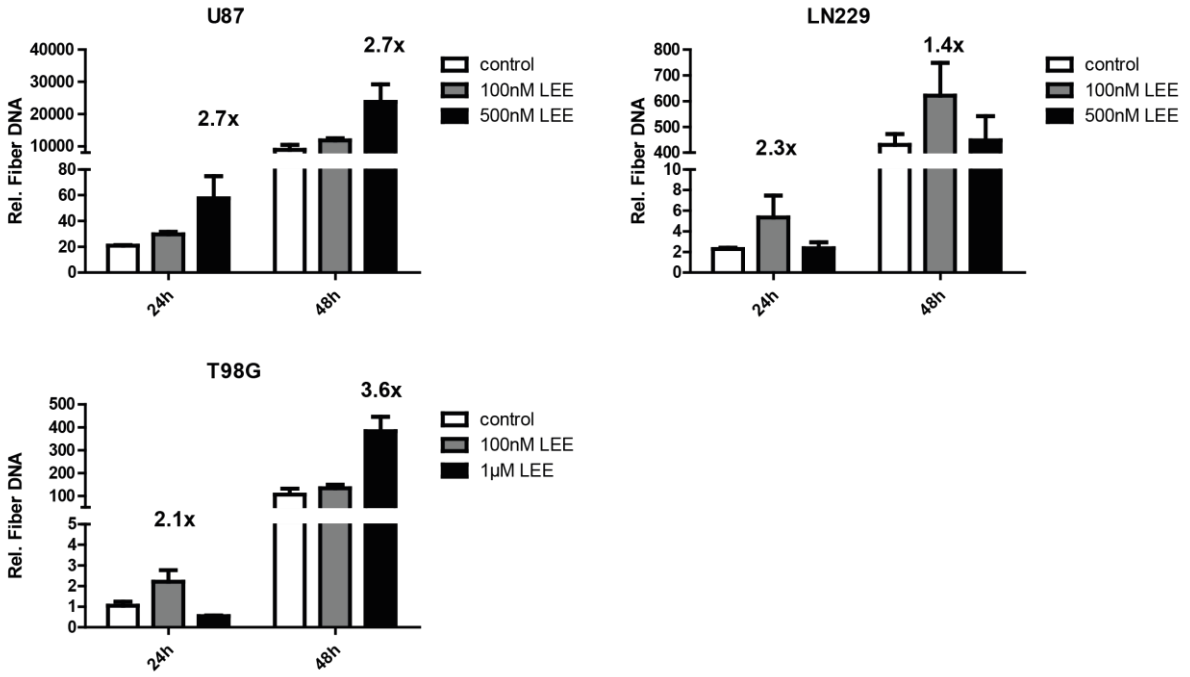

Figure 27: **Ribociclib increased viral replication of XVir-N-31 at indicated timepoints.** Cells were pretreated with LEE011, infected at the next day and analysed after 24h and 48h. Indicated numbers above each graph show the fold changes compared to the control at both analysed timepoints. Error bars S.D.

The replication of XVir-N-31 was increased in all three cell lines. At 24 hours the in U87 cells, higher concentrations led to more replication. In both LN229 and T98G higher replications could be achieved with 100nM LEE011. At 48 hours, In U87 and T98G the replication was increased with higher concentrations of LEE011 (U87: 500nM; T98G: 1µM). In LN229 cells XVir-N-31 replicated at 48 hours with 100nM LEE011, but there was no increase observable with 500nM LEE011, compared to the control.

Increased replication could lead to increased production of infectious particles of XVir-N-31. We therefore investigated if CDK4/6 inhibition with Ribociclib improved infectious particle formation.

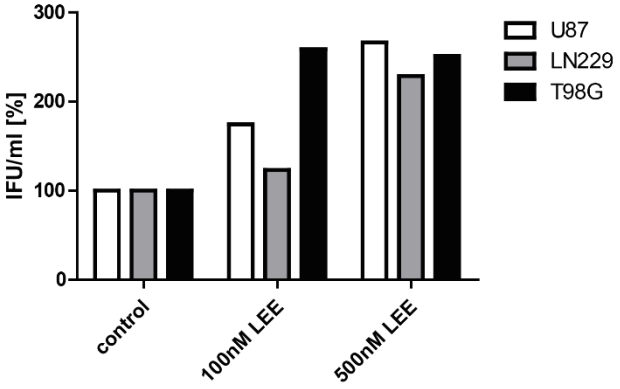

Figure 28: **Ribociclib increased particle formation in all cell lines.** Cells were treated with Ribociclib and infected at the next day (U87, LN229: 20 MOI; T98G: 50 MOI), three day later samples were collected and tested using HEK293 cells, infected with the supernatant.

In all three cell lines an increase in particle formation could be observed in combination of Ribociclib with XVir-N-31. Nearly 3-fold more particles were produced in the samples treated with 500nM LEE011, interestingly in T98G cells similar numbers were achieved already with 100nM LEE011.

Overall, the CDK4/6 Inhibitor Ribociclib, significantly increased the viral potency, replication and particle formation. Although no G1 arrest was achieved in T98G cells, effects were still observable. In comparison to the CDK4/6 inhibitor Abemaciclib all viral parameters benefited.

3.4. Starvation and siRNA against Rb in CDK4/6 resistant T98G cells

Since we were not able to achieve a G1 Arrest with CDK4/6 inhibitors in T98G cells, we tested if starvation or direct downregulation of Rb via siRNA could led to an improvement in viral replication.

XVir-YB-1 dependent induce oncolytic effects in GBM

First, we investigated if serum starved T98G cells would display a G1 arrest, similar to our observations in U87 and LN229, under CDK4/6 inhibitor treatment.

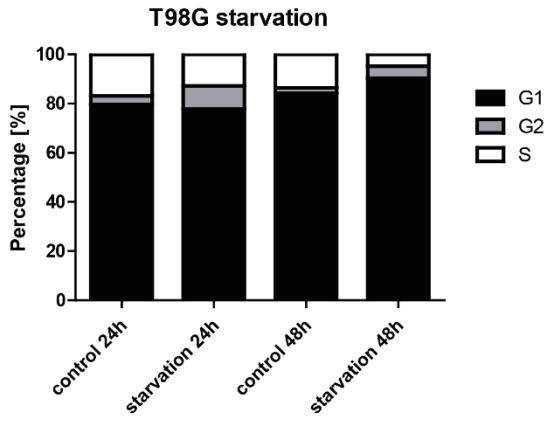

Figure 29: **T98G cells do not show a clear G1 arrest upon starvation.** Cells were seeded and after 24 hours the medium was changed, no longer containing FCS. The cell cycle status was measured at indicated timepoints.

The tested samples already were highly in the G1 phase; therefore no clear G1 Arrest was achieved with starvation at 24h and 48h.

Besides starvation the direct downregulation of Rb is a feasible alternative, we therefore decided to use two different siRNAs targeting the Rb expression. Using western blot we confirmed the downregulation of Rb and pRb with both constructs. Downregulation of Rb did not result in a co-downregulation of E2F1 as experienced when using CDK4/6 inhibitors, which is shown in T98G cell here after 24 hours. The siRNA based downregulation was stable for both timepoints. The starvation sample displayed a small decrease of Rb and E2F1 after 48 hours.

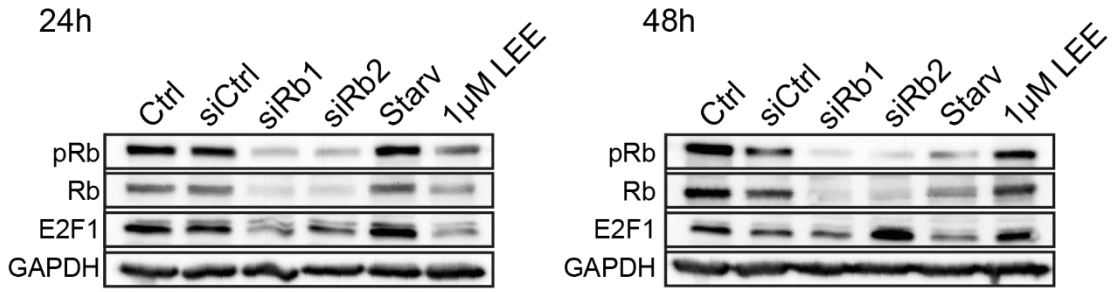

Figure 30: **Downregulation of Rb was achieved using siRNA.** T98G cells either transfected with siRNA, serum starved or treated with 1µM of the CDK4/6 inhibitor LEE011. The expression of cellular proteins was analysed after 24 and 48 hours. As a negative control scrambled siRNA was used.

Based on these results we tested the effect of starvation and siRNA against Rb on viral parameters.

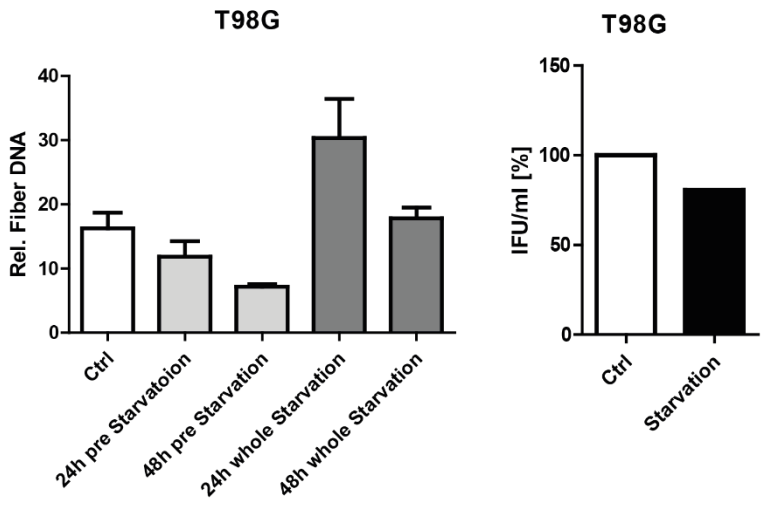

Figure 31: **Starvation does not significantly increase viral replication and particle formation.** Starvation was either applied only previous the infection, and after infection whole medium was added. For complete starvation after the infection again medium without FCS was given to the plates, lysates were conducted at 4h.p.i. and 24h.p.i.. For the viral article formation, the cells were starved as well for the complete experimental procedure. Error bars S.D.

Starvation interferes in several pathways and does not only led to G1 Arrest. We therefore did not observe any strong effect on viral replication of XVir-N-31. Interestingly starving the cells only beforehand, did not allow the cells to recover and thereby allowing better viral replication. The disturbance of cellular pathways as well diminished the ability of the virus to successfully complete its life cycle and haltered the production of infectious viral particles upon starvation.

After these negative results towards starvation we focused to improve viral replication via siRNA, which led to a downregulation of Rb expression.

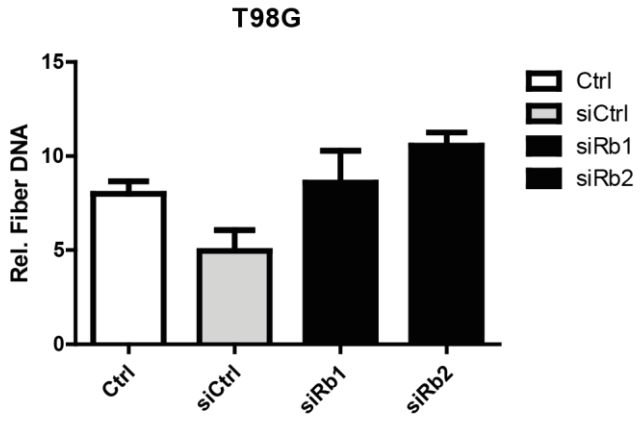

Figure 32: **Downregulation of Rb does not induce replication of XVir-N-31 in T98G cells.** Cells were transfected with two different siRNA sequences targeting Rb and one random siRNA as control. At the next day they were infected with 50 MOI and at 4h.p.i. and 24h.p.i. lysates were done. All values are based on their respective 4h values. Error bars S.D.

Direct downregulation of Rb did not result in an improved replication of XVir-N-31 in T98G cells. This indicates that Rb might not be the target of choice in T98G cells.

3.5. Bromodomain Inhibitors

Besides using CDK4/6 inhibitors in combination with virotherapy, we are currently investigating targeting the epigenetic reader protein BRD4 using the bromodomain inhibitor JQ1. JQ1 has already been published to increase viral infection (Lv, Li et al. 2018), but the effectiveness varies between different cell entities. JQ1 has as well been shown to downregulate CDK4 (Sun et al. 2015). Here we first analysed it is effects on cell viability and cell cycle status, as well as the expression of cell cycle relevant proteins. Then we focused on the impact of a combinatory treatment with XVir-N-31 and the influence on viral potency, replication, and the formation of infectious viral particles.

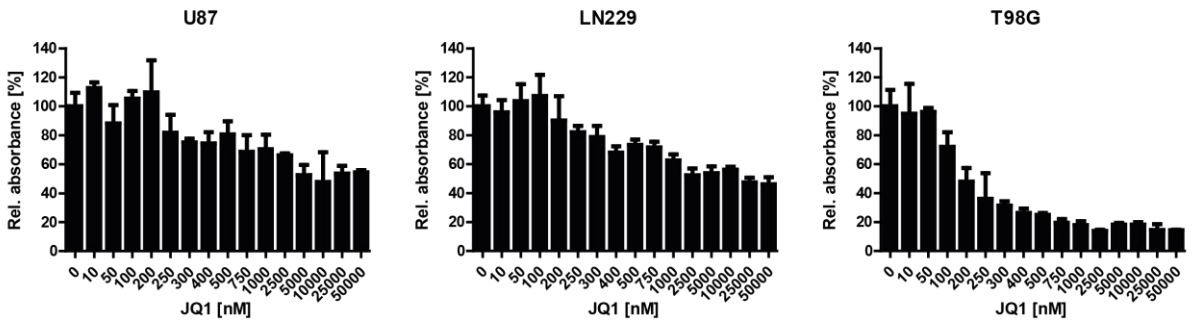

Figure 33: **JQ1 led to a decrease in cell viability in all three GBM cell lines.** Cells were seeded in 96 well plates, after one day treated with LY2835219 and incubated for four days, before fixation with 10% TCA and staining with SRB. The absorption was measured using a plate reader. Error bars S.D.

The bromodomain inhibitor JQ1 led to a decrease of cell viability in all cell lines. Interestingly T98G cells responded the most to higher concentrations of JQ1, whereas both U87 and LN229 did not. Both cell lines had no decrease in cell viability below 60% compared to their respective control. Next we investigated the effects of JQ1 on the cell cycle status.

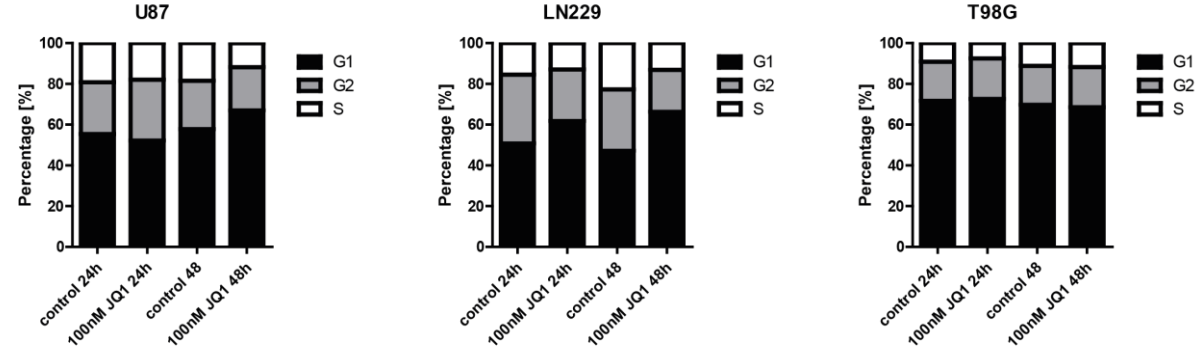

Figure 34: **JQ1 does not alter the cell cycle status in GBM cell lines.** Cells were treated with JQ1 and after 24 hours or 48 hours fixed, stained with PI and analysed for their cell cycle status.

When analysing the cell cycle status of all GBM cell lines, we found no significant alteration after 24 or 48 hours. Only in LN229 a small increase in the G1 phase could be observed, both at the 24h and 48h timepoint. Both U87 and T98G displayed no alteration in their respective cell cycle phases.

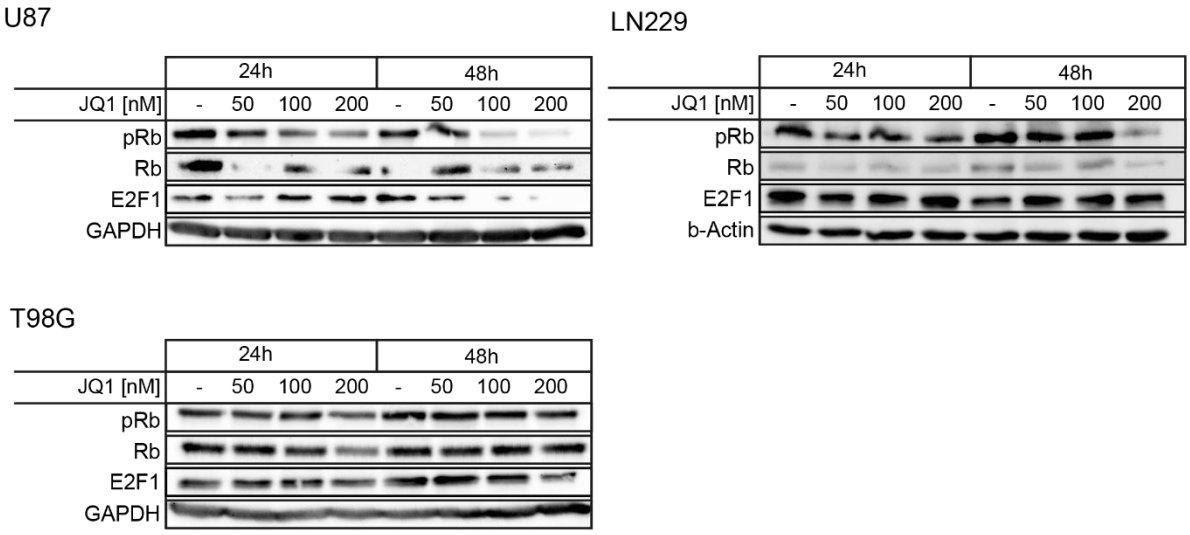

Figure 35: **The bromodomain inhibitor JQ1 decreased pRb in two cell lines after 24 hours.** Cell were treated with different concentrations of JQ1, and the expression of cell cycle proteins was analysed after 24h and 48h.

In U87 cells the treatment with JQ1 led to a strong decrease of pRb after 48h with both 100nM and 200nM JQ1. In LN229 the decrease of pRb was only observable at the 48 hour mark and only with the higher concentration. In T98G cells none of the tested proteins showed a clead changed expression or phosphorylation.

But the effect of JQ1 is not mainly based on alteration of the cell cycle and its related proteins but changing epigenetically both the expression of cellular and viral proteins. We therefore next investigated the effects on viral parameters.

3.5.1. JQ1 increased viral potency, replication and particle formation

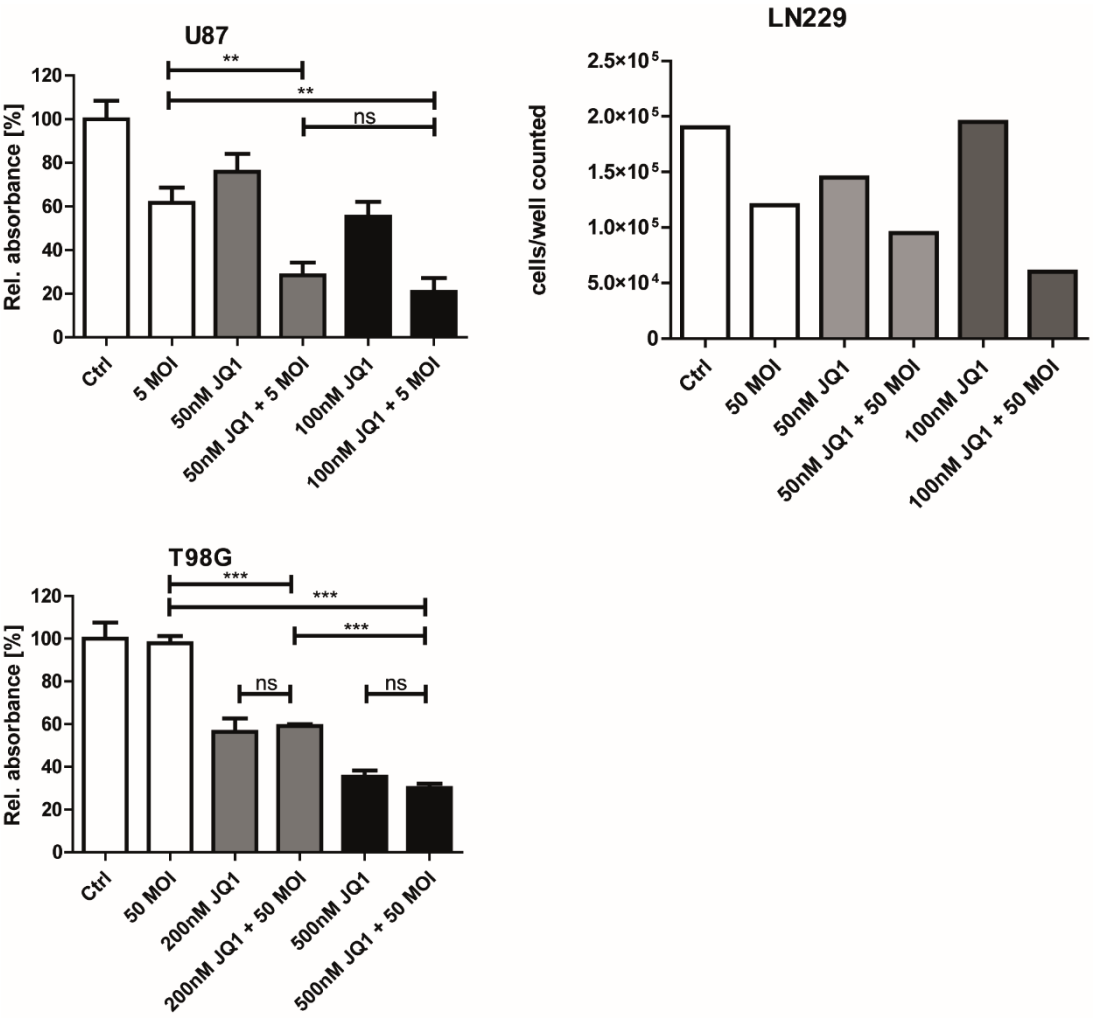

Figure 36: **Viral potency was increases upon JQ1 treatment in two GBM cell lines.** Cells were and infected with different MOIs, then treated with JQ1 1h.p.i. The plated were fixated 4d.p.i. Error bars S.D., statistical analysis is done via students t-tests (ns>0.05; * p≤0.05; ** p≤0.01; *** p≤0.001)

The treatment with JQ1 was highly synergistic with XVir-N-31 in U87 cells ($p < 0.001$). In LN229 the cell survival was decreased with both 50nM and 100nM JQ1. In T98G cells there was no clear decrease in cell survival upon JQ1 treatment, for both 200nM JQ1 and 500nM JQ1, the treatment benefit, originated by the small molecule. Interestingly for two cell lines concentrations as low as 50nM were already capable to increase the viral potency. Next we analysed the effects on viral replication with low concentrations of JQ1.

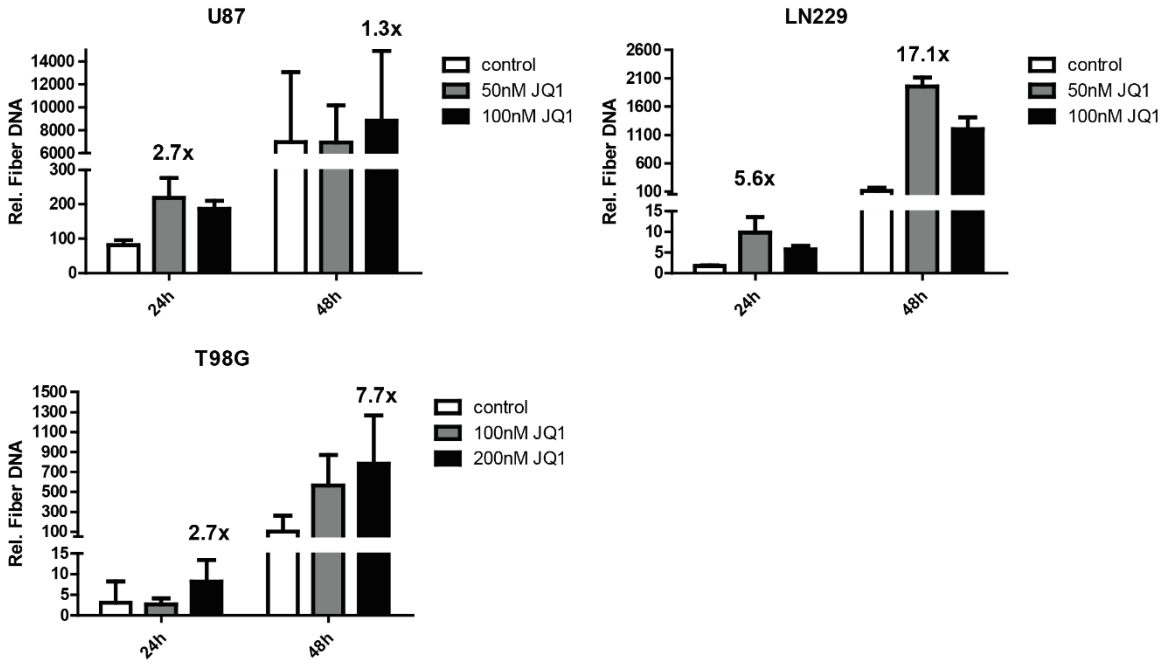

Figure 37: **JQ1 increased viral replication in all cell lines.** Cells were infected with XVir-N-31 (U87, LN229 20 MOI; T98G: 50 MOI) and 1h.p.i. treated with indicated concentrations of JQ1. Lysates were done at 4, 24 and 48h.p.i. The highest fold increases for 24h.p.i. and 48h.p.i. are indicated above the graphs for each cell line. Error bars S.D.

The effects of JQ1 on viral replication differed between the cell lines. In U87 cells at the 24-hour mark, JQ1 led to a three-fold increase in viral replication, which was not longer improved at 48 hours. For LN229 and T98G at 48 hours stronger increases in viral replication could be observed. For LN229 cells 100nM JQ1 already led to negative side effect, no longer increasing viral replication compared to 50nm JQ1. In T98G cells higher concentrations increased the viral replication. Since the replication was increased in all cell lines, we next investigated the capabilities of JQ1 to increase the effective particle formation of XVir-N-31.

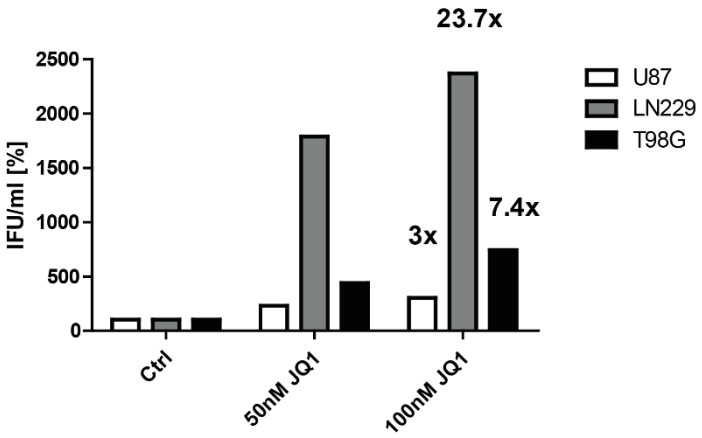

Figure 38: **All cell lines produced more infectious particles of XVir-N-31 in JQ1 treated cells.** Cells were and infected with XVir-N-31 (U87, LN229: 20 MOI; T98G: 50 MOI) and 1h.p.i. treated with different concentrations of JQ1, three day later samples were collected and tested using HEK293 cells, infected with the supernatant. For 100nM JQ1 the fold increases compared to the control are shown above each graph.

The production of infectious particles was increased in all cell lines upon JQ1 treatment, with 50nM and 100nM of JQ1, where the highest increases were observed. Interestingly 200nM of JQ1 already led to less particle formation in all three cell lines tested (data not shown). The smallest increase was observed in U87 cells, but the production of virus in U87 cells was always already high in the control group. In LN229 the highest induction of viral particle formation was observed. T89G cells treated with 100nM JQ1 showed the biggest induction of infectious particle production (7.4 fold).

JQ1 improved all tested viral parameters in low concentrations, in our next step we combined both CDK4/6i and JQ1 to analyse if we can further improve the treatment regime and could lower individual concentrations of either inhibitor, to reach in vivo applicable concentrations.

3.6. Combination of CDK4/6 inhibitor LEE011 and bromodomain inhibitor JQ1

The combination of LEE and JQ1 targets different cellular and viral proteins, here we analysed if this further decreases the expression of cellular proteins and improves the expression of viral proteins.

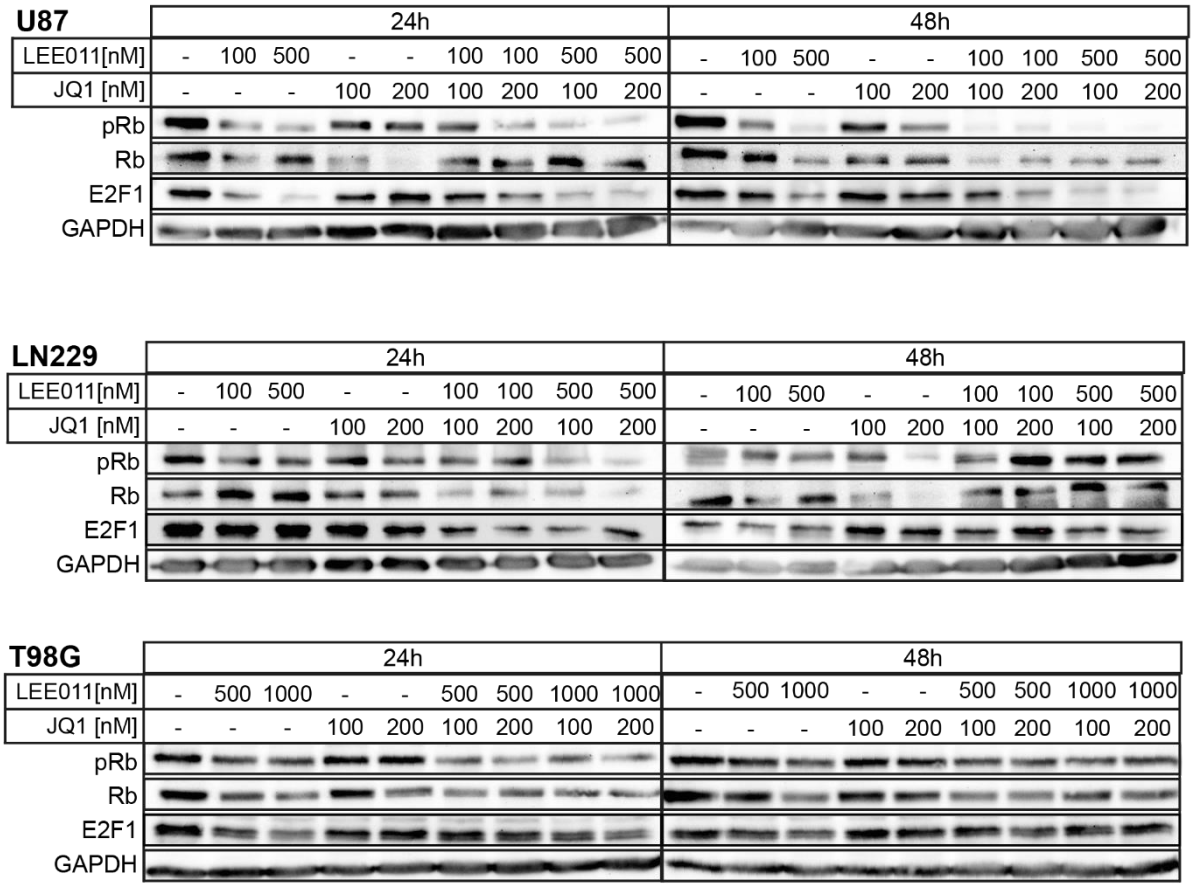

Figure 39: **The combinational approach of LEE011 and JQ1 decreased cellular protein expression.** Cells were treated with LEE011 and JQ1 in different concentrations and protein expression was analysed at indicated timepoints.

Upon CDK4/6 inhibition Rb and E2F1 were reduced in U87 cells. This effect was further improved in the combination with JQ1 at both timepoints. In LN229 the combination led to a decrease in Rb at the 24 hour time point and E2F1 was decreased in all combinatory treatments after 24h. In T98G, which already displayed no alteration in protein expression when treated with LEE011, we observed small decreases in Rb and E2F1, as well as less phosphorylation of Rb at the 24h timepoint. However, after 48h the alteration in the expression was diminished.

Next we investigated the effects on the expression of viral proteins in LN229 and T98G.

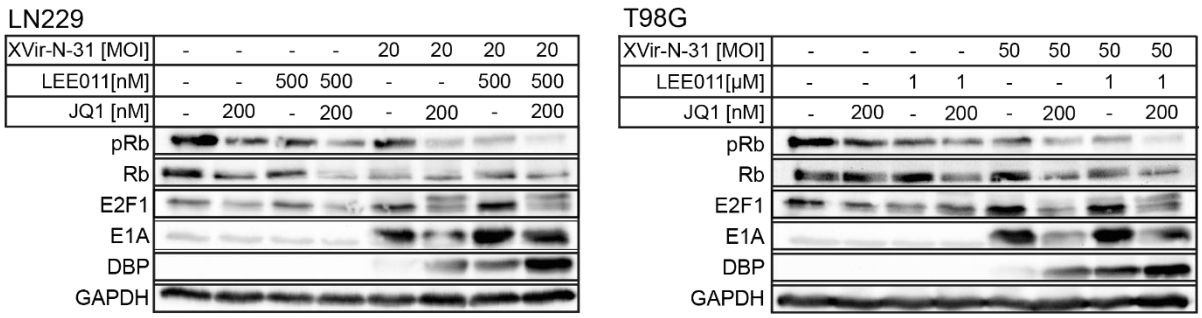

Figure 40: **The combination of LEE011 and JQ1 increased the expression of viral proteins.** Cells were treated with LEE011, at the next day infected with XVir-N-31 and treated with LEE011 and JQ1. 48h.p.i. the protein expression was analysed.

In LN229 the infection with XVir-N-31 decreased the expression of Rb, while the phosphorylation status of Rb did not alter. The combination with either inhibitor led, besides lower Rb expression, also to less phosphorylation of Rb. In the combination with LEE011 the expression of E2F1 was decreased. E1a and DBP was enhanced in the combinatory approach, with the highest increase of DBP in the combination of both inhibitors with XVir-N-31. In T98G cells the expression of Rb and E2F1 was decreased upon LEE011 treatment in combination with XVir-N-31. The DBP expression was increased with both inhibitors, with the most increase in the double treated cells. Next we analysed viral potency of XVir-N-31 upon CDK4/6 inhibition in combination with JQ1 treatment in three GBM cell lines.

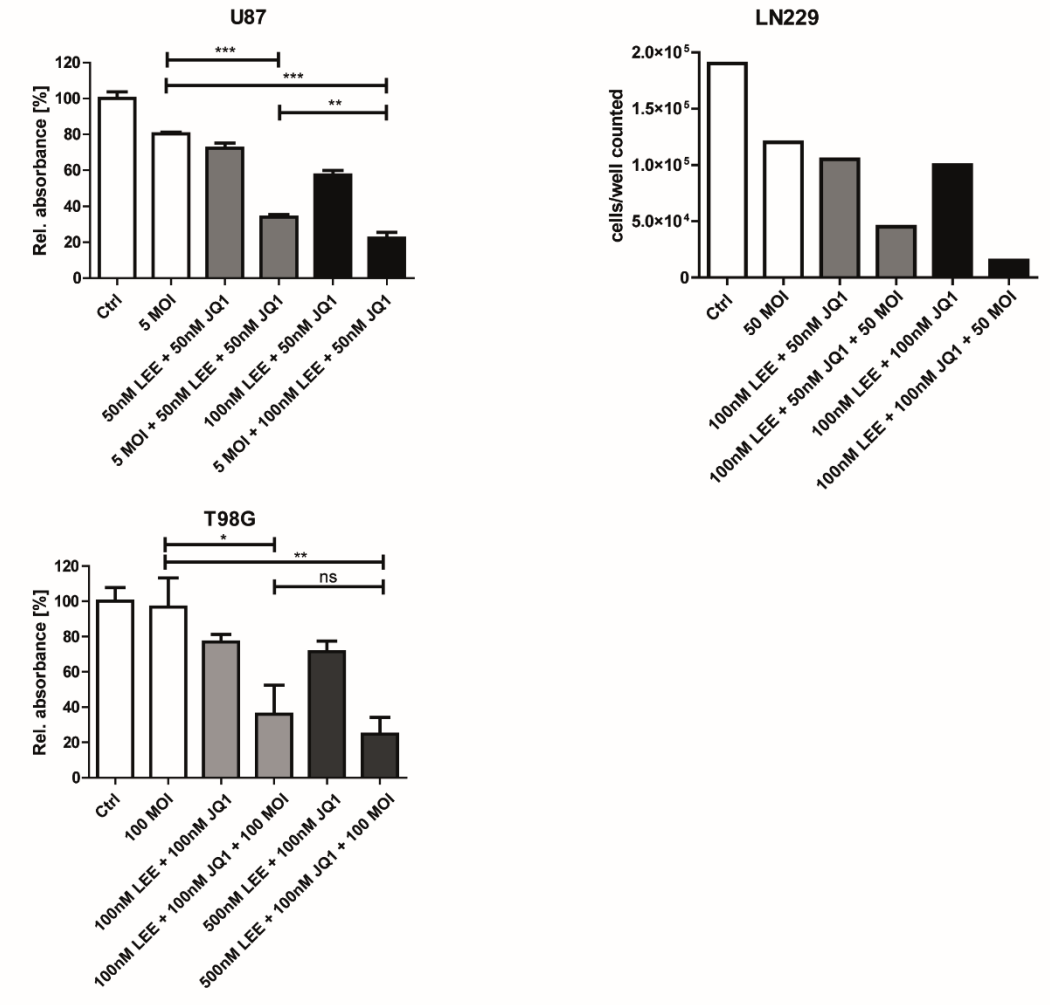

Figure 41: **Combining LEE011 and JQ1 led to an increased viral potency in all tested cell lines.** Cells were treated with LEE011 at the next day infected, after infection both inhibitors were added. U87 and T98G plates were fixed 5d.p.i. and analysed using the SRB assay, LN229 cells were trypsinised and counted. Error bars S.D., statistic analysis is done via students t-tests (ns>0.05; * p≤0.05; ** p≤0.01; *** p≤0.001)

In all cell lines the combination of LEE011 and JQ1 increased the viral potency. In U87 cells concentrations of 50nM were sufficient to significantly decrease cell viability with 5MOI XVir-N-31. For LN229 cells 100nM of LEE011 and JQ1 diminished the cell count over 80% and in higher concentrations, there was no cell survival. In T98G cells the cellular survival is reduced over 70%, this was a much better outcome compared to the mono treatments. Interestingly using low concentrations of only 100nm LEE011 and JQ1 lowered the cell survival significantly. These concentrations did not strongly alter, cell protein expression, here concentrations of 500nM LEE011 and 200nM JQ1 resulted in only small decreases of cellular proteins. Next we investigated the effects of the treatment regime on viral replication of XVir-N-31.

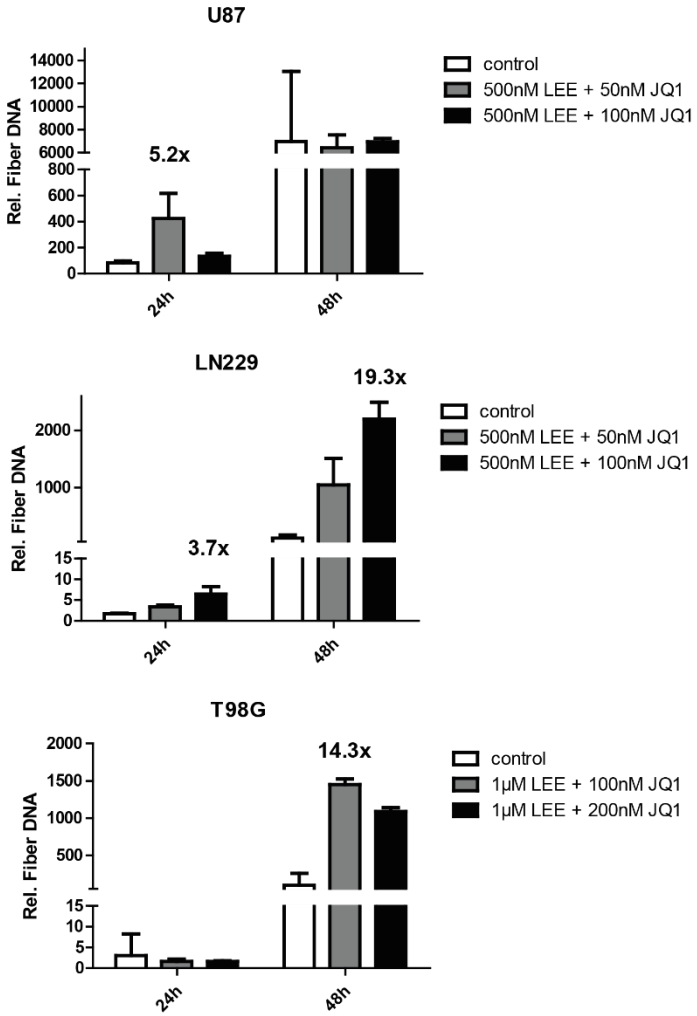

Figure 42: **Combining CDK4/6 inhibitor LEE011 with the bromodomain inhibitor JQ1 increased viral replication of XVir-N.31.** Cells were first treated with LEE011 at the next day infected and 1h.p.i. both inhibitors were added. Samples were drawn at 4h, 24h and 48h. All values are based on their respective 4h values. The highest increase in replication is displayed as the fold changes compared to the controls. Error bars resemble S.D.

In U87 cells the viral potency was increased at the 24 hour mark. At 48 hours the control showed high SD. In LN229 the replication was increased at both timepoints. Here higher concentrations led to more viral replication. In T98G the replication was stronger at the 48 hour mark, using 1µM LEE011 and 200nM JQ1 resulted in less replication compared to only using 100nM JQ1. Since the viral replication was increased in all three cell lines, we investigated the potential of the triple therapy to increase viral particle formation.

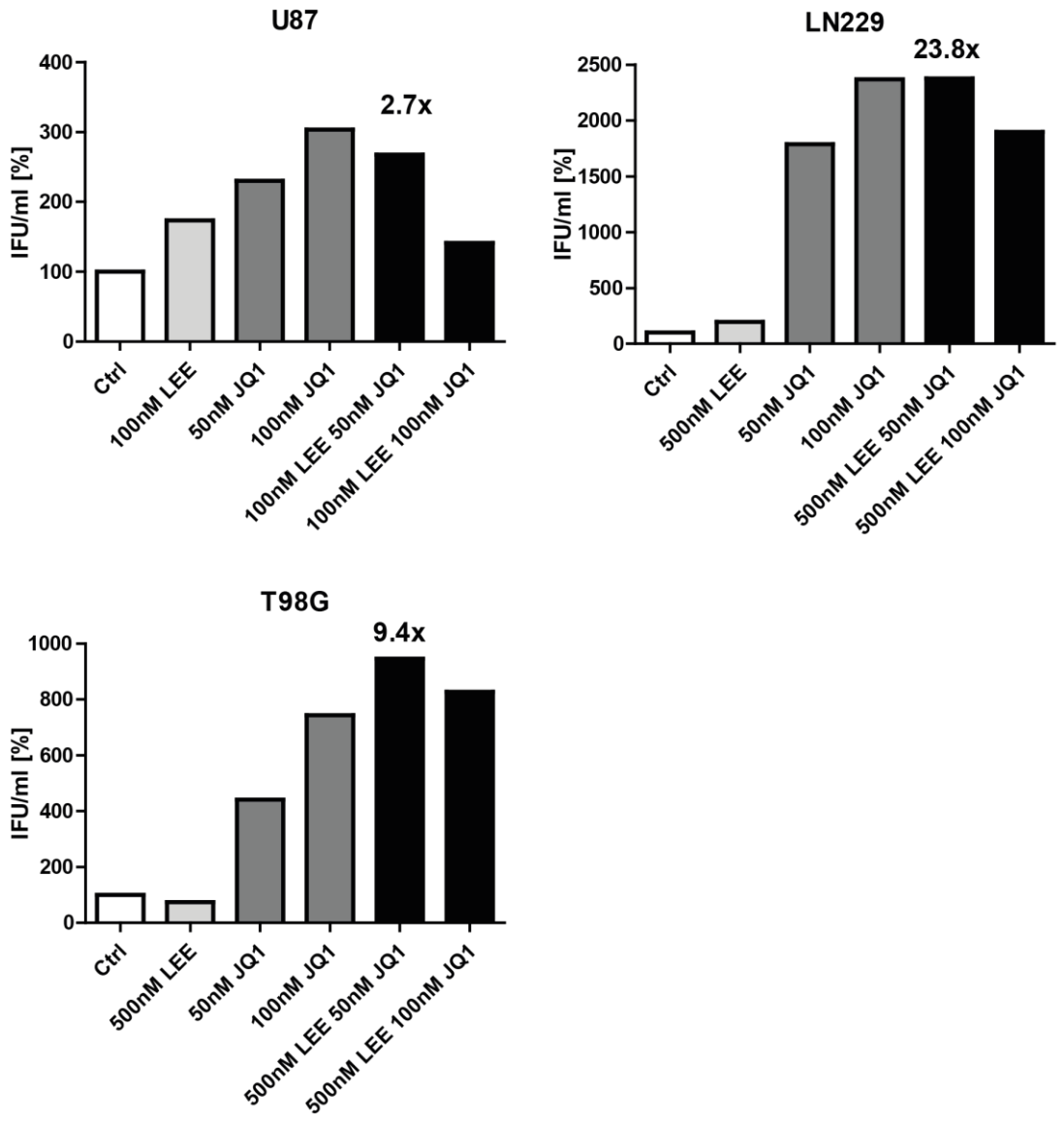

Figure 43: **The particle formation was increased in all tested cell lines upon treatment with LEE011 and JQ1.** The particle formation was tested with different LEE011 and JQ1 concentrations, Cells were infected with XVir-N-31 (U87, LN229: 20 MOI; T98G: 50MOI), three day later samples were collected and tested using HEK293 cells, infected with the supernatant. The most increased combinatory approach is indicated as the fold change compared to the control, above all graphs.

The particle formation was increased in all tested treatment combinations. In U87 the monotherapies led to a stronger increase compared to the combinational therapy. Only 100nM LEE and 50nM JQ1 in combination with virus led to a equal increase. In LN229 and T98G the virus production was strongly increased under JQ1 treatment. LEE011 led only to a small increase in viral replication. The combination of LEE011 and JQ1

improved the production only by a margin. High concentrations of both inhibitors had negative effects on the infectious particle formation, leading to smaller increases.

Combining both CDK4/6 inhibitor LEE011 and bromodomain inhibitor JQ1 increased all tested viral parameters. Compared to the individual treatments lower concentrations of inhibitor were used.

3.7. Comparison of all tested treatment strategies

This chapter compares all used approaches in their capability to improve the viral replication and infectious particle formation.

All three cell lines behave differently when treated with the small molecule inhibitors either alone or in combination, as well as radiation.

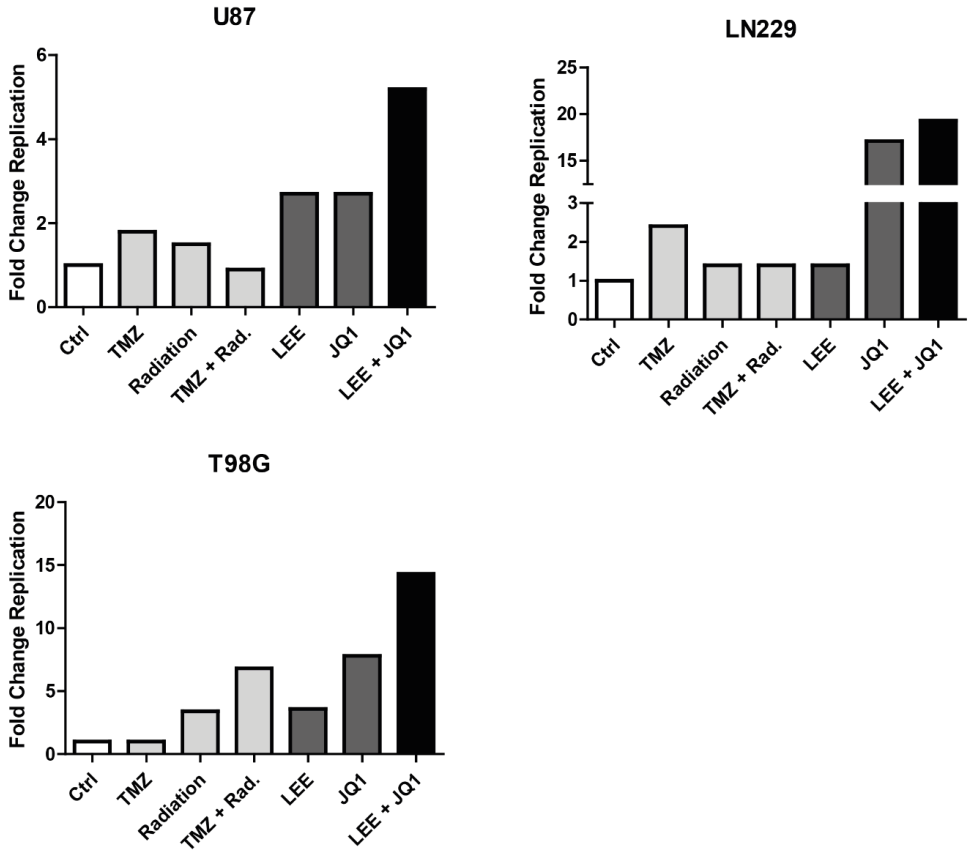

Figure 44: **The treatment with LEE011 and JQ1 led to the highest increase in replication in all three cell lines.** The highest fold change of each compound replication analysis was included for each cell line, For U87 cells the replication 24 h.p.i. was analysed, for LN229 and T98G 48 h.p.i.. All values are based on their respective control at the indicated timepoint.

In U87 cells the replication was analysed after 24h.p.i. since the effects are more prominent in the earlier stages. Both LEE011 and JQ1 had 2.7-fold replication

increases for their own, which combined reached an additive effect of 5.2-fold. In LN229 the effect was purely based on the bromodomain inhibitor JQ1 reaching an increase in replication of 17-fold after 48h.p.i., this effect could only be slightly improved in the combinatory approach reaching over 19-fold. T98G cells show high resistance to both alkylating agents like TMZ and radiation, but the combinatory treatment reached an increase in viral replication of over 6-fold. As seen above T98G cells show a strong resistance to CDK4/6 inhibitors as well as Rb downregulation (Figure 24 & Figure 32). Therefore the effects with LEE011 were lower compared to the “classical” GBM approach, but in combination with JQ1 an increase of 14.3-fold could be achieved, higher then LEE011 alone or JQ1 alone (7.8-fold).

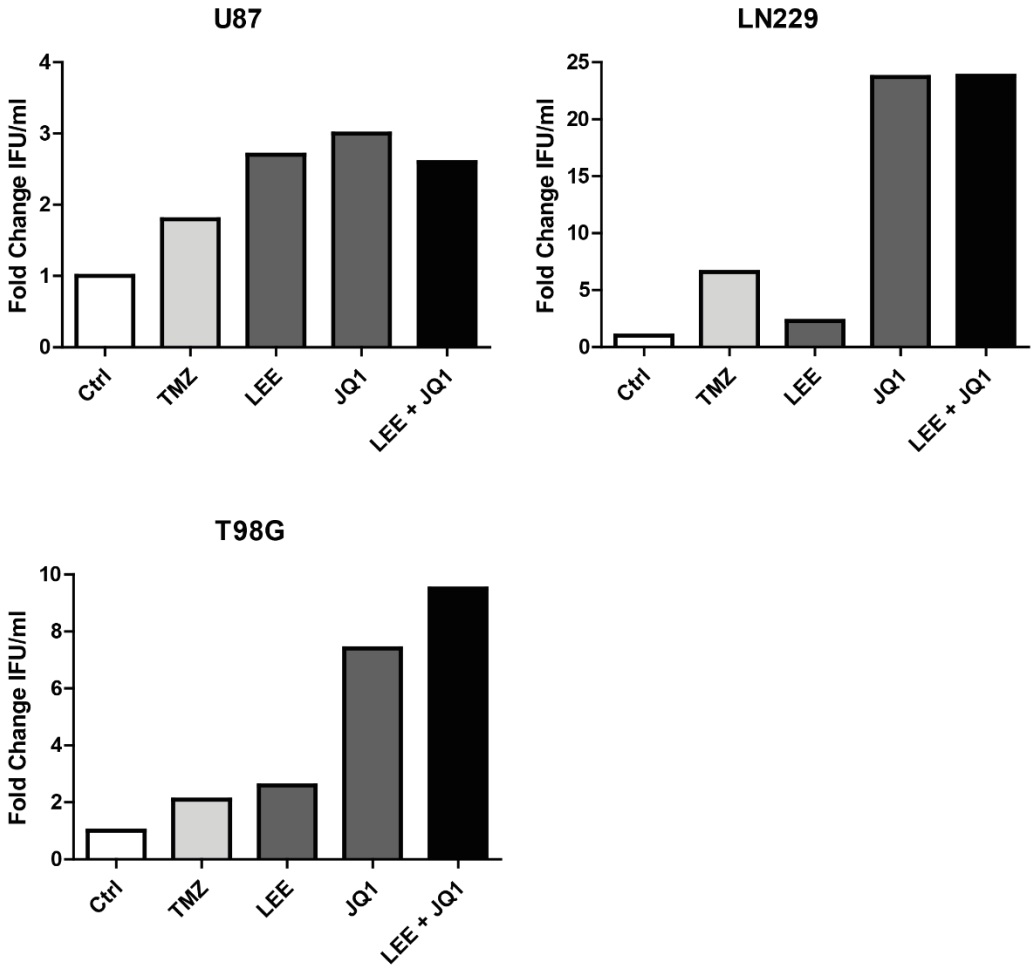

Figure 45: **The production of infectious viral particles could be increased using the bromodomain inhibitor JQ1.** The fold changes of viral particle production were compared in different approaches, respective to their individual control.

Besides the viral replication, the production of infectious viral particles is an important factor for the effectiveness of any oncolytic viral approach, both leading to further viral

spread and the attraction of the immune system. For all tested single approaches JQ1 had the highest impact on the production of IFUs. Only in T98G cells the combination with LEE011 further increases in the particle formation. In LN229 cells the effects of JQ1 lead to over 23-fold more particles formed.

3.8. Analysis the role of Rb in the viral life cycle

The role and Rb and E2F binding sites in the viral genome context can be analysed using specific vectors, that either contain artificial binding sites or on the opposite bear mutations. We therefore created both vector systems, with either 30 artificial E2F-binding sites located in the E3 region (Ad-WT/Trapp) or deleted E2F1 binding sites in the E2-early and the E1 Enhancer region (Ad-WT/2xE2Fm) (Supplementary Figure 3 & Supplementary Figure 4).

3.8.1. Ad-WT/Trapp

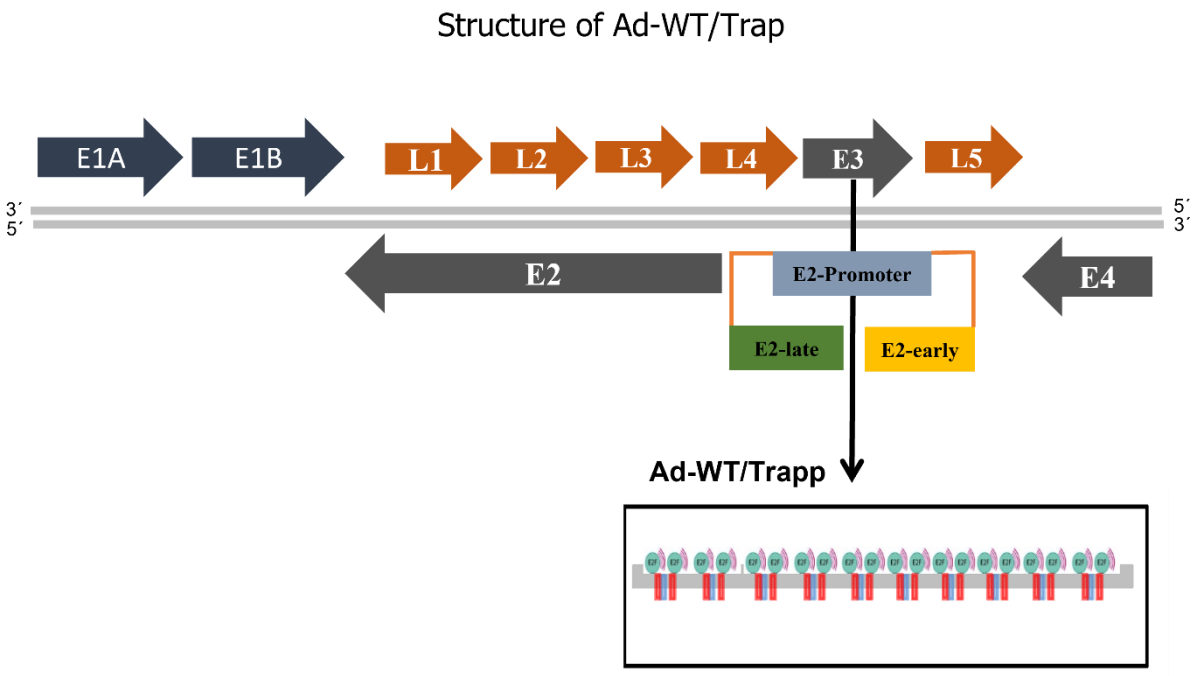

Figure 46: **The viral construct Ad-WT/Trap contains 30 E2F binding sites, located in the viral E3 region.** This allows unfunctional interactions of the cellular E2F proteins with the viral genome, thereby trapping cellular E2Fs, independent of small molecule inhibitors.

A second viral construct, WT Trap, used in our laboratory, bears in the viral E2 region 30 E2F binding sites, this allows the non-functional binding of several E2Fs, thereby limiting the amount of E2Fs binding in the promotor region of E1A and E2-early. Here CDK4/6 inhibitor LEE011 was able to increase the replication 5 fold in U87 cells and 2

fold in T98G cells. As a control a second construct was used bearing the same E2F binding sites, but in a mutated fashion where no binding is possible. Here CDK4/6i only lead to smaller increases of viral replication compared to the non-treated control.

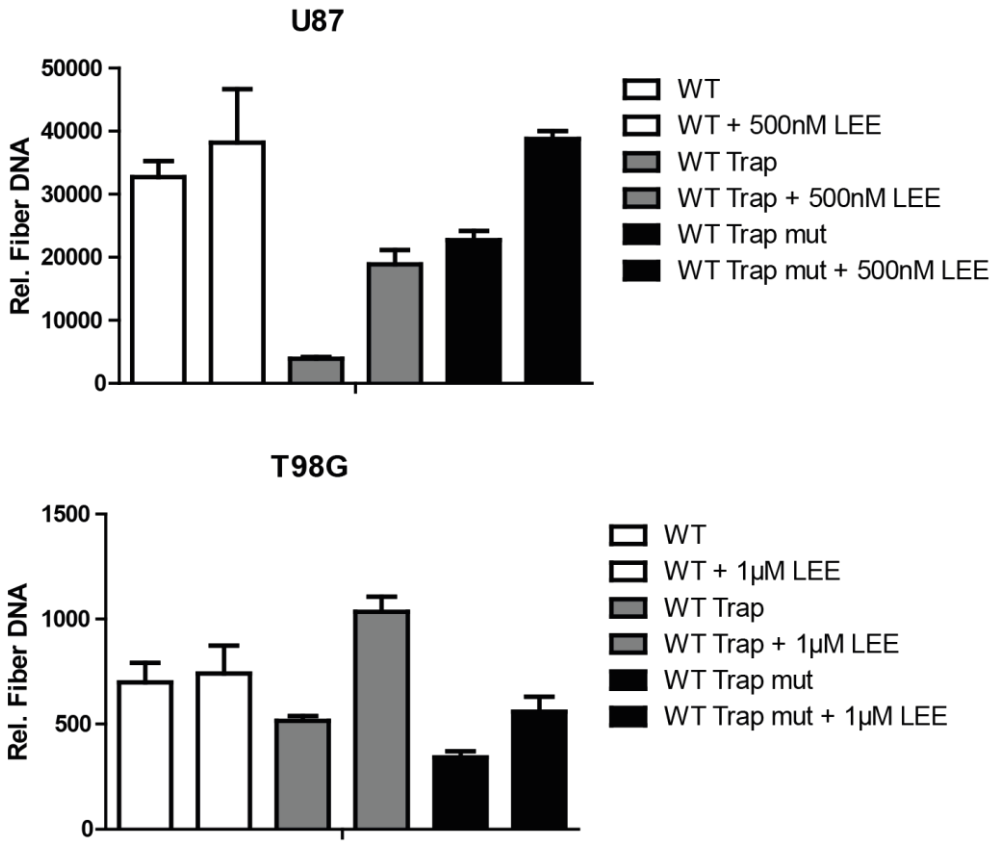

Figure 47: **Comparison of three different adenoviral constructs, in combination with the CDK4/6 inhibitor LEE011.** In U87 and T98G the replication was analysed after 48 hours. All values are based on their corresponding 4 hour value. The error bars S.D.

3.8.2. Ad-WT/2xE2Fm

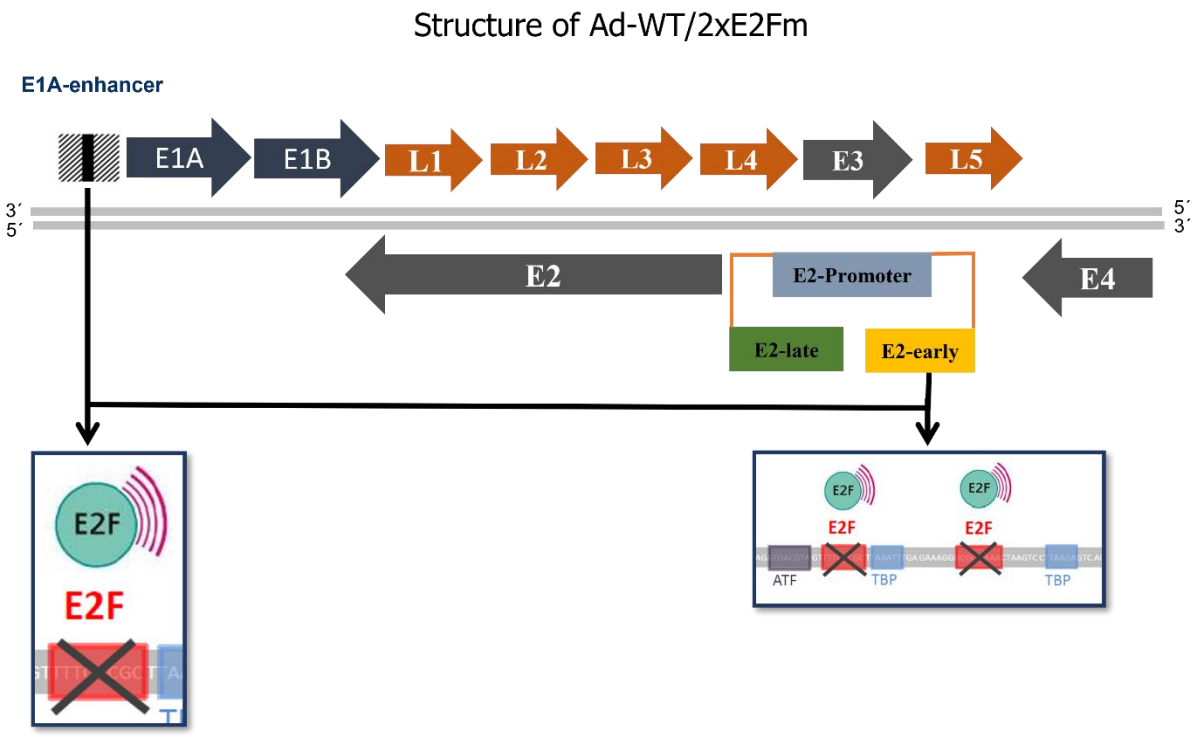

Figure 48: **The viral vector Ad-WT/2xE2Fm contains one mutated E2F core binding site in the viral E1 enhancer region and two mutated E2F binding sites in the viral E2-early promotor.** This leads to much lower transactivation capabilities of E2F1, after infection.

The produced virus exhibited a severe lower replication after 48 hours compared to the control WT adenovirus. When combining the WT 2xE2Fm virus with the CDK4/6i LEE011 or the bromodomain inhibitor JQ1, the viral replication could be increased in two cell lines. The effects were more pronounced using JQ1. The combination of both inhibitors led only in T98G to a further increase of viral replication.

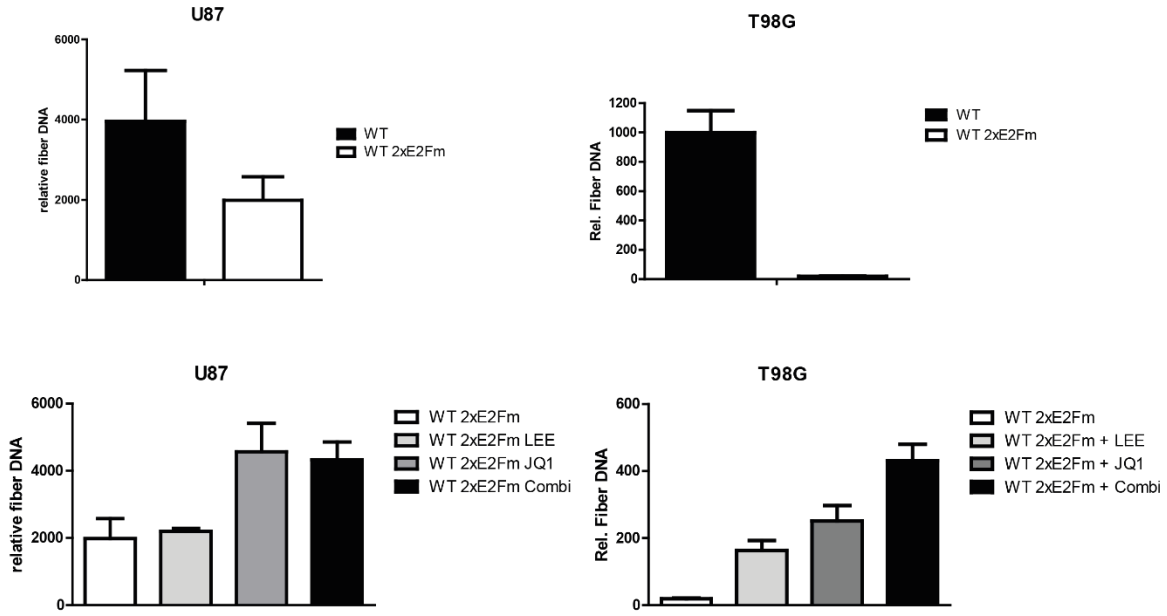

Figure 49: **Comparison of a WT adenovirus with the new viral construct WT 2xE2Fm.** Furthermore, the effects of LEE011 and JQ1 were tested on WT 2xE2Fm, alone and in combination. The replication was analysed after 48 h.p.i. relative to the initial 4h value. Error bars S.D.

4. Discussion

The aim of this thesis was the establishment of a novel combinatory treatment regime for a YB-1 based oncolytic virotherapy in combination with small molecules targeting specific pathways. Furthermore, the therapy was compared to the current treatment, alone as well as in combination with oncolytic adenoviruses. Based on the new insights in virus biology and cell-virus interactions a new viral construct was created to further deepen our molecular understanding.

In detail, we first investigated the effects of radiation and chemotherapy, using temozolomide on glioblastoma cells, thereby analysing the classic treatment regime for GBM (Fig. 7 - Fig. 16). We then shifted our attention to novel targeted therapy using small molecule inhibitors, for CDK4/6 (Fig. 17 - Fig. 31) and the BRD4 protein (Fig. 32 - Fig. 37). In our study we focused on the viral parameters of replication, potency and particle formation as well as consequent cell death. While radiation and temozolomide treatment only induced a small increase in these parameters, CDK4/6i and especially the BRD4 inhibitor JQ1 resulted in a strong increase. Based on the results of CDk4/6 inhibition, we created a new viral vector, independent of E2F induction, by disruption of the E2F binding sites in both the E1 Enhancer and E2 early promotor (Fig. 47 & 48). While the construct itself replicates much weaker, compared to a wildtype adenovirus, the replication is still inducible via JQ1. This could be the first step in proving an E2F1 independent effect of the JQ1 mode of action.

4.1. Oncolytic virotherapy in glioblastoma

Over the past decades several oncolytic adenovirus constructs were created, using several specific deletions in the E1 region. The deletion of 24 bp in the CR2 region of the E1A results in the incapability of the E1A protein to disrupt Rb from its complex (Fueyo, Gomez-Manzano et al. 2000, Heise, Hermiston et al. 2000). Thereby delta24 viral constructs cannot replicate without mutated Rb pathways, a common trait in cancers (Fueyo, Alemany et al. 2003, Lang, Conrad et al. 2018). A second used method was the deletion of the E1B55k coding region in dl1520 (Barker and Berk 1987). This led to the dependency for viral replication on a defective p53 pathway, since E1B55k is responsible for the degradation of p53 (Ries and Korn 2002). Furthermore cancer specific promotors can be used to allow replication only in for example telomerase active cells (Huang, Savontaus et al. 2003). Our research group

is based on the discovery that YB-1, a stress related protein, highly overexpressed in cancer cells, is essential for viral replication. Acting as a transcription factor at the E2 late promotor. Therefore, deletions in the CR3 region of the E1A13S encoding region, results in no transactivation of E1B55k/E4orf6 essential for the translocation of YB-1 into the nucleus (Holm, Bergmann et al. 2002, Holm, Lage et al. 2004). The usage of oncolytic viruses in the treatment of glioblastoma is a focus of our group in the past (Bieler, Mantwill et al. 2006, Mantwill, Köhler-Vargas et al. 2006, Rognoni, Widmaier et al. 2009, Holzmüller, Mantwill et al. 2011, Mantwill, Naumann et al. 2013).

In a first step we tested our oncolytic adenovirus XVir-N-31 on three different glioblastoma cell lines (Figure 7). The cell viability decreased in all three cell lines upon treatment with XVir-N-31, while in U87 and T98G cells a linear regression was observed in LN229 we could observe an “increase” in cell viability in LN229 cells, treated with 10 MOI. This effect observed happens shortly before the infected cells die, the measurement is based on SRB a dye staining, staining all proteins, thereby also the viral proteins produced in the cells. In LN229 cells the release of viral proteins was observed later, compared to T98G and U87 cells.

4.2. Combination of the oncolytic adenovirus XVir-N-31 with classical therapy regime

Our research group has been interested in the treatment of GBM using oncolytic virotherapy for the last two decades. Therefore the effects of radiation (Bieler, Mantwill et al. 2008) and chemotherapy (Holzmüller, Mantwill et al. 2011) have been selectively analysed in previous works. In this project we used further cell lines. For radiotherapy we have already shown U87 cells to react (Figure 9), for the treatment with temozolomide both U87 and LN229 cells have been shown to benefit of the double therapy (Figure 13). T98G cells are highly resistant to TMZ, we therefore included this cell line in our research (Lee 2016). Radiation had in our experiments only a small impact on the cell cycle status, only in LN229 cells we could observe an increase at the 24 hour timepoint (Figure 8). The viral replication and potency were increased upon radiating the cells (Figure 9 & Figure 10). This is in good accordance to already published data.

The treatment of the cell lines with TMZ, did not lead to an increase in G1/G0 phase (Figure 11). All cell lines are adapted to the treatment with TMZ. While U87 does only express a low level of MGMT, T98G is known to highly overexpress MGMT (Lee 2016).

Resistance to chemotherapy is a common feature of recurrent GBM. While the cell cycle was unaffected of the TMZ treatment, both in the FACS analysis as well as on a protein level, there was still an increase in cell killing that could be observed (Figure 13). The replication was increased in U87 and LN229 cells (Figure 14). In all three cell lines the production of infectious particles was measured, while in U87 and T98G cells double the viral progeny were formed in LN229 cells the particle number increased 6-fold (Figure 15). This massive increase in vial particle production was not observed for LN229, beside when treated with TMZ or JQ1 (Figure 45).

The standard therapeutic approach is concurrent treatment with TMZ as well as radiation. Therefore we applied both treatment options simultaneously. This led to further cell killing, compared to the single treatments, but we could observe no further induction of viral caused cell killing (Figure 16). Both treatments in combination seem to be altering the cellular status in a way unsuitable for effective viral replication (Figure 17). This timing issue was already described earlier (Tobias, Thaci et al. 2013). T98G cells highly resistant to TMZ and radiation (Lee 2016, Murad, Alghamian et al. 2018), but it is the only cell line with improved viral parameters in the double treatment. This highlights the effectiveness of the therapeutic approach, cell lines assailable by either one of the treatments benefits of the additional viral infection, and if both therapies fail, these cells are more vulnerable to viral infection as a trade-off in handling both radiation and being resistant to TMZ treatment. Both radiation and TMZ treatment led to increased nuclear YB-1, necessary for activation of the viral E2-late promotor.

4.3. Combination of the oncolytic adenovirus with CDK4/6 Inhibitors

CDK4/6 inhibitors are a group of small molecules targeting the Rb pathway and aim to prevent cell cycle progression and G1 Arrest (Pan, Sathe et al. 2017). Over the past years we have examined the effects of a dual combination using both CDK4/6 inhibitors with oncolytic virotherapy. For GBM two ATP-competitive CDK4/6i are currently in clinical trial, namely Abemaciclib (LY2835219) and Ribociclib (LEE011) and capable of crossing the blood-brain barrier (Wen, Weller et al. 2020, Li, Jiang et al. 2021). The combination of CDK4/6 inhibitors with virotherapy seem at first glance a contradiction, since it is known that viruses promote S-phase induction in order to replicate effectively (Nakajima, Masuda-Murata et al. 1987, Ben-Israel and Kleinberger 2002). But the viral E1A protein is capable of overwriting CDK4/6 induced G1 arrest, furthermore the G1

phase is the natural step for adenoviral infections (Goodrum and Ornelles 1997). This helps the virus by inhibition of the cellular protein synthesis. In this study we investigated the impact of both clinically investigated CDK4/6 inhibitors on their capability to induce G1 arrest, their ability to degrade cell cycle dependent proteins, the promotion of viral parameters and cell killing.

When comparing the IC_{50} values of Abemaciclib and Ribociclib there is a linear regression of cell viability in all three cell lines (Figure 18 & Figure 23). CDK4/6 inhibitors do not lead to apoptosis in their therapeutic window, instead the induced growth arrest halters cellular division, while the untreated control continues to proliferate. Therefore the observed effects in the IC_{50} reflect a gradual decrease in proliferation first, followed by growth arrest and in high concentrations side effects, leading to cytotoxicity. When comparing both used small molecule inhibitors it is clear that LEE011, has a much higher tolerated dose, compared to LY2835219. While the maximal dose of 5µM Abemaciclib resulted in a decrease of over 80%, in all three cell lines treated with Ribociclib 10µM decreases the cell viability only by 50%. In LN229 and U87 even 30µM could not decline the values over 60%, compared to the control. This implies a better compatibility of Ribociclib compared to Abemaciclib. To analyse the G1 arrest induced by the small molecule inhibitors we used a FACS approach (Figure 19 & Figure 24). Both inhibitors lead to a G1 arrest already in low concentrations of 100nM, interestingly the effects were more pronounced with 100nM of Abemaciclib. But with both CDK4/6i a solid S-phase block could be achieved in a dose dependent manner. In T98G cells no G1 arrest was observed in any given concentrations, even with 10µM of LEE011 there was no observable alteration in the distribution of cell cycle phases [data not shown]. T98G cells are in the literature described as sensitive to CDK4/6 inhibition as well as defective of *CDKN2A,B,C* (Michaud, Solomon et al. 2010), but already in this publication the effects are pronounced much weaker compared to U87 and LN229 [Table 1, Michaud, Solomon et al. 2010). Interestingly in serum-starved T98G cells the pre-treatment with the CDK4/6i Palbociclib induced DNA synthesis and Rb phosphorylation via cyclin D3-CDK4/6 complex formation (Paternot, Colleoni et al. 2014). This formation could also prevent the phosphorylation at T172 of CDK4, which correlates to the effectiveness of Palbociclib in breast cancer (Raspé, Coulonval et al. 2017). These results were verified via western blotting, where for U87 and LN229 a small downregulation of Rb and E2F1 was observed as well as decreased phosphorylation of Rb (Figure 25). In T98G cells

the effects were less pronounced, with only small decreases in protein and phosphorylation levels.

Our next step was to analyse viral parameters in the combinatory approach of CDk4/6i and XVir-N-31 infection. For Ribociclib the effects were synergistic in two cell lines, both U87 ($p \leq 0.001$) and LN229 ($p \leq 0.001$) responded to increased levels of inhibitor in addition to viral infection with increased cell killing (Figure 26). In T98G cells there were additive effects observable at a concentration of 1µM LEE011. These effects could not be observed when treating the cells with Abemaciclib (Figure 20). Here 100nM LY showed good effects in U87 and, interestingly, T98G cells. But LN229 did not respond to the combination of CDK4/6i and XVir-N-31. At 1µM LY the side effects resulted in a diminished viral cell lysis in U87 cells. Whereas T98G cells, responded also to 1µM LY. This is in accordance with the results achieved in combination with TMZ and Radiation, were T98G cells proved to be the most resistant (Figure 16). The results of the adverse effects using Abemaciclib were also observable, when analysing the viral replication and particle formation. In both assays the virus performed poorly when the cells were pretreated with high concentrations of LY. In both responding cell lines (U87 and T98G) at a concentration of 1µM the viral replication after 24h was lower compared to the control group (Figure 21). While at 100nM LY the particle formation was increased, again pretreating the cells with 1µM LY had a diminishing effect on the production of viral particles, resulting in less the 20% particles formed compared to the control in U87 and LN229 cells (Figure 22). While these effects strongly oppose a combinatory treatment regime of CDK4/6 and oncolytic adenoviruses, the results with the second CDK4/6i Ribociclib were more promising. Both the replication (Figure 27) and particle formation (Figure 28) were increased under LEE011 treatment. Higher concentrations led to a more pronounced effect.

Since T98G cells did not respond as strongly to CDK4/6i compared to the other cell lines. Starvation of growth factors, via FCS deprivation leads to unspecific growth arrest (Figure 29). The observed growth arrest was not as pronounced, but we could increase the replication in T98G cells, but the increased replication was not accompanied by a higher production of infectious particles (Figure 31). A third option to decrease Rb protein levels in T98G cells is the inhibition via siRNA. We tested two independent siRNAs against Rb. In the western blots we could observe a strong decrease in RB protein level in both used constructs compared to the siCtrl (Figure

30). Interestingly starvation resulted in a decline of Rb only after 48 hours. Maybe the effects observed in the replication and particle formation would be further increased, when the infection only occurred after 48 hours, but longer starvation leads to further decline of cell survival and the viral production would be further decreased. Unfortunately, the inhibition of Rb via siRNA did not lead to a pronounced benefit for viral replication (Figure 32).

All together CDK4/6 inhibitors worked in GBM cell lines. Interestingly the effects were much lower to what we have experienced so far in other tumor entities. For bladder cancer, the combination of a CDK4/6 inhibitor led to a high fold increase in all viral parameters, and the same effect was already observed in head and neck cancer [data not shown]. But since GBM is one of the worst tumor entities in existence even small benefits could be a potential help for the treatment of patients.

Locking the cells in the G1 state resembles the natural environment for adenoviral infections. This allows effective viral cycles in more cells, compared to the untreated. We have already shown that already low MOIs are capable to start effective replication in bladder cancer cells, compared to the same MOIs in untreated cells. The downregulation of Rb is a crucial step priming the cells making it easier for the virus to overcome the natural Rb/E2F blockade, without the need to first crack the complex, removing E2F and stabilizing it for activation of the E1- and E2 early promotor.

4.4. Combination of the oncolytic adenovirus XVir-N-31 with JQ1

JQ1 is a competitive inhibitor of BRD4, known to epigenetically downregulate c-Myc as well as cell cycle proteins like CDK4 and CDK6 (Delmore, Issa et al. 2011, Sun, Shah et al. 2015). We first focussed on cellular parameters altered by JQ1 treatment. To find a good tolerable dose we investigated the toxicity of JQ1 in a dose dependent manner. Interestingly in two of our three cell lines the cell survival was never below 50% compared to the control, even at concentrations of 50µM (Figure 33) . The cell line T98G responded much stronger to the treatment. The treatment with low concentrations of JQ1 did not result in a G1 arrest (Figure 34), but at concentrations of 200nM JQ1, this is in accordance with published data. We observed a downregulation of Rb and its phosphorylation in both U87 and LN229 cells (Figure 35). This could offer an explanation for the increased viral parameters, but the effects are more prominent than the treatment with CDK4/6 inhibitors, where a stronger decrease in Rb and pRb could be observed (Figure 39). But JQ1 does not only target the cell cycle, but in fact

the effects are based on the epigenic alterations caused by the small molecule inhibitor, on both the cellular and viral genome (Sun, Shah et al. 2015, Qiao, Chen et al. 2020). The cell killing (Figure 36) was strongly enhanced as well as the replication (Figure 37) and particle formation (Figure 38), especially the cell line LN229. With JQ1 the replication of XVir-N-31 was 7-fold enhanced in T98G cells, this was the highest induction, experienced with any treatment option. Interestingly the production of viral particles was not strongly increased in U87 cells, compared to the CDK4/6 inhibitor treatment, but they have a very high baseline production, maybe the production capacity is reached. In LN229 cells we achieved an increase in particle production of over 15 times, with concentrations that are reachable in an *in vivo* setting and 5-fold in T89G cells. This really strengthens the value of bromodomain inhibitors as a treatment option in combination with virotherapy. In conclusion all viral parameters were increased.

BET inhibitors have a completely different mode of action compare to CDK4/6 inhibitors, while CDK4/6 prime the cells allowing an easier replication with less viral load. JQ1 only amplifies the expression of viral genes and consequently the replication. This is currently heavily investigated in our lab, we could already show that this increase is E1A independent, and the increase in viral gene expression is observable in both early genes like E1B, E2 early, but as well late genes under the control of the MLP are activated in both a higher extend and earlier in the viral cycle. This effect non the less does not lead to a much higher outcome at the endpoint, instead it just accelerates the viral cycle.

4.5. New triple therapy approach

We now experienced the separated beneficial effects of both CDK4/6i and bromodomain inhibitors on both cellular and viral parameters. On the cellular parameters, the combination led to a further decrease in Rb and its phosphorylation in U87 cells. In LN229 and T89G these effects were more prominent in the first 24 hours. But this could not be the complete explanation for the benefits oberved in the combinatory approach, since the usage of siRNA against Rb did not lead to any significant increase in viral replication. The same holds true for a starvation induced G1 arrest (Figure 31 & Figure 32). Interestingly when analysing the effects on viral proteins we could observe an increase in DNA binding protein (DBP) in both LN229 and T98G cells after 48 h.p.i. and the strongest increase was observed in the triple

therapy approach (Figure 40). These observations transfer also on all other viral parameters, with increased viral potency (Figure 41), viral replication (Figure 42) and particle formation (Figure 43). But each cell line exhibit small differences. U87 cell lines are very responsible to the CDK4/6 inhibitor treatment as well as the JQ1, therefore there is not a much higher cell killing observable in the triple therapy approaches, but since both treatments alone are already beneficial, in the combination the concentration could be further decreased to 50nM of both LEE011 and JQ1. In U87 the effects on viral replication can already be measured strongly at the 24 hour time point. Here the combination led to the highest increase compared to the 48 hour value. If we use higher concentrations of LEE and JQ1 interestingly the combination again decreases the effective production of viral particles. This proves that the effectiveness depends not only on the correct combinations of both inhibitors, but as well on the concentrations and timing. In LN229 the combination of 100nM of both inhibitors was sufficient to decrease cell viability over 95% (Figure 41). The viral replication was increased in all tested combinations, but interestingly the production of viral particles was mostly dependent on JQ1, here 50nM and 100nM JQ1 led to an increase over 20-fold compared to the control. Again higher levels of JQ1 had an adverse effect. The combination of 100nM LEE and 50nM JQ1 was equal to 100nM JQ1. T98G resembled the effects on LN229.

When comparing all tested therapeutic approaches, we could state that the combination of CDK4/6 inhibitors with bromodomain inhibitors display the most prominent treatment option (Figure 44 & Figure 45).

The effects of both strategies interact with the viral cycle in different ways and phases. While CDK4/6 inhibitors seem to prepare the cells for the viral infection and causing increased E1A expression, the bromodomain inhibitor enhances the expression of viral genes independently of E1A. Therefore the optimal timepoints for the treatment, differed as well. While LEE011, was best given 16-24 hours before the infection, simultaneous JQ1 treatment led to the best results. This discriminates both treatment strategies from the classical treatment options, that both led to the accumulation of nuclear YB-1. While the viral replication is in the later phases depended on the expression via the E2-late promotor, the initial infection is a much more unknown system. The role of Rb during the early infection is crucial. While the effects of the E1

proteins on the Rb/E2F complex are studied in a certain degree, conflicting results have emerged.

Based on the results we have obtained to far, we focused on enhancing our knowledge in the molecular mechanisms that are involved in the induced effects of both drugs. For both the CDK4/6 induced priming of the cells as well as the accelerated cell lysis, by Brd4 inhibition via JQ1.

The E2F transcription factors play an important role in the expression of adenoviral early transcripts, both the E1 Enhancer and the E2 early region contain two E2F binding sites. To deepen our knowledge we constructed two adenoviral constructs that gave us the opportunity to shed some light in the importance of cellular Rb and E2Fs. The first construct bears additional 30 artificial E2F binding sites in the E3 region (WT Trap) (Figure 46). This construct alters the activation of the E1 Enhancer and E2 early promotor by trapping E2F. The second construct used in this thesis was created by Klaus Mantwill and myself and has mutated E2F binding sites in both the E1 Enhancer and the E2 early promotor (WT 2xE2Fm) (Figure 48). These are new tools to further allow us to shed light on the importance of E2F in the context of early infection cycles and the molecular mechanisms of both CDK4/6i and bromodomain inhibitors. What we could observe is that the construct with double mutated E2F binding sites, replicates in a much lower extent compared to the WT control. This can be easily explained by the importance of viral E1 at the initiation of the viral cycle.

Loosing these E2F sites result in much lower transcription of viral genes, thereby delaying the initial reprogramming of the cells as well as viral replication (Figure 49). Interestingly using the bromodomain inhibitor JQ1 we were able to increase the viral replication, which is already an astonishing finding. This is interesting because it is a hint for the answer to the question concerning the mode of action of JQ1. We observe that JQ1 activates viral replication independently of E2Fs, because E2Fs are needed for the activation of the E1 and E2 early promotor. This is in good accordance with investigations of a second PhD student in our lab, focussed on understanding the molecular mechanisms of JQ1. When using the Trap mutated adenovirus, we observed that the virus alone was much weaker compared to the control (Figure 47). But using the CDK4/6 inhibitor LEE011, allowed an improvement of the viral replication, at this timepoint we have no explanation off and should be further validated. But these results proved to be not as promising in GBM cell lines. All results lead us to the believe

that the Rb/E2F axis is a difficult target in GBM cells. The usage of JQ1 to induce epigenetic changes improving the viral expression and replication, is a new potential tool. Here the new constructs will help to allow a deeper understanding of the viral mechanisms.

Since these results could only partly explain the effects observed using CDK4/6i and bromodomain inhibitors another factor can not be excluded as an explanation. Here the importance of RNA polymerase II comes into view. RNA polymerase II is interconnected with cell cycle proteins, its transcription activity is regulated by several members of the CDK protein family (Fisher 2017). The positive transcription elongation factor b complex (p-TEFb), consisting of cyclin dependent kinase 9 (CDK9) and cyclin T, is recruited to stalled RNA pol II and stimulates elongation via phosphorylation (Zaborowska, Isa et al. 2016), via binding to the BRD4 protein. This holds true not only in the area of cellular transcription, but as well for viral gene expression. Here the viral E1A protein recruits via the mediator complex RNA pol II (Vijayalingam and Chinnadurai 2013). A negative regulator of p-TEFb is the HEXIM1 protein, limiting viral replication of e.g. HIV-1 (Shimizu, Urano et al. 2007) and works as an opposition to BRD4 (Chen, Yik et al. 2014). Here the Bromodomain inhibitor JQ1 comes into play, resulting in an transient upregulation of transcription via the release p-TEFb from 7SK small nuclear ribonucleoprotein (Bartholomeeusen, Xiang et al. 2012). This transient transcription could be the basis of the massive increase in viral protein expression, observed in our group. We believe that the treatment with JQ1 releases the “brakes” on RNA pol II, resulting in a massive boost of viral proteins. That this effect if only transient, could be seen in, time kinetics done in our lab, where the addition of JQ1, before, during and after infection, resulted in complexly different expression and replication values. Giving JQ1 24 hours before infection was indeed worse compared to concurrent treatment. If the treatment with JQ1 did not exceed 16 hours after infection, there were still positive influences on the viral replication observable. In the combination with the CDK4/6 inhibitor, LEE011, helping to overcome the initial burden for viral replication, by downregulation of the repressive Rb/E2F complex, all viral parameters can be boosted, resulting in the so far optimal approach for virotherapy. Upon completion of my thesis, further work on the mechanism shows that treatment with CDK 4/6 inhibitors increases the activity of RNA polymerase II without affecting the E2F/RB pathway (Prof. Holm personal communication). If this is the case for glioblastoma where also an increase in viral replication is seen without significant

inhibition of E2F/RB expression at low concentration, it could be a possible explanation for the observed effects.

However, the triple therapy of oncolytic adenoviral construct, with CDK4/6 inhibitor LEE011 and bromodomain inhibitor JQ1, proof to be a promising translational treatment strategy. Therefore, future investigations should focus on improving any of these three parameters even further.

4.6. Outlook

The usage of oncolytic virotherapy is an emerging strategy for the treatment of cancer. Over the past decade numerous clinical trials have taken place analysing a huge variety of different oncolytic vectors. For adenoviral constructs several clinical trials are ongoing. During this thesis, we compared different treatment options in combination with our oncolytic adenoviral construct XVir-N-31 to increase both viral oncolysis as well as improving all viral parameters, leading to a higher replication and particle formation. Priming the cells with CDK4/6 inhibitors as well as increasing cell killing via JQ1 are features that can be analysed *in vitro*. While JQ1 has not proven to be of good use in vivo due to its limited pharmacokinetics, better in vivo applicable bromodomain inhibitors are already in clinical trials (Xu, Chen et al. 2018, Li, MacKenzie et al. 2020). As proven already by others the important involvement of the immune system in therapy response is one aspect we could not investigate in vitro. Here lies one of the most critical functions of adenoviral attack on the tumor. The immunogenicity of viral vectors is known for a long time, but the emerging field of immune checkpoint blockaders, like anti-PD-L1 antibodies, enhances this field enormously. The main goal is to turn immune “cold” tumors back to “hot" ones (Kwan, Winder et al. 2021). We and others have already shown the importance of the immune system on virotherapy. While oncolysis may not be the most important feature for virotherapy in vivo, it is fundamentally linked to the immune response. Therefore, improving viral replication and particle formation are not negotiable features of any therapy involving viral constructs. Since a monotherapy with virus does not lead to a strong replication, partnering the therapy with small molecule inhibitors, is the preferred option. During this thesis we successfully established a translational approach. We showed an increase in all viral parameters, with different glioblastoma cell lines, reacting different in all approaches. While the effects differed between all cell lines, there was nonetheless a positive outcome, with the triple therapy in each one. Understanding the

molecular basis of this treatment allows not only to further analyse these effects, but also the improvement of all treatment components. For the success of a virotherapy it is important to attack as many cells as possible in vivo and then replicate and produce as much particle as possible, to improve the immune response the most. A chronic infection is not needed under those circumstances. The next step of taking this approach into an in vivo setup is already taken. Our cooperation partner in the Hertie-Institute for brain research in Tübingen, AG Naumann was able to match PBMCs to the immune signature of U87 cells, allowing them to produce an animal model, to analyse exactly these parameters. The usage of XVir-N-31 proved to benefit the immune parameters critically, improving the tumor infiltration with T cells and the release of cytokines. Fascinatingly the effects did not restrict to the one hemisphere that was injected with XVir-N-31, the immune anti tumor response could also be seen in the second hemisphere, with higher infiltration of T cells. Now the next experiments will be done with the additional knowledge provided by us, using the bromodomain inhibitor JQ1 as well as the CDK4/6 inhibitor LEE011, to further increase the viral parameters and prime the cells for increased access for the virus.

Our group is now further focussed in untangling the exact mode of action that JQ1 provides to benefit the viral gene expression and replication. While we already understand the therapeutic window, being beneficial for the initial expression of viral genes, the complete underlying mechanisms remain uncertain. Further insights are needed, allowing the production of better viral constructs as well as understanding all molecular pathways involved, during the infection.

5. Supplement

5.1. Immunogenicity of viral vector systems

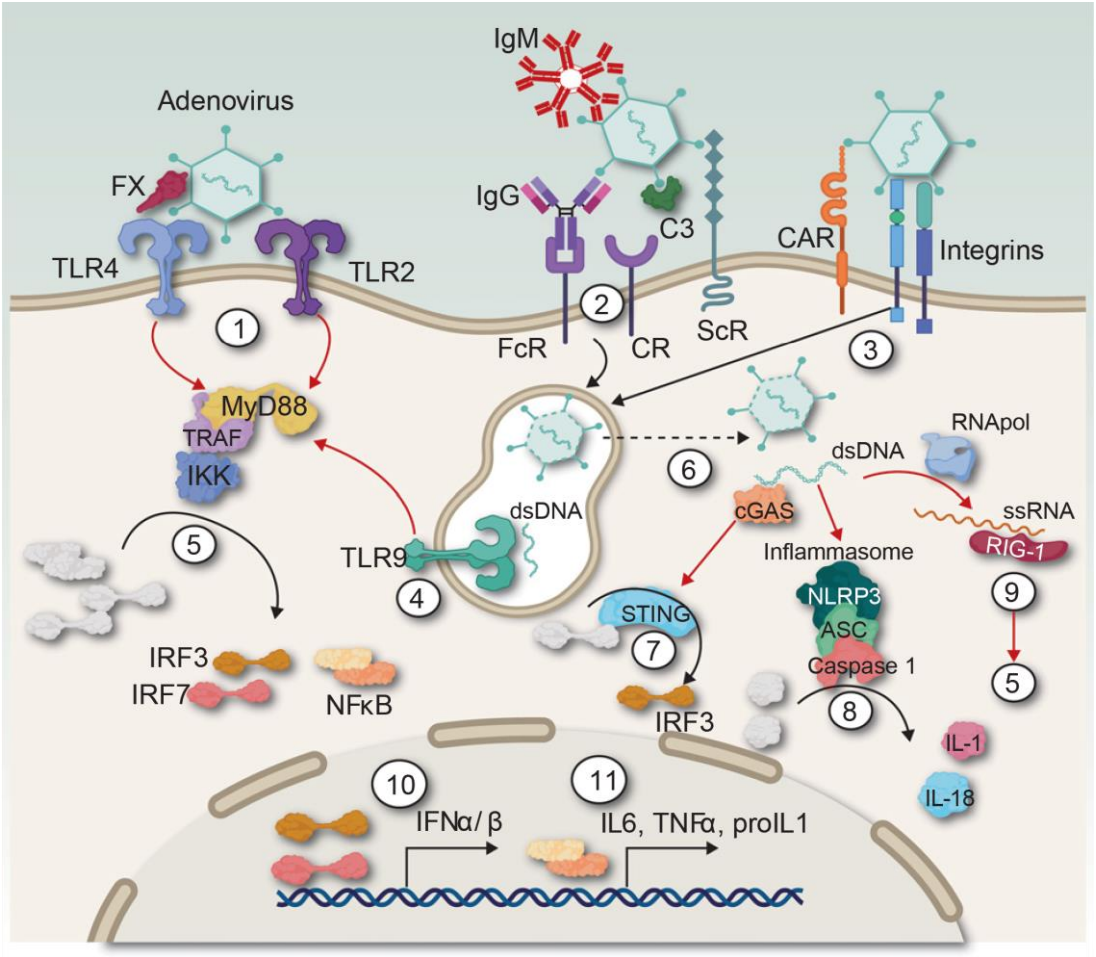

Supplementary Figure 1: Anti-adenovirus immune sensing. The innate sensors to Ads could be divided into the TLR-MyD88 depending pathways or independent (cytosolic sensors). (1) The Ad is recognized by Toll-like receptor 2 (TLR2), or the factor X (FX)-Ad complex is detected by TLR4. Both interactions trigger the MyD88 pathway. (2) The opsonized Ads are captured by Fc receptors (FcR), complement receptors (CRs) or scavenger receptors (ScR), and phagocyted into macrophages, DCs, neutrophils, and monocytes. (3) Adenoviruses could infect cells through CAR/integrins mechanism. (4) The viral dsDNA is detected in the endosome by TLR9 activating the MyD88 pathway, (5) which ends in the activation of IFN-regulating factors (IRFs) 3 and 7, and also the activation of the NFkB transcription factor. (6) The viral DNA in the cytosol induces (7) cyclic GMP-AMP synthase (cGAS) that homodimerizes generating a cyclic guanine adenine monophosphate (cGAMP) which binds to adaptor STING leading to activate IRF3, (8) the inflammasome (NLRP3, ASC, and activated caspases) cleaves pro-IL1 and IL18 into their active form. (9) The adenovirus genome could be transcribed into ssRNA by RNApolIII and activate the RIG-1 sensor, which induces MyD88 cascade. (10) This response ends in the IRF activation promote the IFN type I (a and b) production. (11) NFkB promotes the translation of proinflammatory genes such as IL6, TNFa, proIL1b, among others. Figure adapted from (Farrera-Sal, Moya-Borrego et al. 2021) with permission of the AACR (2021).

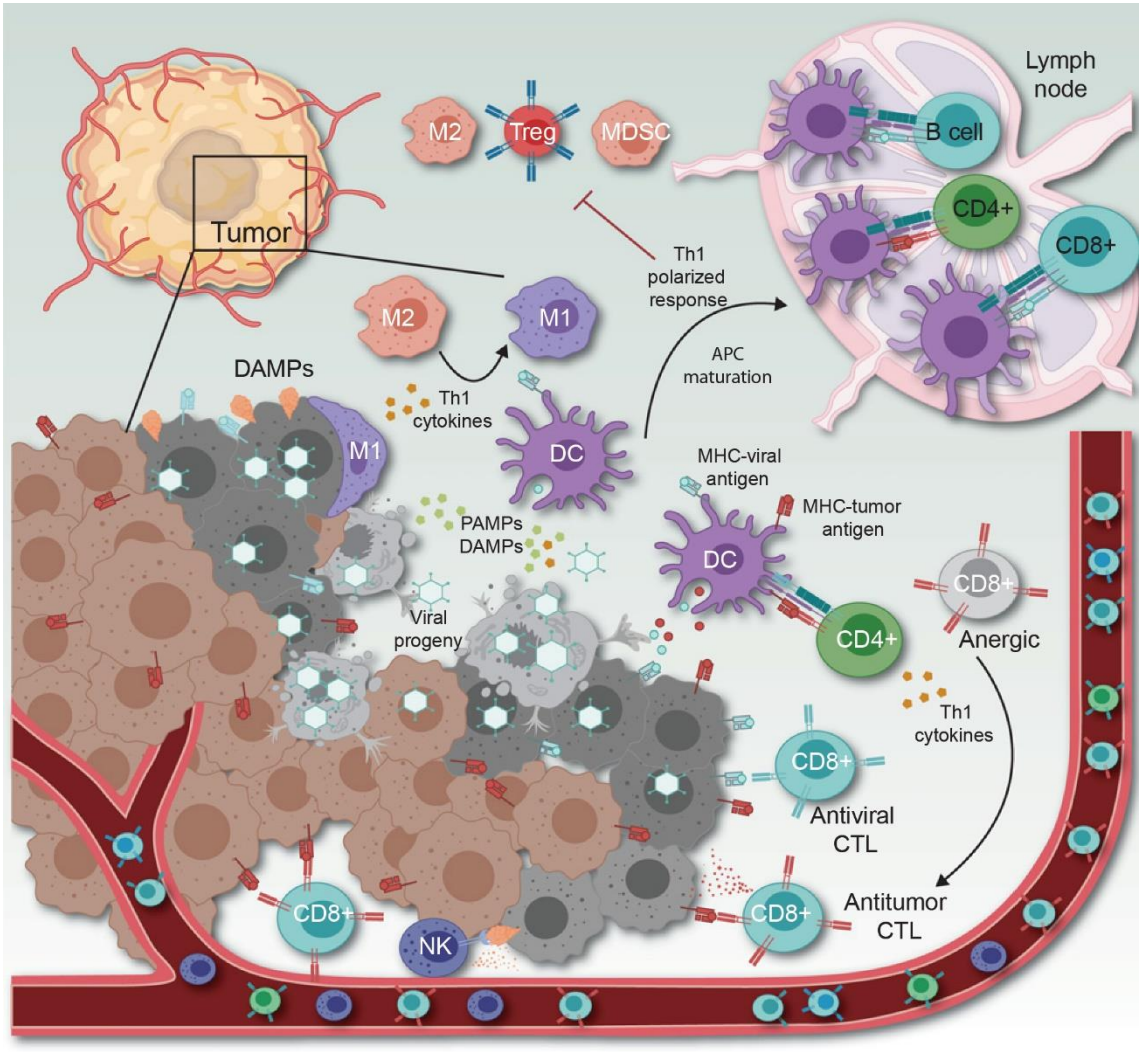

Supplementary Figure 2: Overview of immunovirotherapy and in situ vaccination hypothesis. Tumor-infected cells express DAMPs that could recruit M1 macrophages (blue) among other innate cells and phagocyte the tumor cell (dark gray tumor cell) inducing proinflammatory cytokines (Th1 cytokines). In parallel, the virus induces oncolysis (light gray tumor cells), releasing the viral progeny, PAMPs (green), DAMPs (orange) and tumor (red), and viral (light blue) antigens. These are captured by DCs that mature and transit to the lymph node cross-presenting and activating antitumoral and antiviral lymphocytes (CD8þ, CD4þ, and Bcells). They circulate toward the tumor thanks to a chemokine gradient also induced during the proinflammatory response. The Th1 polarization can revert immunosuppressed phenotypes such M2 macrophages to M1 or anergic T cells to their activation. Moreover, the Th1 polarization in the lymph node avoids the maturation and differentiation of regulatory T cells (Tregs) and myeloid-derived suppressor cells (MDSCs). Figure adapted from (Farrera-Sal, Moya-Borrego et al. 2021) with permission of the AACR (2021).

5.2. Cloning of the new viral vector WT 2xE2Fm

Besides analysing the effects of small molecule inhibitors on both cellular and viral targets, another possibility is directly manipulating the viral genome, disrupting the binding of cellular proteins on viral promotors. We used an already established adenoviral construct, bearing mutations in the two E2F binding sites in the viral E2 promotor (WT E2Fm) and combined it with a mutation of the E2F binding site in the E1 promotor.

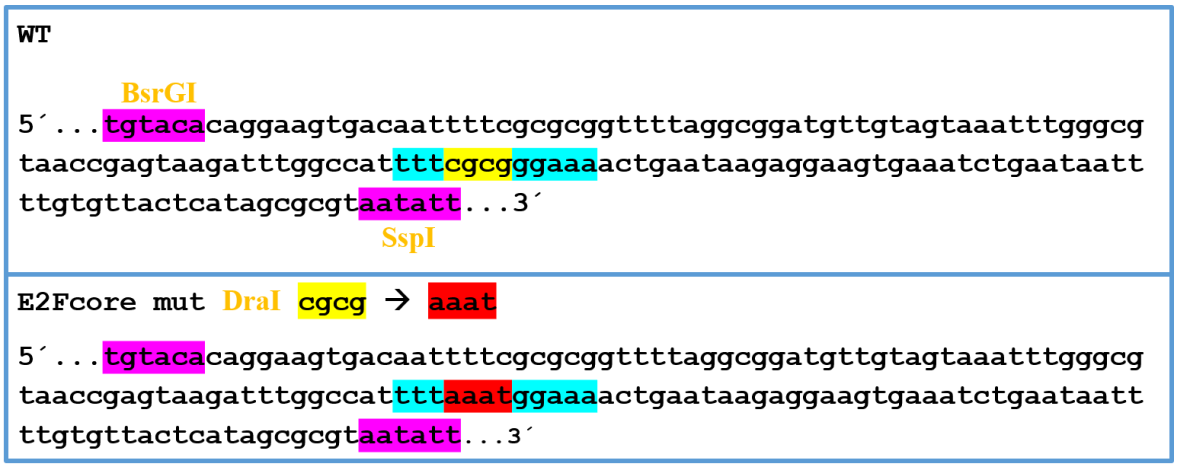

Supplementary Figure 3: Comparison of the WT E1 Enhancer, with a WT E2F binding site and a mutated version used in the new AdWT 2xE2Fm vector.

Mutations were done in a pShuttle AdEasy system using BsrGI and SspI the region containing the E2F binding site was first removed and then exchanged with the same sequence containing a DraI restriction side in the core E2F binding sequence. The pShuttle plasmid was then reintegrated into a backbone already containing the E2F binding site mutations in the E2 region. The plasmids were analysed using restriction analysis in a agarose gel and the specific sides were sequenced to ensure correct insertion and orientation. The finished plasmids were then linearized via XhoI digestions and transfected into HEK293 cells for virus production.

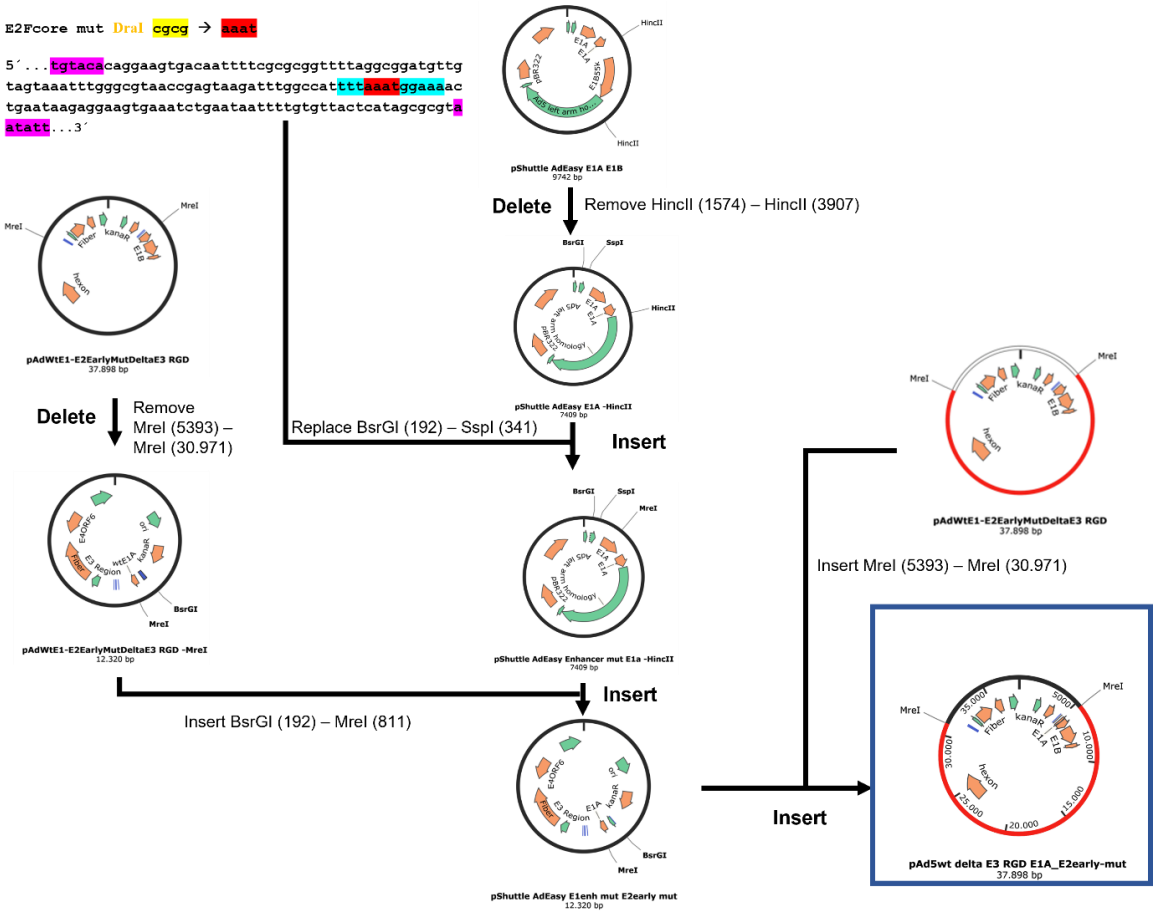

Supplementary Figure 4: Creating of a new Adenoviral construct bearing mutations in E2F binding sites in both the E1 enhancer and the E2 early promotor.

The produced virus exhibited a severe lower replication after 48 hours compared to the control WT adenovirus. When combining the WT 2xE2Fm virus with the CDK4/6i LEE011 or the bromodomain inhibitor JQ1, the viral replication could be increased in two cell lines. The effects were more pronounced using JQ1. The combination of both inhibitors led only in T98G to a further increase of viral replication.

References

Ablack, J. N., P. Pelka, A. F. Yousef, A. S. Turnell, R. J. Grand and J. S. Mymryk (2010). "Comparison of E1A CR3-dependent transcriptional activation across six different human adenovirus subgroups." Journal of virology **84**(24): 12771-12781.

Akaike, Y., Y. Nakane and T. Chibazakura (2021). "Analysis of E1A domains involved in the enhancement of CDK2 activity." Biochemical and Biophysical Research Communications **548**: 98-103.

Avvakumov, N., A. Kajon, R. Hoeben and J. Mymryk (2004). "Comprehensive sequence analysis of the E1A proteins of human and simian adenoviruses." Virology **329**(2): 477-492.

Bandara, L. R. and N. B. La Thangue (1991). "Adenovirus E1a prevents the retinoblastoma gene product from complexing with a cellular transcription factor." Nature **351**(6326): 494-497.

Barker, D. D. and A. J. Berk (1987). "Adenovirus proteins from both E1B reading frames are required for transformation of rodent cells by viral infection and DNA transfection." Virology **156**(1): 107-121.

Bartholomeeusen, K., Y. Xiang, K. Fujinaga and B. M. Peterlin (2012). "Bromodomain and extra-terminal (BET) bromodomain inhibition activate transcription via transient release of positive transcription elongation factor b (P-TEFb) from 7SK small nuclear ribonucleoprotein." Journal of Biological Chemistry **287**(43): 36609-36616.

Ben-Israel, H. and T. Kleinberger (2002). "Adenovirus and cell cycle control." Front Biosci **7**: d1369-d1395.

Berk, A. J. (1986). "Adenovirus promoters and E1A transactivation." Annual review of genetics **20**(1): 45-77.

Bieler, A., K. Mantwill, T. Dravits, A. Bernshausen, G. Glockzin, N. Köhler-Vargas, H. Lage, B. Gansbacher and P. S. Holm (2006). "Novel three-pronged strategy to enhance cancer cell killing in glioblastoma cell lines: histone deacetylase inhibitor, chemotherapy, and oncolytic adenovirus dl520." Human gene therapy **17**(1): 55-70.

Bieler, A., K. Mantwill, R. Holzmüller, K. Jürchott, A. Kaszubiak, S. Stärk, G. Glockzin, H. Lage, A.-L. Grosu and B. Gansbacher (2008). "Impact of radiation therapy on the oncolytic adenovirus dl520: implications on the treatment of glioblastoma." Radiotherapy and Oncology **86**(3): 419-427.

Birzu, C., P. French, M. Caccese, G. Cerretti, A. Idbaih, V. Zagonel and G. Lombardi (2021). "Recurrent glioblastoma: from molecular landscape to new treatment perspectives." Cancers **13**(1): 47.

Blake, M. C. and J. Azizkhan (1989). "Transcription factor E2F is required for efficient expression of the hamster dihydrofolate reductase gene in vitro and in vivo." Molecular and cellular biology **9**(11): 4994-5002.

Blumenthal, R., P. Seth, M. C. Willingham and I. Pastan (1986). "pH-dependent lysis of liposomes by adenovirus." Biochemistry **25**(8): 2231-2237.

Braithwaite, A. and I. Russell (2001). "Induction of cell death by adenoviruses." Apoptosis **6**(5): 359-370.

Brat, D. J., K. Aldape, H. Colman, D. Figrarella-Branger, G. N. Fuller, C. Giannini, E. C. Holland, R. B. Jenkins, B. Kleinschmidt-DeMasters and T. Komori (2020).

"cIMPACT-NOW update 5: recommended grading criteria and terminologies for IDH-mutant astrocytomas." Acta neuropathologica **139**(3): 603-608.

Bressy, C. and K. Benihoud (2014). "Association of oncolytic adenoviruses with chemotherapies: an overview and future directions." Biochemical pharmacology **90**(2): 97-106.

Capper, D., S. Weißert, J. Balss, A. Habel, J. Meyer, D. Jäger, U. Ackermann, C. Tessmer, A. Korshunov and H. Zentgraf (2010). "Characterization of R132H mutation-specific IDH1 antibody binding in brain tumors." Brain pathology **20**(1): 245-254.

Cassany, A., J. Ragues, T. Guan, D. Bégu, H. Wodrich, M. Kann, G. R. Nemerow and L. Gerace (2015). "Nuclear import of adenovirus DNA involves direct interaction of hexon with an N-terminal domain of the nucleoporin Nup214." Journal of virology **89**(3): 1719-1730.

Cenciarini, M., M. Valentino, S. Belia, L. Sforna, P. Rosa, S. Ronchetti, M. C. D'Adamo and M. Pessia (2019). "Dexamethasone in glioblastoma multiforme therapy: mechanisms and controversies." Frontiers in molecular neuroscience **12**: 65.
Chaurasiya, S., N. Chen and S. Warner (2018). "Oncolytic virotherapy versus cancer stem cells: A review of approaches and mechanisms." Cancers **10**(4): 124.

Chaurasiya, S., Y. Fong and S. G. Warner (2021). "Oncolytic Virotherapy for Cancer: Clinical Experience." Biomedicines **9**(4): 419.

Chen, R., J. H. Yik, Q. J. Lew and S.-H. Chao (2014). "Brd4 and HEXIM1: multiple roles in P-TEFb regulation and cancer." BioMed research international **2014**.

Chen, R., M. Zhang, Y. Zhou, W. Guo, M. Yi, Z. Zhang, Y. Ding and Y. Wang (2020). "The application of histone deacetylases inhibitors in glioblastoma." Journal of Experimental & Clinical Cancer Research **39**(1): 1-18.

Chiocca, E. A., F. Nassiri, J. Wang, P. Peruzzi and G. Zadeh (2019). "Viral and other therapies for recurrent glioblastoma: is a 24-month durable response unusual?" Neuro-oncology **21**(1): 14-25.

Choi, A. H., M. P. O'Leary, Y. Fong and N. G. Chen (2016). "From benchtop to bedside: a review of oncolytic virotherapy." Biomedicines **4**(3): 18.

Cohen, A. L., S. L. Holmen and H. Colman (2013). "IDH1 and IDH2 mutations in gliomas." Current neurology and neuroscience reports **13**(5): 345.

Dallaire, F., S. Schreiner, G. E. Blair, T. Dobner, P. E. Branton and P. Blanchette (2015). "The human adenovirus type 5 E4orf6/E1B55K E3 ubiquitin ligase complex enhances E1A functional activity." MSphere **1**(1): e00015-00015.

Delmore, J. E., G. C. Issa, M. E. Lemieux, P. B. Rahl, J. Shi, H. M. Jacobs, E. Kastritis, T. Gilpatrick, R. M. Paranal and J. Qi (2011). "BET bromodomain inhibition as a therapeutic strategy to target c-Myc." Cell **146**(6): 904-917.

Dhingra, A., E. Hage, T. Ganzenmueller, S. Böttcher, J. Hofmann, K. Hamprecht, P. Obermeier, B. Rath, F. Hausmann and T. Dobner (2019). "Molecular evolution of human adenovirus (HAdV) species C." Scientific reports **9**(1): 1-13.

Donati, B., E. Lorenzini and A. Ciarrocchi (2018). "BRD4 and Cancer: going beyond transcriptional regulation." Molecular cancer **17**(1): 164.

Eigenbrod, S., R. Trabold, D. Brucker, C. Erös, R. Egensperger, C. La Fougere, W. Göbel, A. Rühm, H. A. Kretzschmar and J. C. Tonn (2014). "Molecular stereotactic biopsy technique improves diagnostic accuracy and enables personalized treatment strategies in glioma patients." Acta neurochirurgica **156**(8): 1427-1440.

Ellingson, B. M., L. E. Abrey, S. J. Nelson, T. J. Kaufmann, J. Garcia, O. Chinot, F. Saran, R. Nishikawa, R. Henriksson and W. P. Mason (2018). "Validation of postoperative residual contrast-enhancing tumor volume as an independent prognostic factor for overall survival in newly diagnosed glioblastoma." Neuro-oncology **20**(9): 1240-1250.

Farrera-Sal, M., L. Moya-Borrego, M. Bazan-Peregrino and R. Alemany (2021). "Evolving Status of Clinical Immunotherapy with Oncolytic Adenovirus." Clinical Cancer Research.

Filippakopoulos, P., J. Qi, S. Picaud, Y. Shen, W. B. Smith, O. Fedorov, E. M. Morse, T. Keates, T. T. Hickman and I. Felletar (2010). "Selective inhibition of BET bromodomains." Nature **468**(7327): 1067-1073.

Finn, R. S., A. Aleshin and D. J. Slamon (2016). "Targeting the cyclin-dependent kinases (CDK) 4/6 in estrogen receptor-positive breast cancers." Breast Cancer Research **18**(1): 1-11.

Fischer, N. W., A. Prodeus, D. Malkin and J. Gariépy (2016). "p53 oligomerization status modulates cell fate decisions between growth, arrest and apoptosis." Cell Cycle **15**(23): 3210-3219.

Fisher, R. P. (2017). "CDK regulation of transcription by RNAP II: Not over 'til it's over?" Transcription **8**(2): 81-90.

Flak, M. B., C. M. Connell, C. Chelala, K. Archibald, M. A. Salako, K. J. Pirlo, M. Lockley, S. P. Wheatley, F. R. Balkwill and I. A. McNeish (2010). "p21 Promotes oncolytic adenoviral activity in ovarian cancer and is a potential biomarker." Molecular cancer **9**(1): 175.

Fritz, L., L. Dirven, J. C. Reijneveld, J. A. Koekkoek, A. M. Stiggelbout, H. R. W. Pasman and M. J. Taphoorn (2016). "Advance care planning in glioblastoma patients." Cancers **8**(11): 102.

Fueyo, J., R. Alemany, C. Gomez-Manzano, G. N. Fuller, A. Khan, C. A. Conrad, T.-J. Liu, H. Jiang, M. G. Lemoine and K. Suzuki (2003). "Preclinical characterization of the antiglioma activity of a tropism-enhanced adenovirus targeted to the retinoblastoma pathway." Journal of the National Cancer Institute **95**(9): 652-660.

Fueyo, J., C. Gomez-Manzano, R. Alemany, P. S. Lee, T. J. McDonnell, P. Mitlianga, Y.-X. Shi, V. Levin, W. A. Yung and A. P. Kyritsis (2000). "A mutant oncolytic adenovirus targeting the Rb pathway produces anti-glioma effect in vivo." Oncogene **19**(1): 2-12.

Gaspar, N., L. Marshall, L. Perryman, D. A. Bax, S. E. Little, M. Viana-Pereira, S. Y. Sharp, G. Vassal, A. D. Pearson and R. M. Reis (2010). "MGMT-independent temozolomide resistance in pediatric glioblastoma cells associated with a PI3-kinase–mediated HOX/stem cell gene signature." Cancer research **70**(22): 9243-9252.

Gonzalez-Pastor, R., P. S. Goedegebuure and D. T. Curiel (2021). "Understanding and addressing barriers to successful adenovirus-based virotherapy for ovarian cancer." Cancer gene therapy **28**(5): 375-389.

Goodrum, F. D. and D. A. Ornelles (1997). "The early region 1B 55-kilodalton oncoprotein of adenovirus relieves growth restrictions imposed on viral replication by the cell cycle." Journal of Virology **71**(1): 548-561.

Gulati, S., A. S. Jakola, U. S. Nerland, C. Weber and O. Solheim (2011). "The risk of getting worse: surgically acquired deficits, perioperative complications, and functional outcomes after primary resection of glioblastoma." World neurosurgery **76**(6): 572-579.

Harada, J. N. and A. J. Berk (1999). "p53-Independent and-dependent requirements for E1B-55K in adenovirus type 5 replication." Journal of virology **73**(7): 5333-5344.

Harrington, K., D. J. Freeman, B. Kelly, J. Harper and J.-C. Soria (2019). "Optimizing oncolytic virotherapy in cancer treatment." Nature Reviews Drug Discovery: 1.

Hasselbach, L. A., S. M. Irtenkauf, N. W. Lemke, K. K. Nelson, A. D. Berezovsky, E. T. Carlton, A. D. Transou, T. Mikkelsen and A. C. deCarvalho (2014). "Optimization of high grade glioma cell culture from surgical specimens for use in clinically relevant animal models and 3D immunochemistry." JoVE (Journal of Visualized Experiments)(83): e51088.

Hegi, M. E., A.-C. Diserens, T. Gorlia, M.-F. Hamou, N. De Tribolet, M. Weller, J. M. Kros, J. A. Hainfellner, W. Mason and L. Mariani (2005). "MGMT gene silencing and benefit from temozolomide in glioblastoma." New England Journal of Medicine **352**(10): 997-1003.

Heise, C., T. Hermiston, L. Johnson, G. Brooks, A. Sampson-Johannes, A. Williams, L. Hawkins and D. Kirn (2000). "An adenovirus E1A mutant that demonstrates potent and selective systemic anti-tumoral efficacy." Nature medicine **6**(10): 1134-1139.
Hoeben, R. C. and T. G. Uil (2013). "Adenovirus DNA replication." Cold Spring Harbor perspectives in biology **5**(3): a013003.

Holm, P. S., S. Bergmann, K. Jürchott, H. Lage, K. Brand, A. Ladhoff, K. Mantwill, D. T. Curiel, M. Dobbelstein and M. Dietel (2002). "YB-1 relocates to the nucleus in adenovirus-infected cells and facilitates viral replication by inducing E2 gene expression through the E2 late promoter." Journal of Biological Chemistry **277**(12): 10427-10434.

Holm, P. S., H. Lage, S. Bergmann, K. Jürchott, G. Glockzin, A. Bernshausen, K. Mantwill, A. Ladhoff, A. Wichert and J. S. Mymryk (2004). "Multidrug-resistant cancer cells facilitate E1-independent adenoviral replication: impact for cancer gene therapy." Cancer research **64**(1): 322-328.

Holzmüller, R., K. Mantwill, C. Haczek, E. Rognoni, M. Anton, A. Kasajima, W. Weichert, D. Treue, H. Lage and T. Schuster (2011). "YB-1 dependent virotherapy in combination with temozolomide as a multimodal therapy approach to eradicate malignant glioma." International journal of cancer **129**(5): 1265-1276.

Hsu, E., M. A. Pennella, N. R. Zemke, C. Eng and A. J. Berk (2018). "Adenovirus E1A activation domain regulates H3 acetylation affecting varied steps in transcription at different viral promoters." Journal of virology **92**(18): e00805-00818.
Huang, T., M. Savontaus, K. Shinozaki, B. Sauter and S. Woo (2003). "Telomerase-dependent oncolytic adenovirus for cancer treatment." Gene therapy **10**(15): 1241-1247.

Jhanji, V., T. C. Chan, E. Y. Li, K. Agarwal and R. B. Vajpayee (2015). "Adenoviral keratoconjunctivitis." Survey of ophthalmology **60**(5): 435-443.

Jin, J., L. Valanejad, T. P. Nguyen, K. Lewis, M. Wright, A. Cast, L. Stock, L. Timchenko and N. A. Timchenko (2016). "Activation of CDK4 triggers development of non-alcoholic fatty liver disease." Cell reports **16**(3): 744-756.

Jin, X., Y. Yan, D. Wang, D. Ding, T. Ma, Z. Ye, R. Jimenez, L. Wang, H. Wu and H. Huang (2018). "DUB3 promotes BET inhibitor resistance and cancer progression by deubiquitinating BRD4." Molecular cell **71**(4): 592-605. e594.

Knudsen, E. S. and A. K. Witkiewicz (2017). "The strange case of CDK4/6 inhibitors: mechanisms, resistance, and combination strategies." Trends in cancer **3**(1): 39-55.
Kovesdi, I., R. Reichel and J. R. Nevins (1986). "Identification of a cellular transcription factor involved in E1A trans-activation." Cell **45**(2): 219-228.

Kovesdi, I., R. Reichel and J. R. Nevins (1987). "Role of an adenovirus E2 promoter binding factor in E1A-mediated coordinate gene control." Proceedings of the National Academy of Sciences **84**(8): 2180-2184.

Kwan, A., N. Winder and M. Muthana (2021). "Oncolytic Virotherapy Treatment of Breast Cancer: Barriers and Recent Advances." Viruses **13**(6): 1128.

Lam, F. C., S. W. Morton, J. Wyckoff, T.-L. V. Han, M. K. Hwang, A. Maffa, E. Balkanska-Sinclair, M. B. Yaffe, S. R. Floyd and P. T. Hammond (2018). "Enhanced efficacy of combined temozolomide and bromodomain inhibitor therapy for gliomas using targeted nanoparticles." Nature communications **9**(1): 1991.

Lang, F. F., C. Conrad, C. Gomez-Manzano, W. A. Yung, R. Sawaya, J. S. Weinberg, S. S. Prabhu, G. Rao, G. N. Fuller and K. D. Aldape (2018). "Phase I study of DNX-2401 (Delta-24-RGD) oncolytic adenovirus: replication and immunotherapeutic effects in recurrent malignant glioma." Journal of Clinical Oncology **36**(14): 1419.

LaRocca, C. J. and S. G. Warner (2018). "Oncolytic viruses and checkpoint inhibitors: combination therapy in clinical trials." Clinical and translational medicine **7**(1): 1-13.

Le Rhun, E., M. Preusser, P. Roth, D. A. Reardon, M. van den Bent, P. Wen, G. Reifenberger and M. Weller (2019). "Molecular targeted therapy of glioblastoma." Cancer treatment reviews: 101896.

Lee, S. Y. (2016). "Temozolomide resistance in glioblastoma multiforme." Genes & diseases **3**(3): 198-210.

Li, F., K. R. MacKenzie, P. Jain, C. Santini, D. W. Young and M. M. Matzuk (2020). "Metabolism of JQ1, an inhibitor of bromodomain and extra terminal bromodomain proteins, in human and mouse liver microsomes." Biology of reproduction **103**(2): 427-436.

Li, J., J. Jiang, J. Wu, X. Bao and N. Sanai (2021). "Physiologically based pharmacokinetic modeling of central nervous system pharmacokinetics of CDK4/6 inhibitors to guide selection of drug and dosing regimen for brain cancer treatment." Clinical Pharmacology & Therapeutics **109**(2): 494-506.

Lichtenegger, E., F. Koll, H. Haas, K. Mantwill, K.-P. Janssen, M. Laschinger, J. Gschwend, K. Steiger, P. C. Black and I. Moskalev (2019). "The oncolytic adenovirus XVir-N-31 as a novel therapy in muscle-invasive bladder cancer." Human gene therapy **30**(1): 44-56.

Lichtenstein, D. L., K. Toth, K. Doronin, A. E. Tollefson and W. S. Wold (2004). "Functions and mechanisms of action of the adenovirus E3 proteins." International reviews of immunology **23**(1-2): 75-111.

Lim, M., Y. Xia, C. Bettegowda and M. Weller (2018). "Current state of immunotherapy for glioblastoma." Nature reviews Clinical oncology **15**(7): 422-442.

Louis, D. N., A. Perry, G. Reifenberger, A. Von Deimling, D. Figarella-Branger, W. K. Cavenee, H. Ohgaki, O. D. Wiestler, P. Kleihues and D. W. Ellison (2016). "The 2016 World Health Organization classification of tumors of the central nervous system: a summary." Acta neuropathologica **131**(6): 803-820.

Lu, Q., X. Ding, T. Huang, S. Zhang, Y. Li, L. Xu, G. Chen, Y. Ying, Y. Wang and Z. Feng (2019). "BRD4 degrader ARV-825 produces long-lasting loss of BRD4 protein and exhibits potent efficacy against cholangiocarcinoma cells." American Journal of Translational Research **11**(9): 5728.

Lutz, P., M. Rosa-Calatrava and C. Kedinger (1997). "The product of the adenovirus intermediate gene IX is a transcriptional activator." Journal of virology **71**(7): 5102-5109.

Lv, B., J. Li, M. Li, Y. Zhuo, K. Ren, E. Li and G. Yang (2018). "Enhancement of adenovirus infection and adenoviral vector-mediated gene delivery by bromodomain inhibitor JQ1." Scientific reports **8**.

Lv, B., J. Li, M. Li, Y. Zhuo, K. Ren, E. Li and G. Yang (2018). "Enhancement of adenovirus infection and adenoviral vector-mediated gene delivery by bromodomain inhibitor JQ1." Scientific reports **8**(1): 1-10.

Ly, K. I., P. Y. Wen and R. Y. Huang (2020). "Imaging of central nervous system tumors based on the 2016 World Health Organization classification." Neurologic clinics **38**(1): 95-113.

Lynch III, J. P. and A. E. Kajon (2016). Respiratory Viral Infections: Adenovirus: Epidemiology, Global Spread of Novel Serotypes, and Advances in Treatment and Prevention. Seminars in respiratory and critical care medicine, Thieme Medical Publishers.

Lynch, K. L., L. R. Gooding, C. Garnett-Benson, D. A. Ornelles and D. C. Avgousti (2019). "Epigenetics and the dynamics of chromatin during adenovirus infections." FEBS letters **593**(24): 3551-3570.

Mantwill, K., N. Köhler-Vargas, A. Bernshausen, A. Bieler, H. Lage, A. Kaszubiak, P. Surowiak, T. Dravits, U. Treiber and R. Hartung (2006). "Inhibition of the multidrug-resistant phenotype by targeting YB-1 with a conditionally oncolytic adenovirus: implications for combinatorial treatment regimen with chemotherapeutic agents." Cancer research **66**(14): 7195-7202.

Mantwill, K., U. Naumann, J. Seznec, V. Girbinger, H. Lage, P. Surowiak, D. Beier, M. Mittelbronn, J. Schlegel and P. S. Holm (2013). "YB-1 dependent oncolytic adenovirus efficiently inhibits tumor growth of glioma cancer stem like cells." Journal of translational medicine **11**(1): 1-13.

Matthews, H. K., C. Bertoli and R. A. de Bruin (2021). "Cell cycle control in cancer." Nature Reviews Molecular Cell Biology: 1-15.

Matzuk, M. M., M. R. McKeown, P. Filippakopoulos, Q. Li, L. Ma, J. E. Agno, M. E. Lemieux, S. Picaud, N. Y. Richard and J. Qi (2012). "Small-molecule inhibition of BRDT for male contraception." Cell **150**(4): 673-684.

McBride, A. A., A. Warburton and S. Khurana (2021). "Multiple Roles of Brd4 in the Infectious Cycle of Human Papillomaviruses." Frontiers in Molecular Biosciences: 727.

Meier, O. and U. F. Greber (2004). "Adenovirus endocytosis." The Journal of Gene Medicine: A cross-disciplinary journal for research on the science of gene transfer and its clinical applications **6**(S1): S152-S163.

Melin, B. S., J. S. Barnholtz-Sloan, M. R. Wrensch, C. Johansen, D. Il'Yasova, B. Kinnersley, Q. T. Ostrom, K. Labreche, Y. Chen and G. Armstrong (2017). "Genome-wide association study of glioma subtypes identifies specific differences in genetic susceptibility to glioblastoma and non-glioblastoma tumors." Nature genetics **49**(5): 789-794.

Michaud, K., D. A. Solomon, E. Oermann, J.-S. Kim, W.-Z. Zhong, M. D. Prados, T. Ozawa, C. D. James and T. Waldman (2010). "Pharmacologic inhibition of cyclin-dependent kinases 4 and 6 arrests the growth of glioblastoma multiforme intracranial xenografts." Cancer research **70**(8): 3228-3238.

Miller, T. W., N. A. Traphagen, J. Li, L. D. Lewis, B. Lopes, A. Asthagiri, J. Loomba, J. De Jong, D. Schiff and S. H. Patel (2019). "Tumor pharmacokinetics and pharmacodynamics of the CDK4/6 inhibitor ribociclib in patients with recurrent glioblastoma." Journal of neuro-oncology: 1-10.

Miura, T. A., J. L. Cook, T. A. Potter, S. Ryan and J. M. Routes (2007). "The interaction of adenovirus E1A with p300 family members modulates cellular gene expression to reduce tumorigenicity." Journal of cellular biochemistry **100**(4): 929-940.

Montaño-Samaniego, M., D. M. Bravo-Estupiñan, O. Méndez-Guerrero, E. Alarcón-Hernández and M. Ibáñez-Hernández (2020). "Strategies for Targeting Gene Therapy in Cancer Cells With Tumor-Specific Promoters." Frontiers in Oncology **10**: 2671.

Moore, A. E. (1952). "Viruses with oncolytic properties and their adaptation to tumors." Annals of the New York Academy of Sciences **54**(6): 945-952.
Mudryj, M., S. H. Devoto, S. W. Hiebert, T. Hunter, J. Pines and J. R. Nevins (1991). "Cell cycle regulation of the E2F transcription factor involves an interaction with cyclin A." Cell **65**(7): 1243-1253.

Murad, H., Y. Alghamian, A. Aljapawe and A. Madania (2018). "Effects of ionizing radiation on the viability and proliferative behavior of the human glioblastoma T98G cell line." BMC research notes **11**(1): 1-6.

Muster, V. and T. Gary (2020). "Incidence, Therapy, and Bleeding Risk—Cancer-Associated Thrombosis in Patients with Glioblastoma." Cancers **12**(6): 1354.

Nakajima, T., M. Masuda-Murata, E. Hara and K. Oda (1987). "Induction of cell cycle progression by adenovirus E1A gene 13S-and 12S-mRNA products in quiescent rat cells." Molecular and cellular biology **7**(10): 3846-3852.

Nemajerova, A., F. Talos, U. Moll and O. Petrenko (2008). "Rb function is required for E1A-induced S-phase checkpoint activation." Cell Death & Differentiation **15**(9): 1440-1449.

Nguyen, D. X., L. A. Baglia, S. M. Huang, C. M. Baker and D. J. McCance (2004). "Acetylation regulates the differentiation-specific functions of the retinoblastoma protein." The EMBO journal **23**(7): 1609-1618.

O'leary, B., R. S. Finn and N. C. Turner (2016). "Treating cancer with selective CDK4/6 inhibitors." Nature reviews Clinical oncology **13**(7): 417-430.

O'Shea, C. C., L. Johnson, B. Bagus, S. Choi, C. Nicholas, A. Shen, L. Boyle, K. Pandey, C. Soria and J. Kunich (2004). "Late viral RNA export, rather than p53 inactivation, determines ONYX-015 tumor selectivity." Cancer cell **6**(6): 611-623.
Ohgaki, H. and P. Kleihues (2013). "The definition of primary and secondary glioblastoma." Clinical cancer research **19**(4): 764-772.

Ohtani, K., J. Degregori and J. R. Nevins (1995). "Regulation of the cyclin E gene by transcription factor E2F1." Proceedings of the National Academy of Sciences **92**(26): 12146-12150.

Ostrom, Q. T., M. Adel Fahmideh, D. J. Cote, I. S. Muskens, J. M. Schraw, M. E. Scheurer and M. L. Bondy (2019). "Risk factors for childhood and adult primary brain tumors." Neuro-oncology **21**(11): 1357-1375.

Ostrom, Q. T., J. Edelson, J. Byun, Y. Han, B. Kinnersley, B. Melin, R. S. Houlston, M. Monje, K. M. Walsh and C. I. Amos (2021). "Partitioned glioma heritability shows subtype-specific enrichment in immune cells." Neuro-oncology.

Palermo, R. D., H. M. Webb and M. J. West (2011). "RNA polymerase II stalling promotes nucleosome occlusion and pTEFb recruitment to drive immortalization by Epstein-Barr virus." PLoS pathogens **7**(10): e1002334.

Pan, Q., A. Sathe, P. C. Black, P. J. Goebell, A. M. Kamat, B. Schmitz-Draeger and R. Nawroth (2017). "CDK4/6 inhibitors in cancer therapy: a novel treatement strategy for bladder cancer." Bladder Cancer **3**(2): 79-88.

Pasteur, L. (1885). Méthode pour prévenir la rage après morsure.

Pastori, C., M. Daniel, C. Penas, C.-H. Volmar, A. L. Johnstone, S. P. Brothers, R. M. Graham, B. Allen, J. N. Sarkaria and R. J. Komotar (2014). "BET bromodomain proteins are required for glioblastoma cell proliferation." Epigenetics **9**(4): 611-620.
Paternot, S., B. Colleoni, X. Bisteau and P. P. Roger (2014). "The CDK4/CDK6 inhibitor PD0332991 paradoxically stabilizes activated cyclin D3-CDK4/6 complexes." Cell cycle **13**(18): 2879-2888.

Pelka, P., J. N. Ablack, J. Torchia, A. S. Turnell, R. J. Grand and J. S. Mymryk (2009). "Transcriptional control by adenovirus E1A conserved region 3 via p300/CBP." Nucleic acids research **37**(4): 1095-1106.

Pelka, P., M. S. Miller, M. Cecchini, A. F. Yousef, D. M. Bowdish, F. Dick, P. Whyte and J. S. Mymryk (2011). "Adenovirus E1A directly targets the E2F/DP-1 complex." Journal of virology **85**(17): 8841-8851.

Philips, A., D. L. Henshaw, G. Lamburn and M. J. O'Carroll (2018). "Authors' Comment on "Brain Tumours: Rise in Glioblastoma Multiforme Incidence in England 1995–2015 Suggests an Adverse Environmental or Lifestyle Factor"." Journal of environmental and public health **2018**.

Philips, A., D. L. Henshaw, G. Lamburn and M. J. O'Carroll (2018). "Brain tumours: rise in glioblastoma multiforme incidence in England 1995–2015 suggests an adverse environmental or lifestyle factor." Journal of environmental and public health **2018**.

Phillips, H. S., S. Kharbanda, R. Chen, W. F. Forrest, R. H. Soriano, T. D. Wu, A. Misra, J. M. Nigro, H. Colman and L. Soroceanu (2006). "Molecular subclasses of high-grade glioma predict prognosis, delineate a pattern of disease progression, and resemble stages in neurogenesis." Cancer cell **9**(3): 157-173.

Portman, N., S. Alexandrou, E. Carson, S. Wang, E. Lim and C. E. Caldon (2019). "Overcoming CDK4/6 inhibitor resistance in ER-positive breast cancer." Endocrine-related cancer **26**(1): R15-R30.

Qi, J. (2014). "Bromodomain and extraterminal domain inhibitors (BETi) for cancer therapy: chemical modulation of chromatin structure." Cold Spring Harbor perspectives in biology **6**(12): a018663.

Qiao, H., X. Chen, Q. Wang, J. Zhang, D. Huang, E. Chen, H. Qian, Y. Zhong, Q. Tang and W. Chen (2020). "Tumor localization of oncolytic adenovirus assisted by pH-degradable microgels with JQ1-mediated boosting replication and PD-L1 suppression for enhanced cancer therapy." Biomaterials science **8**(9): 2472-2480.

Quillien, V., A. Lavenu, L. Karayan-Tapon, C. Carpentier, M. Labussière, T. Lesimple, O. Chinot, M. Wager, J. Honnorat and S. Saikali (2012). "Comparative assessment of 5 methods (methylation-specific polymerase chain reaction, methylight, pyrosequencing, methylation-sensitive high-resolution melting, and immunohistochemistry) to analyze O6-methylguanine-DNA-methyltranferase in a series of 100 glioblastoma patients." Cancer **118**(17): 4201-4211.

Ranger, A. M., Y. K. Patel, N. Chaudhary and R. V. Anantha (2014). "Familial syndromes associated with intracranial tumours: a review." Child's Nervous System **30**(1): 47-64.

Raspé, E., K. Coulonval, J. M. Pita, S. Paternot, F. Rothé, L. Twyffels, S. Brohée, L. Craciun, D. Larsimont and V. Kruys (2017). "CDK 4 phosphorylation status and a linked gene expression profile predict sensitivity to palbociclib." EMBO molecular medicine **9**(8): 1052-1066.

Rehman, H., A. W. Silk, M. P. Kane and H. L. Kaufman (2016). "Into the clinic: Talimogene laherparepvec (T-VEC), a first-in-class intratumoral oncolytic viral therapy." Journal for immunotherapy of cancer **4**(1): 1-8.

Ren, K., W. Zhang, X. Chen, Y. Ma, Y. Dai, Y. Fan, Y. Hou, R. X. Tan and E. Li (2016). "An epigenetic compound library screen identifies BET inhibitors that promote HSV-1 and-2 replication by bridging P-TEFb to viral gene promoters through BRD4." PLoS pathogens **12**(10): e1005950.

Ries, S. and W. Korn (2002). "ONYX-015: mechanisms of action and clinical potential of a replication-selective adenovirus." British journal of cancer **86**(1): 5-11.

Roa, W., P. Brasher, G. Bauman, M. Anthes, E. Bruera, A. Chan, B. Fisher, D. Fulton, S. Gulavita and C. Hao (2004). "Abbreviated course of radiation therapy in older patients with glioblastoma multiforme: a prospective randomized clinical trial." Journal of clinical oncology **22**(9): 1583-1588.

Rognoni, E., M. Widmaier, C. Haczek, K. Mantwill, R. Holzmüller, B. Gansbacher, A. Kolk, T. Schuster, R. Schmid and D. Saur (2009). "Adenovirus-based virotherapy enabled by cellular YB-1 expression in vitro and in vivo." Cancer gene therapy **16**(10): 753.

Russell, W. (2000). "Update on adenovirus and its vectors." Journal of general virology **81**(11): 2573-2604.

Russell, W. (2009). "Adenoviruses: update on structure and function." Journal of General Virology **90**(1): 1-20.

Sato-Dahlman, M., B. L. Roach and M. Yamamoto (2020). The Role of Adenovirus in Cancer Therapy, Multidisciplinary Digital Publishing Institute.

Schaer, D. A., R. P. Beckmann, J. A. Dempsey, L. Huber, A. Forest, N. Amaladas, Y. Li, Y. C. Wang, E. R. Rasmussen and D. Chin (2018). "The CDK4/6 inhibitor abemaciclib induces a T cell inflamed tumor microenvironment and enhances the efficacy of PD-L1 checkpoint blockade." Cell reports **22**(11): 2978-2994.

Seifried, L., S. Talluri, M. Cecchini, L. Julian, J. Mymryk and F. Dick (2008). "pRB-E2F1 complexes are resistant to adenovirus E1A-mediated disruption." Journal of virology **82**(9): 4511-4520.

Shimizu, S., E. Urano, Y. Futahashi, K. Miyauchi, M. Isogai, Z. Matsuda, K. Nohtomi, T. Onogi, Y. Takebe and N. Yamamoto (2007). "Inhibiting lentiviral replication by HEXIM1, a cellular negative regulator of the CDK9/cyclin T complex." Aids **21**(5): 575-582.

SongTao, Q., Y. Lei, G. Si, D. YanQing, H. HuiXia, Z. XueLin, W. LanXiao and Y. Fei (2012). "IDH mutations predict longer survival and response to temozolomide in secondary glioblastoma." Cancer science **103**(2): 269-273.

Stavrakaki, E., C. M. Dirven and M. L. Lamfers (2021). "Personalizing oncolytic virotherapy for glioblastoma: in search of biomarkers for response." Cancers **13**(4): 614.

Stummer, W., A. Novotny, H. Stepp, C. Goetz, K. Bise and H. J. Reulen (2000). "Fluorescence-guided resection of glioblastoma multiforme utilizing 5-ALA-induced porphyrins: a prospective study in 52 consecutive patients." Journal of neurosurgery **93**(6): 1003-1013.

Stupp, R. (2005). "European Organisation for Research and Treatment of Cancer Brain Tumor and Radiotherapy Groups; National Cancer Institute of Canada Clinical Trials Group. Radiotherapy plus concomitant and adjuvant temozolomide for glioblastoma." N Engl J Med **352**: 987-996.

Sun, B., B. Shah, W. Fiskus, J. Qi, K. Rajapakshe, C. Coarfa, L. Li, S. G. Devaraj, S. Sharma and L. Zhang (2015). "Synergistic activity of BET protein antagonist-based combinations in mantle cell lymphoma cells sensitive or resistant to ibrutinib." Blood, The Journal of the American Society of Hematology **126**(13): 1565-1574.

Sung, H., J. Ferlay, R. L. Siegel, M. Laversanne, I. Soerjomataram, A. Jemal and F. Bray (2021). "Global cancer statistics 2020: GLOBOCAN estimates of incidence and mortality worldwide for 36 cancers in 185 countries." CA: a cancer journal for clinicians **71**(3): 209-249.

Swaminathan, S. and B. Thimmapaya (1996). "Transactivation of adenovirus E2-early promoter by E1A and E4 6/7 in the context of viral chromosome." Journal of molecular biology **258**(5): 736-746.

Tamimi, A. F. and M. Juweid (2017). "Epidemiology and outcome of glioblastoma." Exon Publications: 143-153.

Taspinar, M., S. Ilgaz, M. Ozdemir, T. Ozkan, D. Oztuna, H. Canpinar, J. A. Rey, A. Sunguroğlu, J. S. Castresana and H. C. Ugur (2013). "Effect of lomeguatrib–temozolomide combination on MGMT promoter methylation and expression in primary glioblastoma tumor cells." Tumor Biology **34**(3): 1935-1947.

Täuber, B. and T. Dobner (2001). "Molecular regulation and biological function of adenovirus early genes: the E4 ORFs." Gene **278**(1-2): 1-23.

Thangamathesvaran, L., R. Shah, R. Verma and O. Mahmoud (2018). "Immune checkpoint inhibitors and radiotherapy—concept and review of current literature." Annals of translational medicine **6**(8).

Tobias, A. L., B. Thaci, B. Auffinger, E. Rincón, I. V. Balyasnikova, C. K. Kim, Y. Han, L. Zhang, K. S. Aboody and A. U. Ahmed (2013). "The timing of neural stem cell-based virotherapy is critical for optimal therapeutic efficacy when applied with radiation and chemotherapy for the treatment of glioblastoma." Stem cells translational medicine **2**(9): 655-666.

Tribouley, C., P. Lutz, A. Staub and C. Kedinger (1994). "The product of the adenovirus intermediate gene IVa2 is a transcriptional activator of the major late promoter." Journal of virology **68**(7): 4450-4457.

Tucha, O., C. Smely, M. Preier and K. W. Lange (2000). "Cognitive deficits before treatment among patients with brain tumors." Neurosurgery **47**(2): 324-334.
Vähä-Koskela, M. J., J. E. Heikkilä and A. E. Hinkkanen (2007). "Oncolytic viruses in cancer therapy." Cancer letters **254**(2): 178-216.

Verhaak, R. G., K. A. Hoadley, E. Purdom, V. Wang, Y. Qi, M. D. Wilkerson, C. R. Miller, L. Ding, T. Golub and J. P. Mesirov (2010). "Integrated genomic analysis identifies clinically relevant subtypes of glioblastoma characterized by abnormalities in PDGFRA, IDH1, EGFR, and NF1." Cancer cell **17**(1): 98-110.

Vijayalingam, S. and G. Chinnadurai (2013). "Adenovirus L-E1A activates transcription through mediator complex-dependent recruitment of the super elongation complex." Journal of virology **87**(6): 3425-3434.

Weller, M., T. Cloughesy, J. R. Perry and W. Wick (2013). "Standards of care for treatment of recurrent glioblastoma—are we there yet?" Neuro-oncology **15**(1): 4-27.
Weller, M., M. van den Bent, M. Preusser, E. Le Rhun, J. C. Tonn, G. Minniti, M. Bendszus, C. Balana, O. Chinot and L. Dirven (2021). "EANO guidelines on the diagnosis and treatment of diffuse gliomas of adulthood." Nature Reviews Clinical Oncology **18**(3): 170-186.

Weller, M., M. Van Den Bent, J. C. Tonn, R. Stupp, M. Preusser, E. Cohen-Jonathan-Moyal, R. Henriksson, E. Le Rhun, C. Balana and O. Chinot (2017). "European Association for Neuro-Oncology (EANO) guideline on the diagnosis and treatment of adult astrocytic and oligodendroglial gliomas." The lancet oncology **18**(6): e315-e329.

Wen, P. Y., M. Weller, E. Q. Lee, B. A. Alexander, J. S. Barnholtz-Sloan, F. P. Barthel, T. Batchelor, R. S. Bindra, S. M. Chang and E. A. Chiocca (2020). "Glioblastoma in Adults: A Society for Neuro-Oncology (SNO) and European Society of Neuro-Oncology (EANO) Consensus Review on Current Management and Future Directions." Neuro-oncology.

Whyte, P., H. Ruley and E. Harlow (1988). "Two regions of the adenovirus early region 1A proteins are required for transformation." Journal of virology **62**(1): 257-265.

Wick, W., T. Gorlia, M. Bendszus, M. Taphoorn, F. Sahm, I. Harting, A. A. Brandes, W. Taal, J. Domont and A. Idbaih (2017). "Lomustine and bevacizumab in progressive glioblastoma." New England Journal of Medicine **377**(20): 1954-1963.
Wick, W., M. Weller, M. Van Den Bent, M. Sanson, M. Weiler, A. Von Deimling, C. Plass, M. Hegi, M. Platten and G. Reifenberger (2014). "MGMT testing—the challenges for biomarker-based glioma treatment." Nature Reviews Neurology **10**(7): 372-385.

Wu, Y., Y. Zhang, H. Pi and Y. Sheng (2020). "Current therapeutic progress of CDK4/6 inhibitors in breast cancer." Cancer Management and Research **12**: 3477.

Xu, L., Y. Chen, A. Mayakonda, L. Koh, Y. K. Chong, D. L. Buckley, E. Sandanaraj, S. W. Lim, R. Y.-T. Lin and X.-Y. Ke (2018). "Targetable BET proteins-and E2F1-dependent transcriptional program maintains the malignancy of glioblastoma." Proceedings of the National Academy of Sciences **115**(22): E5086-E5095.

Young, C. (2003). The structure and function of the adenovirus major late promoter.
Yust-Katz, S., J. J. Mandel, J. Wu, Y. Yuan, C. Webre, T. A. Pawar, H. S. Lhadha, M. R. Gilbert and T. S. Armstrong (2015). "Venous thromboembolism (VTE) and glioblastoma." Journal of neuro-oncology **124**(1): 87-94.

Zaborowska, J., N. F. Isa and S. Murphy (2016). "P-TEFb goes viral." Bioessays **38**: S75-S85.

Zajchowski, D. A., H. Boeuf and C. Kédinger (1987). "E1a inducibility of the adenoviral early E2a promoter is determined by specific combinations of sequence elements." Gene **58**(2-3): 243-256.

Zhang, W. and M. J. Imperiale (2003). "Requirement of the adenovirus IVa2 protein for virus assembly." Journal of virology **77**(6): 3586-3594.

Zhu, J., G. D. Gaiha, S. P. John, T. Pertel, C. R. Chin, G. Gao, H. Qu, B. D. Walker, S. J. Elledge and A. L. Brass (2012). "Reactivation of latent HIV-1 by inhibition of BRD4." Cell reports **2**(4): 807-816.

Zhu, X., K. Enomoto, L. Zhao, Y. J. Zhu, M. C. Willingham, P. Meltzer, J. Qi and S.-y. Cheng (2017). "Bromodomain and extraterminal protein inhibitor JQ1 suppresses thyroid tumor growth in a mouse model." Clinical Cancer Research **23**(2): 430-440.